Investigating the role of nidogens, a family of basement membrane proteins, at the neuromuscular junction in health and disease

---

Ione Frederica Greensmith Meyer

Institute of Neurology

UCL

Primary Supervisor: Professor Giampietro Schiavo

Secondary Supervisor: Professor Elizabeth Fisher

Thesis submitted for the degree of

Doctor of Philosophy in Molecular Neuroscience

2019

Declaration

I, Ione Meyer confirm that the work presented in this thesis is my own. Where information has been derived from other sources, I confirm that this has been indicated in the thesis.

Abstract

The basement membrane is a specialised form of the extracellular matrix that surrounds cells and tissues to provide structural support, regulate tissue development and modulate homeostatic signalling. Despite the ubiquitous presence of this matrix throughout the body, dysregulation of individual components can result in tissue-specific human diseases. Recently nidogens, a family of basement membrane glycoproteins, have been identified as candidate genes in a family with hydrocephalus and muscle weakness. Increasing evidence suggests that nidogens are involved in signalling processes underlying neurological function and development, and certain nidogen isoforms appear to be specific to the neuromuscular junction (NMJ). My aim was to investigate the active signalling role of nidogens at the NMJ using a combination of biochemical and imaging techniques. As the basement membrane can play an important role in tissue remodelling, I investigated the changes in expression profile of nidogens in conditions of NMJ plasticity. Expression was measured during postnatal muscle maturation and disease progression in a model of amyotrophic lateral sclerosis (ALS) - the $SOD1^{G93A}$ mouse. As neurotrophins are crucial to the development and maintenance of motor neurons and NMJs, I also investigated the interaction of nidogens with several trophic molecules. My work shows that nidogens are internalised by motor neurons and may be co-transported with neurotrophin receptors inside signalling endosomes. While expression of nidogens appears unaffected by disease progression in the $SOD1^{G93A}$ mouse, there may be increased levels of nidogens and altered isoform expression during early postnatal muscle maturation. I also introduce a novel nidogen-1 knock-out mouse model, which displays neurological phenotypes and compensatory upregulation of nidogen-2 in certain tissues. Defining the nidogen signalling complex and its downstream pathways will increase our understanding of the homeostatic mechanisms governing the NMJ and provide new targets for therapeutic strategies to maintain neuromuscular function in pathological conditions.

Impact Statement

Basement membranes are complex networks of extracellular molecules that surround most cell types and all tissues in the body. They not only provide structural support to protect against mechanical deformation and stress but are also critical regulators of morphogenesis and patterning during tissue development, cellular remodelling and homeostatic signalling pathways. Participation of the basement membrane in these processes is not merely as a passive, permissive substrate and the dynamic capabilities of this extracellular matrix are beginning to be appreciated.

The work presented in this thesis aims to shed some light on the specific signalling functions of a family of components of this basement membrane; nidogens. Specifically, this study examines the role of nidogens within the neuromuscular system at the interface between motor neuron terminals and muscle fibres, known as the neuromuscular junction. I present evidence that while nidogens are expressed throughout the neuromuscular system, they are enriched at the neuromuscular junction (NMJ). In addition, I show that nidogens may interact with receptors on motor neurons that are critical for their survival and function and can undergo intracellular trafficking in these cells. This represents an important step in our understanding of how basement membrane components may interact with cell surface receptors.

Increasing our understanding of the active signalling role played by basement membranes at the NMJ, and building a picture of the interactors, has far reaching benefits. Several neurological diseases display significant degeneration at the NMJ, which has a direct consequence in the severity of motor deficits. Recent work has indicated that treatments with growth factors, molecules that promote cell survival, to preserve this synapse may ameliorate these disease symptoms. However, several clinical trials targeting growth factors have led to limited success. Other work has shown that engineering growth factors with a strong affinity for the basement membrane, significantly increases their efficacy. These growth factor variants may therefore be a viable option for therapy. Identification of novel signalling pathways involving the entry of nidogens into motor neuron terminals may represent an important addition to this therapeutic strategy. If nidogen already localises to the site of degeneration, the NMJ, and is also able

to be internalised into neurons, engineering growth factors with increased affinity for this family of proteins may significantly improve the efficiency of treatments and reduce systemic side effects.

In addition, this pathway could be optimised for drug delivery systems outside of growth factor treatments. If nidogens are able to enter motor neuron terminals and be retrogradely transported back to the spinal cord, this will represent a privileged pathway of entry to the CNS. This has been a notorious complication for neurological disease treatments, as the blood brain barrier prevents the majority of exogenously applied drugs from reaching the target tissue. However, hijacking the nidogen pathway, as indeed the tetanus neurotoxin seems to have done, will bypass this important physiological barrier.

The work presented in this thesis thereby represents an important step in our understanding of nidogen with important implications in the treatment of many devastating neurological diseases.

Acknowledgements

Firstly a thank you must be said
To all the students I may have led,
Astray with cake club,
Who joined me at the pub,
And stopped me from losing my head.

To all the members of ION 5th Floor,
I've never had such fun at work before.
For your help and the jokes,
I thank all you folks,
I'll remember you forever more.

A special thank you of course must go,
To Nicol who's honestly been a hero,
If I needed advice,
She was there in a trice,
Fuelled by nine espresso.

For teaching me all about muscle dissection,
And sharing the woes of the damn cryosection,
I thank James of course,
Who had perforce,
To put up with my constant distraction.

I must mention Alex, for all his support
And being more patient than I could have thought,
If two theses, one house,
Has somehow not doused
His good humour, it's not been for naught.

Thank you to Lizzy for keeping me calm,
Her voice of reason allayed my alarm.
If over the years,
I've expressed a few fears,
She's stopped them from doing me harm.

And finally Gipi, I cannot deny,
I've learned quite a lot as time has gone by,
I truly am glad,
To have been part of your lab,
But now little boss must say goodbye.

Table of Contents

Table of Figures

Table of Tables

Abbreviations

ACh	acetylcholine	MBP	myelin basic protein
AChE	acetylcholine esterase	MDC1A	merosin-deficient congenital muscular dystrophy type 1A
AChR	acetylcholine receptor	MuSK	muscle-specific kinase
AKT	protein kinase B	NCAM	neural cell adhesion molecule
ALS	amyotrophic lateral sclerosis	NF	neurofilament
BBB	blood brain barrier	NMJ	neuromuscular junction
BDNF	bone derived neurotrophic factor	NT-3/4	neurotrophin-3/4
bHLH	basic helix-loop-helix	OLIG2	oligodendrocyte transcription factor
BMP	bone morphogenic protein	OPC	oligodendrocyte precursor cell
BTX	bungarotoxin	$P75^{NTR}$	p75 neurotrophin receptor
c-FN	cellular fibronectin	PDGF	platelet derived growth factor
CNS	central nervous system	PECAM1	platelet endothelial cell adhesion molecule
DGC	dystrophin-glycoprotein complex	p-FN	plasma fibronectin
Dpp	decapentaplegic	PLA	proximity ligation assay
ECM	extracellular matrix	PND	postnatal day
EDL	extensor digitorum longus	PNS	peripheral nervous system
ERK	extracellular-signal-regulated kinase	PNSA	PVL-negative *S. aureus*
FGF	fibroblast growth factor	PPSA	PVL-positive *S. aureus*
FGFR	fibroblast growth factor receptor	RET	rearranged during transfection proto-oncogene
GAPDH	glyceraldehyde 3-phosphate dehydrogenase	SJS	Schwartz-Jampel syndrome
GC	gastrocnemius	SOD1	superoxide dismutase 1
GDNF	glial derived neurotrophic factor	SOL	soleus
GFAP	glial fibrillary acidic protein	SOX10	SRY-Box 10 transcription factor
GFRα1	GDNF family receptor alpha 1	SV2	synaptic vesicle protein 2
HcT	TeNT heavy chain C-terminal fragment	TA	tibialis anterior
HSPG	heparan sulfate proteoglycan	TeNT	tetanus neurotoxin
KO	knock-out	TP	total protein
LAR	leukocyte antigen-related protein	TrkB	tropomyosin-related kinase receptor B
LRP4	LDL receptor-related protein 4	VEGF	vascular endothelial growth factor

Chapter 1. Introduction

1.1 Basement Membranes

1.1.1 What are basement membranes?

The extracellular matrix (ECM) is a complex network of secreted molecules that assemble as two specialised structures: the interstitial matrix and the pericellular matrix. The interstitial matrix comprises the fibrillar connective tissue which fills the extracellular space. The pericellular matrix is also known as the basement membrane, and exists as a dense, layered macromolecular network that underlies epithelial and endothelial cells as well as muscle fibres, adipocytes and cells of the nervous system (Laurila and Leivo, 1993; Timpl, 1989). The basement membrane, first observed in muscle tissue in 1840, was initially considered to simply provide structural support and compartmentalise cells and tissues (Bowman, 1840). Subsequent work suggests that this structural support is crucial for the ability to sustain multi-organ life forms. Strikingly, the appearance of the basement membrane during evolution coincided with the advent of multicellularity (Hynes, 2012; Ozbek et al., 2010; Sherwood, 2015). As the ECM components involved in basement membrane formation are missing from the genetic makeup of single-celled organisms, this suggests a role for the basement membrane in the evolution of more complex organisms and the ability to generate discrete tissues and organs (Fidler et al., 2017). However, more recent investigations into the structure and function of the basement membrane have revealed additional roles for this matrix in the modulation of cell behaviour during development, remodelling and homeostasis.

1.1.2 Composition of the basement membrane

The basement membrane is made up of a wide range of large molecules that self-assemble into the insoluble, highly cross-linked polymer matrix (Kalluri, 2003). This matrix is predominantly comprised of four key members: laminins, collagens (particularly type IV collagens), heparan sulfate proteoglycans (HSPGs) and nidogens (also known as entactins). Although these are the main components, a plethora of other molecules are involved in cross-linking within the basement membrane and adhesion of the matrix to plasma membranes and/or connective tissue (see Table 1.1). The variety of these other components, in

addition to the existence of several isoforms of each of the main members, generates significant diversity in the final composition of basement membranes (Timpl and Brown, 1994). Differences in the precise make-up of the basement membrane, depending on its localisation or its temporal expression during development or remodelling, result in specific functional characteristics relevant for particular tissues.

Component	Molecular mass (approx.)	Variants	Location	Interactors
Laminin	400-900 kDa (monomer)	12 viable combinations from 5 α, 3 β and 3 γ chain genes	Basement membrane	Integrins, dystroglycan, nidogens, laminin, fibulins, sulfated glycolipids, agrin
Collagen IV	600 kDa (monomer)	α1α1α2, α3α4α5, α5α5α6	Basement membrane	Collagen IV, nidogens, perlecan
Nidogen-1	150 kDa	Proteolytic fragments, alternative splice variants	Basement membrane	Collagen IV, laminin, perlecan, fibulins
Nidogen-2	200 kDa	Proteolytic fragments	Basement membrane	Collagen IV, laminin, perlecan, fibulins
Perlecan	480 kDa	Alternative splicing variants	Basement membrane, interstitial matrix	Collagen IV, laminin, fibronectin, nidogen-1, nidogen-2, heparin, fibulin, dystroglycan, integrins, sulphated glycolipids
Agrin	400 kDa	Alternative splicing variants	Basement membrane, transmembrane (isoform 2 only)	Laminin, integrins, sulphated glycolipids, dystroglycan, heparin (Y^+ agrin)
Fibronectin	250 kDa (monomer)	Alternative splicing variants	Basement membrane and interstitial matrix (insoluble form), plasma (soluble form)	Integrins (classically α5β1), heparan sulfates
Collagen VI	500 kDa (monomer)	α1α2αX (where X is α3/4/5)	Interface of basement membrane and stroma	Collagen I, II, IV, VI, XIV, perlecan, fibulin, heparan sulfates, integrins
Fibulin-1 and -2	90-100 kDa (-1), 200 kDa (-2)	Alternative splicing variants of fibulin-1	Basement membrane, interstitial matrix	Fibronectin, collagen VI, nidogen-1, nidogen-2, perlecan, laminin, integrins
Usherin	170 kDa (extracellular) or 600 kDa (transmembrane)	-	Basement membrane, transmembrane	Collagen IV, fibronectin
Bamacan	138 kDa	-	Basement membrane	Heparan sulfates
Nephronectin	90 kDa	-	Extracellular	Integrin (α8β1)

Netrins	75 kDa	6 different genes	Extracellular (netrin-1, -3, -4, -5), cell surface (netrin-G1, -G2)	Heparan sulfates
Dystroglycan	160 kDa (α subunit), 40 kDa (β subunit)	-	Cell surface (α subunit), transmembrane (β subunit)	Laminin, agrin, perlecan,
Integrins	Range	24 combinations from 18 α subunit genes and 8 β subunit genes	Transmembrane	Laminin, perlecan, agrin, fibronectin, collagen VI, nephronectin

Table 1.1 Key basement membrane components and associated molecules

The main components of the basement membrane are outlined, along with key interactors at the cell surface. Approximate molecular weights and molecular or genetic variants are described along with localisation and interaction partners. The interactors listed are those relevant for basement membrane formation and maintenance.

1.1.2.1 Laminins

Laminins are trimeric glycoproteins formed from one each of three different subunits, α, β and γ. There are 11 genes for the laminin subunits, encoding five α chains, three β chains and three γ chains (Miner and Yurchenco, 2004). These chains assemble into heterotrimers through the formation of a triple-stranded α-helical coiled-coil domain (Aumailley, 2013; Paulsson et al., 1985). The resulting heterotrimers have a cruciform structure with three short arms and one long arm, each with integral globular domains (see Figure 1.1; Engel et al., 1981). Despite the potential for a large number of laminin heterotrimer combinations, there appears to be a restriction to compatible subunits, resulting in only 16 isoforms being identified to date (Aumailley et al., 2005; Macdonald et al., 2010; Yurchenco, 2015). Interestingly, comparative analysis of different laminin isoforms indicate that they differ in their induction of proliferation, differentiation and adhesion via their interactions with cell surface receptors and stimulation of transcription factor cascades (Turck et al., 2005). The different laminin isoforms display diverse binding repertoires and tissue distribution patterns, contributing to the functional specificity of the basement membrane (Domogatskaya et al., 2012).

1.1.2.2 Collagens

Collagens are another genre of trimeric extracellular matrix molecules. Collagens have a characteristic triple-helical domain and are comprised of three α chains. There are currently 28 identified members of the collagen superfamily (types I-

XXVIII), which differ according to their component α chains (Ricard-Blum, 2011). The existence of different isoforms and splicing variants of the individual α chains generates even more diversity. A subgroup of this superfamily encompasses the fibrillar collagens, which assemble into ordered striated fibrils and are part of the interstitial matrix (Exposito et al., 2010). Collagens I, II, III, V and XI are members of this subgroup and are found in the majority of connective tissues and cartilage (Ricard-Blum, 2011). In contrast to the fibrillar collagens, collagen IV forms polygonal sheet-like lattices instead of elongated fibres, and is the most abundant component of the basement membrane. There are six α chain genes for collagen IV: α1(IV) and α2(IV), which are ubiquitously expressed throughout the body, and α3(IV)-6(IV), which display a greater degree of tissue specificity (Khoshnoodi et al., 2008). Similarly to laminins, despite the large number of possible combinations, there are only three collagen IV heterotrimers assembled: α1α1α2, α3α4α5 and α5α5α6 (Bai et al., 2009). These heterotrimers form hexagonal networks through end-to-end interactions between their C-terminal globular NC1 domains, as well as interactions between their N-terminal 7S domains (see Figure 1.1; Casino et al., 2018; Yurchenco and Ruben, 1987; Yurchenco and Schittny, 1990). Lateral intermolecular sulfilimine bonds help stabilise this three-dimensional lattice (Vanacore et al., 2009).

1.1.2.3 Heparan sulfate proteoglycans (HSPGs)

HSPGs are glycoproteins with covalently attached heparan sulfate side chains, and can be lipid-anchored, transmembrane, or secreted into the extracellular milieu (Farach-Carson and Carson, 2007). Perlecan and agrin belong to the secreted subgroup of HSPGs and are important members of the basement membrane. Perlecan is a modular proteoglycan with a diverse portfolio of interaction partners, which implicate it in a wide range of physiological processes, from wound healing and angiogenesis, to lipid metabolism and regulation of skeletal muscle morphology (Gubbiotti et al., 2017; Yamashita et al., 2018).

Conversely, agrin appears to have more conserved roles in synapse development as well as an emerging role in maturation of the innate immune system (Daniels, 2012; Mazzon et al., 2012). Agrin-deficient mice produced lower numbers of mature monocyte-derived cells and macrophages from these animals displayed defects in phagocytic activity (Mazzon et al., 2012). The signalling pathways behind the role of agrin in immune cell maturation remain unclear. The

role of agrin in promoting formation and maintenance of neuromuscular junctions (NMJs) on the other hand, has been an area of intense investigation for many years. Agrin secreted by presynaptic motor neuron terminals forms a complex with LRP4 (low-density lipoprotein receptor related protein 4) and MuSK (muscle-specific kinase), which initiates downstream intracellular signalling pathways to direct postsynaptic acetylcholine receptors (AChRs) into discrete clusters (Kim et al., 2008; Zhang et al., 2008; Zong et al., 2012). Agrin thereby mediates the refinement of precisely apposed pre- and post-synaptic compartments required for rapid and efficient neurotransmission.

There are several different isoforms of agrin resulting from insertions at two specific sites (Z and Y in mammals) due to alternative splicing (Burgess et al., 2000, 1999). At the C-terminal Z site, splicing can incorporate either 8, 11 or 19 amino acids, and these isoforms of agrin (Z^+ agrin) display up to 1000-fold greater activity in promoting acetylcholine receptor (AChR) clustering at the NMJ than Z^- agrin (Burgess et al., 1999). Splicing events that introduce four amino acids into the Y site of agrin (Y^+ agrin) confer the ability to bind heparin, and this has been shown to further increase the efficacy of Z^+ agrin in AChR clustering (Ferns et al., 1993; O'Toole et al., 1996). This suggests that interaction with other extracellular molecules bearing heparan sufate chains, such as those found in the basement membrane, can modulate the activity of agrin.

1.1.2.4 Fibronectin

In addition to the core members of the basement membrane, other extracellular molecules can interact and become incorporated into this matrix. Fibronectin is an extracellular dimeric glycoprotein encoded by a single gene but with many alternative splicing variants (ffrench-Constant, 1995). There are two main forms of fibronectin. One is a soluble form secreted by hepatocytes into blood plasma (p-FN), where it is an important player in the formation of fibrin clots and aggregation of platelets (Wang et al., 2014). The other form is known as cellular fibronectin (c-FN) and is secreted by various cell types for incorporation into the insoluble extracellular matrix, where it associates with collagens, heparin and integrins to modulate tissue morphogenesis, remodelling and angiogenesis (Wakui et al., 1990).

1.1.2.5 Fibulins

Fibulins are a family of eight extracellular matrix proteins which share a general structure of a C-terminal fibulin module preceded by EGF-like domains (Nakamura, 2018). Fibulin-1 and -2 are large molecules present in the basement membrane as well as the interstitial matrix. Fibulin-1 interacts with laminin, nidogens and fibronectin, while fibulin-2 also weakly binds collagen IV and perlecan (Balbona et al., 1992; Brown et al., 1994; Pan et al., 1993; Sasaki et al., 1995). Fibulins have a wide array of functions, including cell migration and basement membrane assembly, as a result of their interactions between the ECM and the plasma membrane.

1.1.3 Basement membrane assembly

Basement membrane deposition is initiated by the formation of a laminin polymer network, which self-assembles via interactions between its N-terminal short arms under high local concentrations (Figure 1.1; (Cheng et al., 1997; Colognato et al., 1999; Li and Thompson, 2003; Yurchenco et al., 1992). Integrins are transmembrane heterodimers, composed of α and β subunits, crucial for cellular adhesion and the transmission of extracellular cues to intracellular signalling pathways (Hynes, 2002). Laminins interact with integrins (particularly β1 integrins), promoting the concentration of laminin at competent cell surfaces, and interference of these interactions has been shown to negatively impact basement membrane formation (Aumailley et al., 2000; Li et al., 2002). Laminin also binds to the cell surface-associated α-dystroglycan via the laminin α1 and α2 C-terminal globular domains (Gee et al., 1993). Dystroglycan is comprised of non-covalently associated α and β subunits, where the α subunit is exposed on the cell surface and the β subunit is a transmembrane polypeptide that interacts intracellularly with dystrophin to form the dystrophin glycoprotein complex (DGC; Ibraghimov-Beskrovnaya et al., 1992). Binding of dystrophin to F-actin completes the link between the cytoskeleton and the basement membrane (Montanaro et al., 1999; Way et al., 1992).

Integrins also bind to many other components of the basement membrane, thereby concentrating these molecules in the vicinity of each other where they can interact to build up the basement membrane (Hynes, 2002). Collagen IV also self-assembles, as previously described, and the formation of intermolecular covalent bonds and branched polymers confer a high degree of tensile strength

and the ability to withstand mechanical stresses on the basement membrane (Timpl et al., 1981; Vanacore et al., 2009). The laminin and collagen IV networks are linked via interactions of both molecules with nidogens and perlecan in addition to auxiliary extracellular components (Aumailley et al., 1993, 1989; Behrens et al., 2012; Costell et al., 1999; McKee et al., 2007). This recruitment and assembly of extracellular molecules results in a stepwise formation of the complex layered basement membrane (Figure 1.1; Hohenester and Yurchenco, 2013).

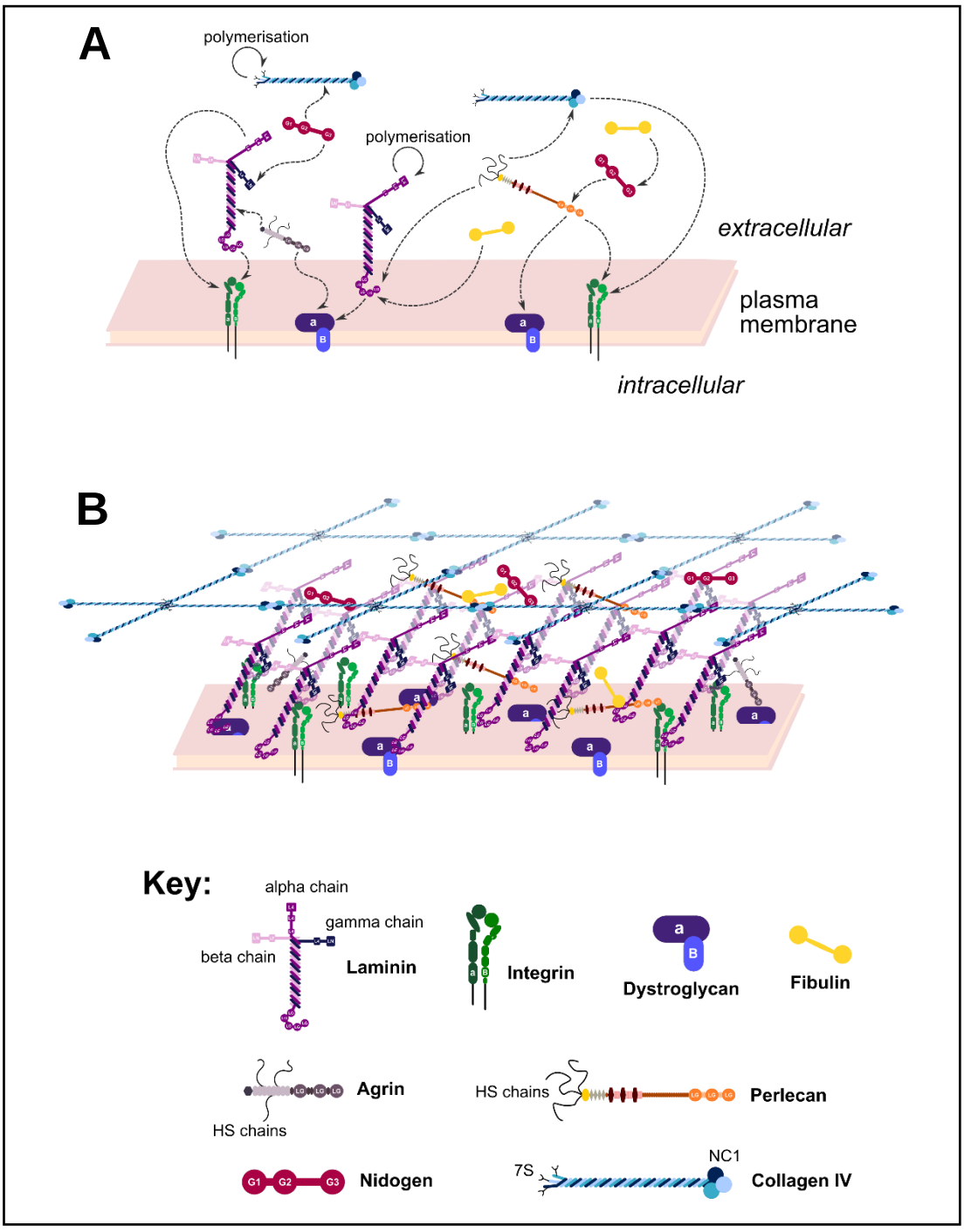

Figure 1.1 Basement membrane assembly

(A) Black arrows indicate interactions between the key components of the basement membrane in the extracellular space. Laminin adheres to cell surfaces via interactions with integrins and dystroglycan. High local concentrations of laminin promote the self-assembly of laminin networks. Collagen IV also polymerises to form a collagenous mesh. Recruitment of nidogens and perlecan create intermolecular links between the two lattices in addition to reinforcing adhesion of the assembling basement membrane to cell surfaces. Agrin also facilitates binding of the laminin network to cell surfaces via interaction with laminin and dystroglycan. **(B)** This stepwise polymerisation and recruitment of interacting molecules results in the formation of a dense layered extracellular matrix that adheres tightly to cell surfaces.

1.1.4 Role in normal physiology and disease

Basement membrane components have been implicated in a wide range of diseases as causative or contributing factors. The importance of the basement membrane for the normal development and maintenance of tissue and cell function is thereby underlined by the disastrous consequences of its dysregulation. Interestingly, despite the association of the basement membrane with tissues throughout the body, the majority of mutations in individual components of this matrix often result in tissue specific pathologies. This further highlights the existence of tissue-specific basement membranes with different compositions and distinct functions.

A primary role of the basement membrane is as a physical barrier and selective permeability filter to enable homeostatic control by regulating the cellular microrenvironment. In many basement membrane diseases this barrier function is subverted or destroyed. For example, Alport syndrome is a genetic disorder characterised by renal dysfunction, progressive sensorineural hearing loss and visual abnormalities (Hudson et al., 1992; Kashtan, 2017). These symptoms are caused by missense or nonsense mutations in the genes for type IV collagen α chains, which results in reduced expression of mutated α chains, altered composition of the basement membranes in the kidney, cochlea and visual system, and a subsequent increase in their susceptibility to proteolytic degradation (Hudson et al., 1992; Zeisberg et al., 2006). This degradation compromises the integrity of the basement membrane in the organs expressing the affected α chain. Thinning of the glomerular basement membrane in the kidney leads to proteinuria and progressive renal failure (Savige, 2014; Zeisberg et al., 2006). In the cochlea, insufficient adhesion between the tissues and affected basement membrane result in separation of the organ of Corti from the basilar membrane, which impairs the transmission of sound to the cochlear nerve (Ungar et al., 2018).

Goodpasture’s syndrome is another disease of the basement membrane affecting the kidney, and results in progressive nephritis and pulmonary haemorrhage, due to the impaired structural integrity of the basement membrane (Pedchenko et al., 2011). This syndrome is an autoimmune disease, where autoantibodies against the type IV collagen α3 chain are produced and target the

basement membranes of specific organs for cellular attack (Lerner et al., 1967; Turner et al., 1992).

The particular ultrafiltration requirements of the lungs and kidney mean that the basement membranes in these tissues are particularly susceptible to perturbations in their composition. However, other tissues, such as those of the central nervous system (CNS) and musculoskeletal system, can also be dramatically affected. The basement membrane is crucial to tissue patterning during development of the CNS as well as playing an important role in the homeostasis of mature organs. Familial porencephaly is a devastating rare neurological disease affecting neonates, which involves the development of fluid-filled cavities in the cerebral hemisphere. Infants present with a range of clinical symptoms such as macrocephaly, developmental delay, seizures, spastic hemiplegia and speech impairments. Mutations in the gene for collagen IV α1 chain are strongly associated with the development of familial porencephaly and are believed to cause cerebral haemorrhages and degeneration during brain development and parturition due to loss of the CNS vasculature resistance to mechanical stresses (Gould et al., 2005; van der Knaap et al., 2006).

Mutations in a number of extracellular matrix components are associated with congenital muscular dystrophies. Dominant and recessive autosomal mutations in the collagen VI genes lead to a clinical spectrum of myopathies presenting with muscle weakness and joint laxity (reviewed in Bönnemann, 2011). Merosin-deficient congenital muscular dystrophy type 1A (MDC1A) occurs as a result of mutations in the *LAMA2* gene which encodes the laminin-α2 chain protein (Helbling-Leclerc et al., 1995; Tomé et al., 1994). This leads to severe inflammation, fibrosis and degeneration of muscle tissue, with patients often dying in their early teenage years due to respiratory failure (Lisi and Cohn, 2007). Several mouse models of MDC1A exist. *DyW* mice lack *Lama2* gene function due to insertion of a β-galactosidase gene and neomycin resistance cassette downstream of the α2 chain start codon (Kuang et al., 1998). The *dy/dy* and *dy^{2J}* mice are spontaneously occurring mutants that either lack laminin-α2 expression completely or express a truncated and partially functional variant respectively (Meier and Southard, 1970; Michelson et al., 1955). The early muscle fibre necrosis and tissue fibrosis observed in patients with MDC1A, as well as mouse models of the disease (*DyW* and *dy/dy* mice), demonstrate a critical role for

laminin-α2 in myogenesis and the preservation of muscle tissue integrity (Mehuron et al., 2014). Composition and organisation of the basement membrane at specific loci has important implications for tissue function. In skeletal muscle, the basement membrane associated with the sarcolemma of myofibres is vital for linking adjacent fibres and thereby for the generation of coordinated contractile force (Sanes, 2003). This linkage involves the Z-line associated costameres; rectilinear concentrations of sarcolemmal surface receptors, such as integrins and α-dystroglycan, as well as cytoskeletal components, such as vinculin and talin (Peter et al., 2011). The basement membrane components laminin-α2, type IV collagen, perlecan and nidogens are enriched at costameres, but this lattice-like distribution becomes disorganised in the *dy^{2J}* mouse model of MDC1A from 6.5 weeks of age (Yurchenco et al., 2004). This suggests an important role for laminin-α2 in maintenance of costameric structures and therefore efficient muscle force transduction, which is supported by the severe muscle weakness displayed by MDC1A patients and mouse models.

Schwartz-Jampel syndrome (SJS), or chondrodystrophic myotonia, is another neuromuscular disease resulting from dysregulation of basement membrane components. This autosomal recessive disease is caused by hypomorphic mutations in the *HSPG2* gene encoding perlecan, which result in reduced secretion of the extracellular protein (Arikawa-Hirasawa et al., 2002; Nicole et al., 2000; Stum et al., 2006). SJS patients display muscle stiffness with short stature, skeletal abnormalities and a characteristic fixed facial expression due to reduced facial mobility as a result of loss of perlecan function (Arikawa-Hirasawa et al., 2002; Mallineni et al., 2012). Independent evidence gleaned from a mouse model of SJS and a human patient indicates that perlecan mutations may lead to peripheral nerve hyperexcitability and defective presynaptic maintenance of the NMJ (Bangratz et al., 2012; Bauché et al., 2013). These data suggest an important role for perlecan in sustaining contact between nerve terminals and postsynaptic muscle in addition to organising myelinating Schwann cells along peripheral nerves.

1.1.5 Pathogens and the basement membrane

While internal dysregulation of basement membrane components is one mechanism of disease, external pathogens can also target these extracellular

molecules to gain a foothold within the human body. The gastrointestinal tract is constantly exposed to substances from the external environment, and therefore has developed a range of innate defence mechanisms to protect it from pathogenic insults, including maintenance of an acidic environment, secretion of antimicrobial enzymes and active humoral and cellular immune systems (Pelaseyed et al., 2014; Sarker and Gyr, 1992). In the event that pathogens manage to overcome these defences, there remains a constant shedding of the epithelial lining of the gastrointestinal lumen to reduce the likelihood of colonisation and propagation of infection into the blood circulation (Williams et al., 2015). However, certain bacterial strains have developed mechanisms to circumvent these obstacles. *Shigella* is a species of bacteria that causes dysentery and fever. Among other virulence factors, *Shigella* secretes OspE, which interacts with integrin-linked kinase to increase surface expression of β1 integrins and thereby maintain adhesion of epithelial cells to the basement membrane (Kim et al., 2009; Miura et al., 2006). This in turn promotes retention of the infected epithelium allowing efficient replication and spread of the bacterium.

Panton-Valentine leucocidin (PVL)-positive *Staphylococcus aureus* (PPSA) strains are a causative agent of severe necrotising pneumonia, which is characterised by fever, acute respiratory distress and high mortality (Gillet et al., 2002). The symptoms of PPSA infection are much more severe than those of PVL-negative (PNSA) strains. Interestingly PPSA strains were found to associate with exposed regions of the basement membrane in necrotic lesions in lung tissue and displayed a greater affinity for laminins and collagens I and IV than PNSA strains (de Bentzmann et al., 2004). This opportunistic adherence to damaged epithelium thereby facilitates bacterial colonisation and increased virulence.

In another example of pathogens taking advantage of basement membrane components to gain entry to the body, nidogens were found to facilitate the onset of spastic paralysis upon intoxication with the tetanus neurotoxin (TeNT; Bercsenyi et al., 2014). TeNT binds to neuromuscular junctions and is internalised into motor neuron terminals before being trafficked to the spinal cord where it blocks inhibitory neurotransmission to induce paralysis (Deinhardt et al., 2006). TeNT is able to bind to nidogens, which are subsequently internalised by motor neurons along with the neurotoxin (Bercsenyi et al., 2014). The authors

showed that this interaction between TeNT and nidogens was an important rate limiting step in tetanus pathology as blocking the interaction ameliorated the reduction in muscle force observed and delayed the onset of paralysis in mice injected with the full-length toxin. Basement membrane components have therefore become targeted by pathogens to subvert host organism defences.

Taken together, these examples from the literature and clinic show the critical roles of basement membranes in the maintenance of normal tissue physiology. The importance of tissue-specific function and distribution of basement membrane components is revealed by the effects of mutations or downregulation of these proteins on certain organs. However, the specific signalling roles of basement membrane proteins in different tissues and cells are still being discovered.

1.1.6 Passive matrix or signalling platform?

In the last decade, significant progress has been made in our understanding of the basement membrane as more than simply a passive supportive matrix. Accumulating evidence shows the importance of basement membranes in essential signalling processes that underlie the development and patterning of tissues, as well as the maintenance of cellular function and response to injury and disease. Basement membranes are crucial for cell polarity and the determination of tissue size and shape (reviewed in Morrissey and Sherwood, 2015). The mechanisms by which basement membrane components are involved in homeostatic and responsive processes are still being uncovered, but their participation in growth factor signalling appears to be a key pathway for modulating cell behaviour (Ruoslahti and Yamaguchi, 1991).

Growth factors are soluble, secreted proteins that are important for cell growth, differentiation, survival, maintenance and migration. Several different mechanisms by which extracellular matrix interactions modulate growth factor signalling have been described. These mechanisms reveal diverse roles such promotion of growth factor receptor complexes, sequestration of growth factors, and establishment of developmental gradients.

Basement membranes can act as a reservoir for growth factors and have been described as ‘solid-phase agonists’, referring to their ability to act as a mediator of molecular signalling (Trelstad, 1988). In some cases, basement membrane

components interact with growth factors to sequester the active molecules and prevent downstream signalling, while in other scenarios the interaction serves to concentrate the molecules at physiologically relevant sites.

The affinity of growth factors for the basement membrane components and the strength of their binding to this matrix can regulate their diffusion through the extracellular space. This can facilitate the formation of growth factor signalling gradients, which are extremely important in development and repair of tissue after injury.

There are 22 members of the fibroblast growth factor (FGF) family in mammals, which regulate proliferation, differentiation and migration of cells during tissue remodelling (Ornitz and Itoh, 2016). FGFs can be categorised into three main groups according to their diffusion characteristics; intracrine, hormonal, and paracrine (Beenken and Mohammadi, 2009). Intracrine FGFs are cytosolic proteins and do not signal via the FGF receptor (FGFR). Hormonal and paracrine FGFs diffuse away from their secretory cells to varying extents based on their affinities for heparins within the extracellular space. While hormonal FGFs have relatively weak affinities and are able to diffuse large distances within the bloodstream, paracrine FGFs have moderate to strong interactions and are therefore retained in closer proximity to their site of secretion via association with the basement membrane (Folkman et al., 1988). Indeed, this has been shown for two members of the FGF family, FGF-7 and FGF-10, which possess different morphogenetic properties as a result of their different binding affinities for HSPG and their subsequent dissimilar diffusion gradients (Makarenkova et al., 2009).

Another example includes Decapentaplegic (Dpp), a bone morphogenic protein (BMP) growth factor of the transforming growth factor (TGF)-β superfamily, which acts as a critical regulator of cell fate and tissue patterning in *Drosophila* (Podos and Ferguson, 1999). Type IV collagens have been shown to interact with Dpp in *Drosophila*, and mediate both the establishment of the growth factor gradient by limiting its diffusion, and its downstream signalling via promotion of Dpp receptor complex formation (Wang et al., 2008). The basement membrane thereby acts as a critical regulator of growth factor gradient profiles, and alterations to binding affinities of growth factors or the distribution of extracellular interaction partners can have dramatic effects on the morphological development of cells and tissues.

Release of growth factors from the basement membrane is just as important as their adhesion to this matrix. Downstream signalling pathways can require the internalisation of growth factors along with their cell surface receptors to initiate certain cascades, which means that the growth factors must be released from the basement membrane. Degradation of HSPGs by extracellular proteases has been shown to liberate FGF from the basement membrane as a soluble factor, thereby allowing temporal control of the released signalling potential from the basement membrane (Saksela and Rifkin, 1990; Vlodavsky et al., 1987). However, degradation of HSPGs does not completely free FGF, just mobilises it. FGF released from the basement membrane can still be bound to heparin, and formation of the active FGF signalling complex with its receptor and its biological activity is greatly enhanced by interaction of both the ligand and receptor with HSPGs (Schlessinger et al., 2000; Yayon et al., 1991). Activation of FGFRs involves their dimerisation within the plasma membrane and subsequent cross-phosphorylation via their intracellular tyrosine kinase domains (Bellot et al., 1991). Resolution of the crystal structure of active FGFR1 dimers revealed that heparin binds to two FGF1 ligands and the FGFR1, thereby forming a ternary complex which facilitates the assembly of an active signalling complex (Pellegrini et al., 2000). Heparin therefore acts as an important modulator of FGF signalling via its actions as a cofactor for receptor transduction and as a molecular reservoir. Indeed, engineering of growth factors, such as vascular endothelial growth factor (VEGF), bone morphogenic protein (BMP) and platelet derived growth factor (PDGF), with enhanced affinity to the basement membrane has been shown to amplify their effects on wound healing (Martino et al., 2014). However, it was not shown whether this was due to the matrix acting as a coreceptor, as for FGF signalling, or if simply a greater retention at the wound site promoted local activity.

Binding to the basement membrane does not always mean that growth factor participation in signalling is restricted. Instead of sequestering growth factors for release and temporal control of signalling initiation, contact with the basement membrane can direct signalling to an alternative route. VEGF-A is a potent growth factor responsible for initiation and patterning of neovasculature in angiogenesis (Takahashi and Shibuya, 2005). While cleavage events mediated by matrix metalloproteases can regulate the bioavailability of VEGF, it has also been shown that soluble VEGF-A or a matrix-bound form influence the downstream signalling

cascades to result in different morphogenic signals (Chen et al., 2010; Lee et al., 2005). Pleiotropic growth factors can therefore be directed towards certain pathways as a result of the context of their presentation, where interactions with basement membrane components can play a key role.

These studies show that the basement membrane is an important modulatory platform, responsible for the efficient signal transduction and tight spatial control of growth factor signalling during development. Since different basement membrane components interact with distinct growth factors and bioactive molecules, the site-specific composition of this extracellular matrix confers unique functional properties.

1.1.7 Specialisation at the neuromuscular junction

The basement membrane in skeletal muscle surrounds the individual muscle fibres in addition to its association with endothelial tissue and innervating nerves. The basement membrane is also present at the NMJ where it lies between the motor neuron terminal and the muscle end plate (Sanes, 2003). It is involved in the adhesion of the terminal to the post-synaptic membrane, as evidenced by the loss of pre- and post-synaptic apposition under treatment with basement membrane-specific proteases (Betz and Sakmann, 1973). The basement membrane at this site does not interfere with efficient neuronal signal transduction as it allows neurotransmitters to permeate the synaptic cleft (Land et al., 1984). In fact, specific actions of the extracellular components enhance the efficiency of neurotransmission. For example, acetylcholine esterase (AChE) is tethered to the basement membrane at the NMJ (McMahan et al., 1978). The tethering action appears to be mediated by perlecan and optimises the efficient termination, and therefore temporal control, of ACh-mediated neurotransmission at the NMJ by precisely localising the degrading enzyme to the relevant sites (Arikawa-Hirasawa et al., 2002).

Basement membrane components may be responsible for localising more than just enzymes to the NMJ. Notably, upon denervation, innervating axons are able to reinnervate precise synaptic sites, targeting the post-synaptic compartments within sub-micron accuracy (Nguyen et al., 2002). While this represents regrowth along the nerve basement membrane and Schwann cell channels, it also suggests specific attracting guidance molecules present on the post-synaptic membrane that refine targeting. Indeed, studies have revealed the existence of

several synapse-specific basement membrane components, such as laminin and collagen isoforms, which as previously discussed, cause neuromuscular disease when mutated (Patton, 2000; Sanes et al., 1990). In addition to targeting roles, basement membrane components also seem to be necessary for the maturation of synaptic specialisations. Active zones in pre-synaptic terminals at the NMJ fail to form in mice lacking laminin-β2, which is enriched at this type of synapse, and these mice have severe neuromuscular defects resulting in early lethality (Noakes et al., 1995). Voltage-gated calcium channels at the NMJ bind to laminin-β2, and mediate the anchorage of essential presynaptic active zone components, such as Bassoon and Piccolo, to this site (Chen et al., 2011). The essential role of laminin-β2 in maintenance of efficient NMJs is underlined by the severe congenital myasthenic syndrome caused by truncation mutations of this basement membrane component (Maselli et al., 2009).

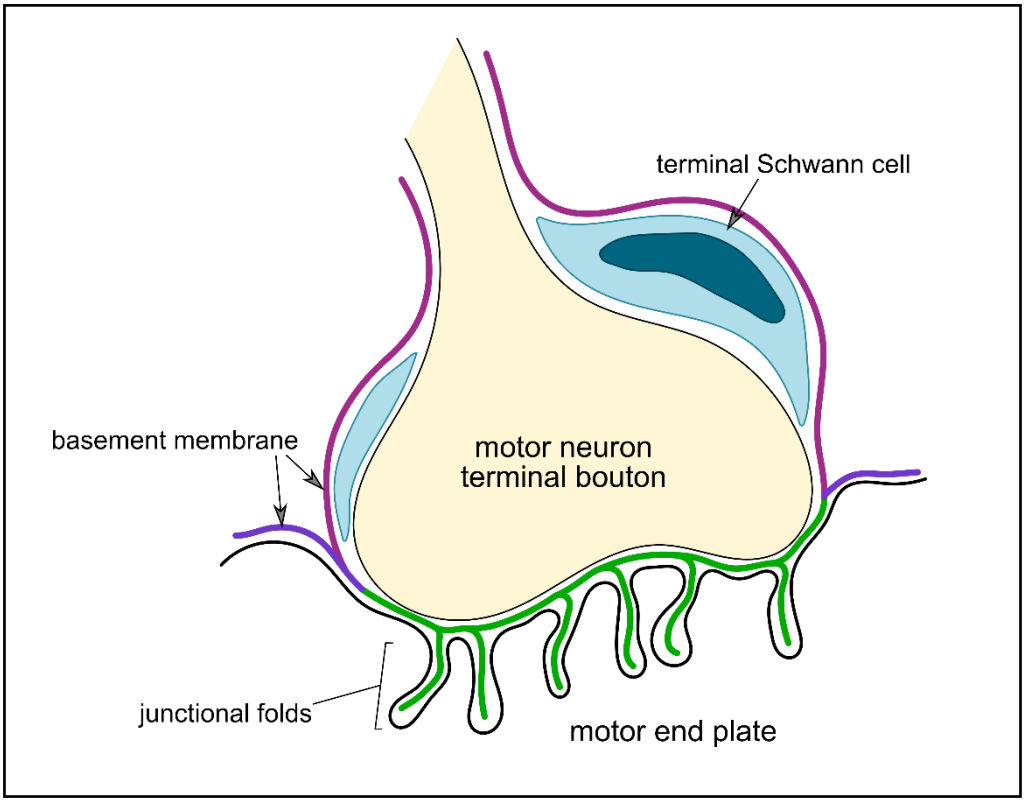

Figure 1.2 Basement membrane at the neuromuscular junction

The basement membrane is present within the synaptic cleft between motor neuron terminal boutons and the motor end plate (green), at extrasynaptic sites on the muscle sarcolemma (purple) and surrounding the Schwann cells and axon (pink). Adapted from Sanes, 2003.

As previously mentioned, there are number of different isoforms of agrin. The inclusion of amino acids at the Z splice site confers significant AChR-clustering activity, which is a vital stage in the initial formation of distinct NMJs. Interestingly, agrin is not just expressed at the NMJ, but is found throughout the sarcolemma of the muscle, as well as widely distributed in the CNS. However, the expression profiles of the specific isoforms vary. While the NMJ presents Z^+ agrin secreted by the motor neuron terminals, the myofibres secrete Z^- agrin, which displays reduced AChR clustering activity but is important in maintaining the connections between myofibres and the basement membrane through its interactions with the dystrophin glycoprotein complex (Gesemann, 1995). These data emphasise the importance of site-specific basement membrane components or variants.

However, while our understanding of the development and maintenance of the mammalian NMJ has been significantly increased in recent years, there is still progress to be made in identifying modulatory synapse specific components.

1.2 The Nidogen Family

Nidogens, also known as entactins, are a family of secreted glycoproteins. There are two nidogen isoforms in vertebrates; nidogen-1 and nidogen-2, in contrast to the single nidogen found in invertebrates (Carlin et al., 1981). The vertebrate nidogen genes (*NID1* and *NID2*) are located on different chromosomes and share only 46% sequence identity (Kohfeldt et al., 1998). However, sequence predictions, confirmed by electron microscopy and rotary shadowing experiments on the recombinant proteins, have indicated that both nidogens consist of three globular domains (G1-3; Durkin et al., 1988; Kohfeldt et al., 1998). G1 and G2 are located at the N-terminal region and are connected by a flexible linker domain, while the C-terminal G3 domain is connected to G2 via a rod-like domain (Figure 1.3; Fox et al., 1991; Kohfeldt et al., 1998).

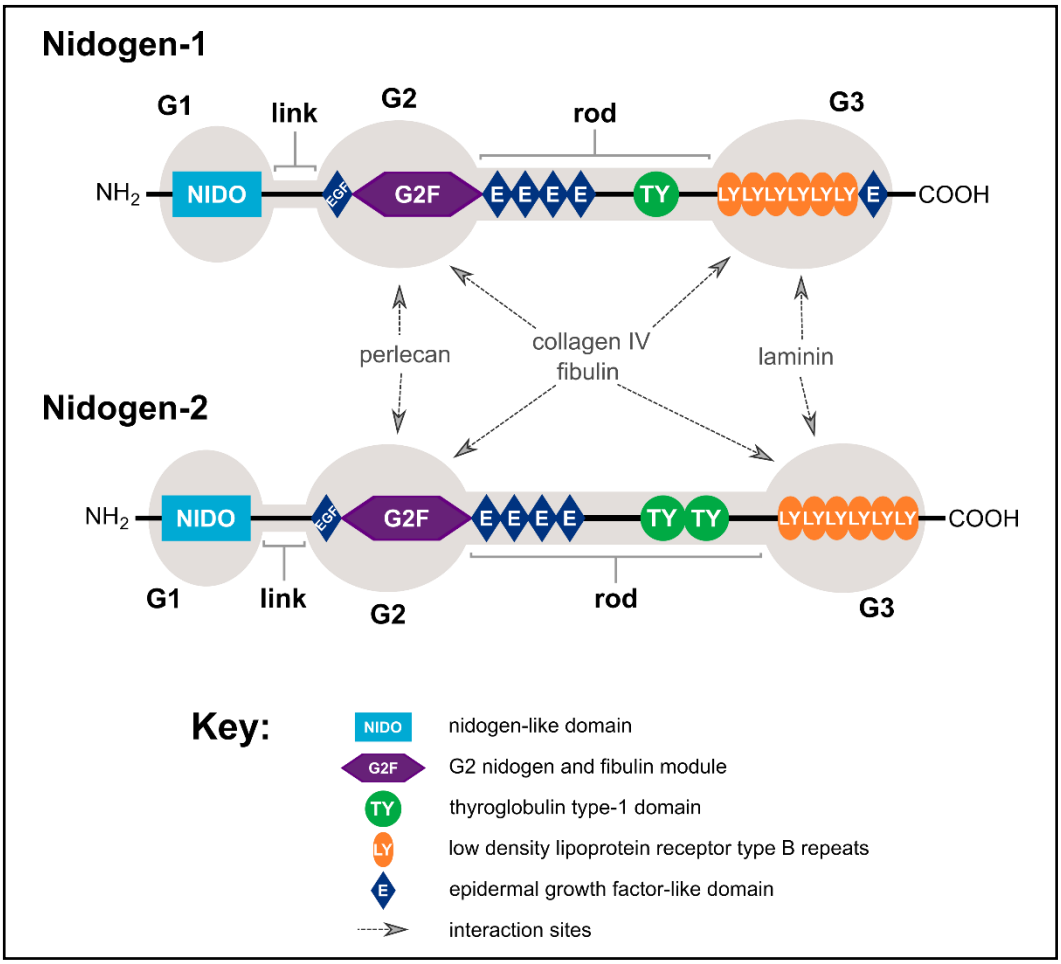

Figure 1.3 Domain structure of nidogen-1 and nidogen-2

Nidogen-1 and nidogen-2 share a similar structure of three globular domains (G1-3) joined by a short flexible link region and a rod domain. The G2 domain binds to basement membrane components perlecan, collagen IV and fibulin. G3 also harbours binding sites for collagen IV and fibulin as well as laminin. The function of the NIDO domain remains unclear.

Nidogens have been shown to form stable complexes with other components of the basement membrane, such as type IV collagen and laminin (Aumailley et al., 1989; Dziadek et al., 1985). The G2 domain of nidogens is responsible for binding to collagen IV and the HSPG perlecan (Hopf et al., 2001, 1999; Ries et al., 2001). The C-terminal G3 domain of nidogens binds to the short arm of the laminin γ-chain (Ries et al., 2001). As these interactions occur via different binding sites on nidogens, these globular proteins can form ternary complexes within the basement membrane, indicating a role for nidogens in linking and stabilising these polymer networks during basement membrane formation and maintenance (Figure 1.3; Fox et al., 1991; Timpl and Brown, 1996). While the binding affinities of the two nidogens for collagen IV and fibulin are comparable, nidogen-2

displays lower affinities for perlecan and laminin than nidogen-1 (Kohfeldt et al., 1998; Miosge et al., 2002; Salmivirta et al., 2002; Sasaki et al., 1995). The similar binding profiles of the two nidogens suggests that they may be able to functionally compensate for one another.

The majority of the evidence for the interactions of nidogens has come from *in vitro* studies and suggests a crucial role for nidogen in the development and maintenance of basement membranes throughout the body. However, generation of single knock-out (KO) models yielded viable and fertile animals with overtly normal basement membranes (Murshed et al., 2000; Schymeinsky et al., 2002). As previously mentioned, the overlapping expression patterns and binding repertoires of the two nidogens could represent a redundancy in the system, explaining why the knock-out of the single genes fails to result in an overt phenotype. Consistent with this hypothesis, lack of both nidogens results in embryonic lethality due to major defects in lung and cardiac development (Bader et al., 2005). Interestingly, even in these mice, the basement membrane abnormalities are restricted to a few tissues and most basement membranes appear ultrastructurally normal. This suggests that nidogens may have tissue-specific, non-structural roles, which may include intracellular signalling pathways.

1.2.1 A non-structural role for nidogens

In light of the strong and specific interactions of nidogens with components of the basement membrane, it was surprising that animal models lacking single nidogen isoforms were apparently unaffected. However, upon closer examination, subtle phenotypes have emerged. Despite an earlier nidogen-1 KO mouse model showing no anatomical or phenotypical abnormalities (Murshed et al., 2000), an alternative mouse generated by targeting a different exon resulted in the development of neurological phenotypes including seizure-like activity and temporary hind limb paralysis, despite intact NMJs (Dong et al., 2002). Further investigation revealed epileptiform activity in the hippocampus of mutant animals despite an absence of gross morphological anomalies (Köhling et al., 2006; Vasudevan et al., 2010). Murshed and colleagues generated their nidogen-1 knock out model by excising exon 3 from the *Nid1* gene via loxP recombination. Dong and colleagues used a targeting vector insertion strategy to delete exon 1, translation initiation sites and part of the promoter region of *Nid1*. While the groups used different strategies to mutate the *Nid1* gene, both reported complete

ablation of mRNA and protein levels of nidogen-1, so it is unclear why the neurological phenotype was not observed in both studies. However, these conflicting results demonstrate a need for further investigation into the role of nidogen-1 and suggest a potential role for this protein in regulation of neuronal excitability and plasticity.

In a nidogen-2 KO mouse model, Fox and colleagues found topological changes at the NMJ despite the lack of a detectable neuromuscular phenotype (Fox et al., 2008). This abnormal topology included fragmented distributions of acetylcholine receptors (AChRs), which appeared in more mature mice, suggesting a deficit with the maintenance rather than a developmental impairment. Even with these topological alterations, the pre- and post-synaptic elements remained precisely apposed at the NMJ and no muscle fibre degeneration was observed. This suggests that nidogen-2 could play a role in maintenance of receptor positioning at this peripheral synapse, for which nidogen-1 cannot compensate.

Further evidence indicating a synaptic role for nidogens was found in a *C. elegans nid1* KO model. In contrast to the mouse models, this mutant did show mislocalisation of pre- and post-synaptic markers along the dorsal and ventral nerve cords, along with altered synaptic transmission and pathological motor phenotypes (Ackley et al., 2003). The more severe phenotype observed in *C. elegans* mutants may result from the presence of a single nidogen gene in this species, and therefore a lack of compensation. Several studies also showed mispositioning of axons in *C. elegans nid1* KO mutants as a result of inappropriate crossing of the ventral midline and incorporation into the left instead of the right axon tract (Bhat and Hutter, 2016; Kim and Wadsworth, 2000). These studies reveal a likely role for nidogen-1 in targeting of axons during development and establishment of efficient synaptic connections. Whether this is an active signalling role, or as a permissive directional cue remains to be seen.

Recent work from our laboratory has also suggested a role for nidogens at the mammalian NMJ. As previously mentioned, nidogens were shown to be necessary for the binding of the TeNT to the NMJ and its subsequent toxicity (Bercsenyi et al., 2014). Co-administration *in vivo* of a nidogen peptide with the full-length neurotoxin significantly ameliorated the reduction in muscle force produced by TeNT intoxication alone. This indicated that TeNT gained entry to motor neurons via a nidogen-dependent route. Nidogens were shown to be

internalised into motor neurons along with the binding fragment of the TeNT (Bercsenyi et al., 2014). This suggests the presence of an endogenous signalling pathway involving the mobilisation of nidogens from the basement membrane and its subsequent entry to neurons in signalling endosomes (Schmieg et al., 2014). The nature of this pathway remains unclear.

1.2.2 Implications for nidogens in development and disease

The two nidogen isoforms appear to have mainly overlapping expression patterns throughout the basement membranes of mammalian tissues, particularly during embryogenesis (Salmivirta et al., 2002). However, the concentrations of nidogen-2 were found to be dramatically lower than those of nidogen-1 in adult tissues. This was particularly striking in skeletal muscle, where nidogen-2 equalled only 2.8% of the concentration of nidogen-1 (Salmivirta et al., 2002). Indeed, in skeletal and cardiac muscle, differences in the localisation of the two nidogens have been observed. While nidogen-1 was found to be ubiquitously expressed throughout the basement membranes surrounding blood vessels, nerves, cardiocytes and myotubes, nidogen-2 appeared mainly restricted to the nerves and vasculature in these tissues (Kohfeldt et al., 1998). A subsequent investigation revealed that in cross-sections of muscle, nidogen-2 was enriched at sites colocalising with α-bungarotoxin, a marker of the post-synaptic AChRs (Fox et al., 2008). Interestingly, at birth and in the first postnatal week nidogen-2 was present throughout the extrasynaptic basement membrane but became restricted to NMJs by postnatal day (PND) 21. In nidogen-2 knock out mutants, no NMJ abnormalities were observed in the first three postnatal weeks, but in adult mice the synapses appeared fragmented (Fox et al., 2008). This suggests that, while nidogen-2 may not be necessary for the initial stages of synapse formation, it is an essential component of the machinery that develops or stabilises the mature organisation of the mammalian NMJ.

As previously discussed, mutations in several extracellular matrix proteins have been reported to cause human neuromuscular disease. Recently, mutations in nidogen genes have also been identified in human diseases with a neurological spectrum of phenotypes. *NID1* was identified as a candidate gene in a family with hydrocephalus, muscle weakness and global developmental delay during whole-exome sequencing of consanguineous families with neurogenetic diagnoses (Alazami et al., 2015). Another study reported a nonsense mutation in the *NID1*

gene in a family with Dandy-Walker malformation, a disease characterised by abnormal development of the cerebellum (Darbro et al., 2013). Although functional validation of these mutations is lacking, taken together with data from animal knock out mutants, these data suggest a possible signalling role for nidogens in the neuromuscular system.

1.3 Project Aims

As discussed above, there is increasing evidence that nidogens are not merely structural proteins of the basement membrane, but are involved in signalling processes underlying neurological function. While interactions of nidogens with other components of the basement membrane have been identified and mapped to specific domains, the involvement of these extracellular glycoproteins in intracellular signalling pathways remains unexplained. It is possible that, in a similar mechanism to the HSPGs, nidogens may sequester growth factors via specific interactions and cleavage events may release them for internalisation. It may be that nidogens themselves are able to act upon cell surface receptors directly. It is interesting that the binding fragment of the tetanus neurotoxin (HcT) was shown to be internalised into motor neuron terminals at the NMJ along with nidogens (Bercsenyi et al., 2014). This argues the existence of an endogenous signalling pathway which involves nidogen uptake by motor neurons. My project therefore aimed to uncover novel interactors and signalling mechanisms of nidogens at this crucial synapse to better understand the role of this relatively understudied basement membrane component.

To begin addressing this question, I aimed to investigate the expression pattern of the two nidogen isoforms, nidogen-1 and nidogen-2, in neuromuscular tissue. I decided to examine the expression across a range of skeletal muscles, to see if these displayed different profiles over maturation.

During disease states, differential regulation of protein expression can reveal specific functions of proteins in pathology or protection from damage. This can thereby shed light on the basal physiological roles of expressed factors. To get a clearer picture of the role of nidogens at the NMJ, I have examined the expression profiles of the two isoforms during disease progression in the $SOD1^{G93A}$ mouse model of amyotrophic lateral sclerosis (ALS), which shows presymptomatic motor neuron pathology and subsequent NMJ denervation.

As there have been conflicting reports of the phenotypes observed in nidogen-1 KO mice, there is a need to further examine the consequences of genetic ablation. To this end, I also investigated a novel nidogen-1 KO mouse model generated by collaborators at MRC Harwell. This model harbours a floxed *Nid1* allele and offers the potential to produce developmentally-regulated or tissue-specific conditional nidogen-1 KO mice.

Finally, as HcT has been shown to bind to nidogens, I decided to investigate known interactors of HcT as possibly endogenous binding partners of nidogens. Understanding the binding repertoire of nidogens should give a clearer picture of the role these proteins may play in signalling or targeting pathways at the NMJ.

By understanding the distribution of nidogens throughout the neuromuscular system, and identifying interactors, we can start to reveal how nidogens can provide more than just structural support to neurons and their synapses. This project could thereby lead to a greater understanding of the dynamic role of basement membrane components and uncover novel targets for therapeutic intervention in debilitating neuromuscular diseases.

Chapter 2. Methods

2.1 Mice

All experiments using animals were carried out under license from the UK Home Office in accordance with the Animals (Scientific Procedures) Act 1986 (Amended Regulations 2012). Biological replicates consisted of single tissues from different mice.

2.1.1 Wild-type C57BL/6J – SJL mixed background mice

C57BL/6 crossed with SJL-Elite strain to increase breeding capacity. Both genders were used in experiments.

C57BL/6 strain origin:

Developed by C.C. Little in 1921, from a mating of Miss Abby Lathrop's stock that also gave rise to strains C57BR and C57L. Strains 6 and 10 separated about 1937. Transfer to The Jackson Laboratory in 1948 from Hall. To NIH in 1951 from The Jackson Laboratory at F32. To Charles River in 1974 from NIH Laboratory at F32. To Charles River in 1974 from NIH.

SJL-Elite strain origin:

Selected by James Lambert in 1955 from 3 different strains of Swiss Webster brought to Jackson Laboratory between 1938 and 1943. This strain was introduced to CNRS-CSEAL, Orleans, France, in 1978, and acquired by IFFA CREDO in 1990 at the 114th generation. To Charles River in 1997.

2.1.2 Nidogen-1 conditional knock out mice

Nidogen-1 conditional knock out mice were generated in collaboration with colleagues at the MRC Harwell Institute and International Mouse Phenotyping Consortium (IMPC), using a targeting vector from the European Mouse Mutant Cell Repository (EuMMCR) (Figure 2.1; Dickinson et al., 2016)). This vector flanks critical exons with loxP sites thereby conferring conditional potential. Mice expressing the reporter-tagged (β-galactosidase) insertion with conditional potential *(Nid1$^{tm1a(EUCOMM)Hmgu}$)* were crossed with mice expressing Cre recombinase under the ubiquitous actin promoter, resulting in deletion of the *neo* cassette and exons 2 and 3 of the *Nid1* gene. Deletion of these critical exons and the upstream polyadenylation sequence results in a global knock out for *Nid1*

expression. Heterozygous and homozygous mice of both genders were investigated.

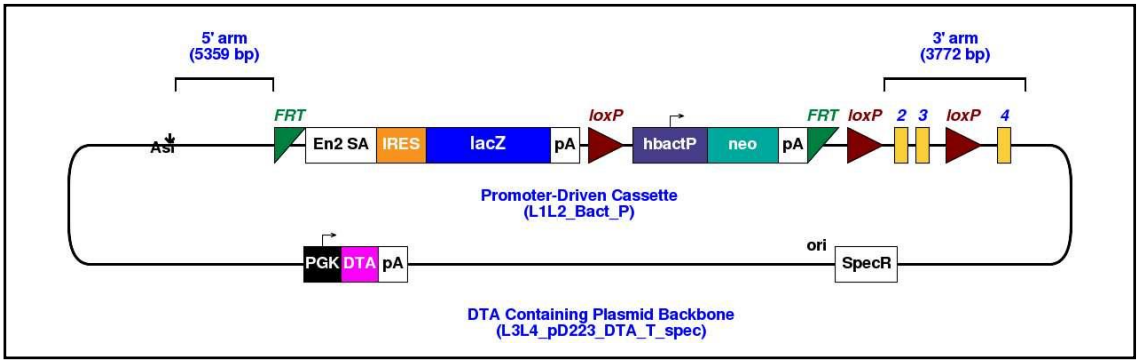

Figure 2.1 Nid1 promoter-driven targeting vector

Vector contains a reading frame-independent LacZ gene trap cassette consisting of an En2 splice acceptor site (En2-SA), internal ribosome entry site (IRES), *lacZ* gene, and polyadenylation signal (pA). Downstream is a neomycin resistance cassette containing the *neo* gene, driven by the human β-actin promoter, with a second pA site. These two selection cassettes are flanked by flippase (Flp) recombinase target (FRT) sequences to allow excision via Flp-FRT site-specific recombination. The *neo* cassette is also flanked separately by loxP sites, as are the critical exons 2 and 3 from the *Nid1* gene. Cre-mediated recombination thereby excises both the *neo* cassette and exons 2 and 3, resulting in gene knock out. Figure from International Mouse Phenotyping Consortium with permission (http://www.mousephenotype.org/).

2.1.3 SOD1^{G93A} C57BL/6J - SJL transgenic mice

Transgenic mice hemizygous for an inserted mutant human *SOD1* gene (G93A) on a C56BL/6-SJL mixed background (B6SJL-Tg[SOD1^{G93A}]1Gur/J) were acquired from The Jackson Laboratory. Hemizygous males were mated with wild-type C56BL/6-SJL F1 generation females to obtain experimental colonies. Mouse genotypes were confirmed using DNA extracted from ear biopsies and PCR amplification of the human *SOD1* transgene as described below. Only female SOD1^{G93A} and age-matched wild type littermates were used.

2.1.4 SOD1^{G93A} Genotyping

PCRs used two sets of primer pairs to amplify the human *SOD1* transgene and an internal positive control gene. Primer pair IMR0042 and IMR0043 amplified the control gene fragment (324 bp) while primer pair IMR0113 and IMR0114 amplified the transgene fragment (236 bp).

Primer sequences:

Primer *IMR0042* 5'- CTA GGC CAC AGA ATT GAA AGA TCT -3'

Primer *IMR0043* 5'- GTA GGT GGA AAT TCT AGC ATC ATC -3'

Primer *IMR0113* 5'- CAT CAG CCC TAA TCC ATC TGA -3'

Primer *IMR0114* 5'- CGC GAC TAA CAA TCA AAG TGA -3'

For crude DNA extraction, ear biopsies were incubated with 120 µl DirectPCR Lysis Reagent (Viagen, 102-T) plus 0.1 mg/ml Proteinase K (Sigma, P2308) at 55°C on a shaking block (800 rpm) overnight. Reactions were stopped by incubation at 85°C for 30 minutes.

PCRs comprised 1 µl extracted DNA, 0.125 µl of each primer (final concentration of 0.5 µM), 15 µl of a ready to use PCR mix containing Taq polymerase in 1.1x reaction buffer (2.75 mM $MgCl_2$) with 220 µM dNTPs and blue agarose loading dye (MegaMix Blue 2MMB, Microzone), and 8.5 µl nuclease-free H_2O to make 25 µl reaction volumes.

PCR conditions:

1. Initial denaturation 95°C (3 minutes)
2. Denaturation 95°C (30 seconds)
3. Annealing 60°C (30 seconds)
4. Extension 72°C (45 seconds)
5. Final extension 72°C (2 minutes)
6. Maintain at 4°C

Steps 2-4 were repeated for 35 cycles.

Amplified PCR samples were separated at 50 V for 45 minutes on a 1.5% agarose-Tris-borate-EDTA (TBE) gel containing ethidium bromide.

2.2 Tissue Dissection

Prior to dissection, mice were euthanized by intraperitoneal injection of a lethal overdose (>150 mg/kg) of sodium pentobarbital (Euthatal, Merial).

1.1.1 Sciatic nerve dissection

The overlying fur and skin were removed from the hindlimb and lower back of the mouse. The mouse was pinned out in supine position and the thigh muscles were

removed by blunt dissection along the inter-muscular fascia to expose the sciatic nerve underneath. The connective tissue surrounding the nerve was blunt dissected to release the nerve before removal. The sciatic was cut proximally at the level of the sciatic foramen, and distally just after the nerve branches into the sural, common peroneal and tibial nerves – at the popliteal fossa. The nerve segment was then pinned to a silicone mount to maintain the nerve in a straight orientation at a slight stretch for fixation. The nerve was immersed in 4% paraformaldehyde (PFA) in phosphate buffered saline (PBS, see Section 2.8) and incubated at 4°C for 1 hour before transfer to a solution of 20% sucrose in PBS to cryoprotect the tissue overnight at 4°C. To freeze, the nerve was embedded in OCT freezing compound (TissueTek®) in aluminium foil moulds. These moulds were then frozen on dry ice and kept at -20°C for short-term or -80°C for long-term storage before cryosectioning (see Section 2.3).

2.2.1 Hindlimb muscle dissection

The mouse was prepared and pinned as for sciatic dissection. To remove the posterior hindlimb muscles (gastrocnemius, GC, and soleus, SOL) the calcaneal tendon was grasped and severed to release the distal ends of the GC and the SOL. The connective tissue overlying the muscles was blunt dissected away to release them from the leg. The calcaneal tendon was used to pull the muscles up towards the knee until the proximal SOL tendon was visible. This was severed and used to isolate the SOL from the GC. The distal tendons were separated to completely release the SOL. The GC was cut at the knee to release it for removal. The mouse was turned over and pinned out again to access the anterior hindlimb muscles (tibialis anterior, TA, and extensor digitorum longus, EDL). The distal tendon of the TA was identified at the ankle, isolated and severed. This was then used to gently pull back the TA towards the knee, blunt dissecting the overlying fascia from either side of the muscle to release it from the leg. The proximal TA was cut at the point of insertion into the knee. The distal tendon of the EDL was identified, severed and used to pull it away from the leg as for the TA. The EDL was removed by cutting the proximal tendon.

Muscles were collected for sectioning or for tissue lysis for western blotting. All muscles for sectioning were immersed in OCT and allowed to equilibrate briefly before mounting onto a cork disc and submerging in isopentane chilled with liquid nitrogen. These were then stored at -80°C until sectioning (see Section 2.3).

Muscles for tissue lysates were placed into Eppendorfs, snap frozen in liquid nitrogen immediately upon sampling and stored at -20°C for a brief time before lysis (see Section 2.5.1).

Lumbrical muscles were dissected from adult wild-type mice as described previously (Sleigh et al., 2014).

2.2.2 Brain dissection

To begin extraction of the brain, the mouse was first decapitated. The overlying fur and skin were removed to expose the skull. A cut through the skull was made down the midline of the interparietal bone, and the two halves of the skull bones were prised away from the midline and broken off. This was continued rostrally until the brain was completely exposed. A small curved spatula was slid underneath the brain to sever the optical and cranial nerves before lifting the brain free of the skull. Brains were placed in Eppendorfs, immediately snap frozen in liquid nitrogen and stored at -20°C for a brief time before lysis (see Section 2.5.1).

2.2.3 Spinal cord dissection

The mouse was pinned out in supine position and fur and tissue overlying the spine was removed. A clean transverse cut through the whole spinal column was made at the base of the skull and a vertebral laminectomy performed to expose the spinal cord down to the sacrum. The spinal cord was then gently lifted out of the vertebral foramen, severing the nerve roots to release the cord completely.

For western blot samples, cords were placed in Eppendorfs, immediately snap frozen in liquid nitrogen and stored at -20°C for a short time before lysis. For spinal cord cryosections, cardiac perfusion fixation was performed prior to dissection. After lethal injection of sodium pentobarbital animals were perfused first with 20 ml PBS at rate of 2 ml/min, and then 20 ml of 4% PFA in PBS. Lumbar spinal cords were dissected as above and post-fixed by immersion in 4% PFA-PBS at 4°C for 24 hours. Samples were moved to 20% sucrose-PBS for cryoprotection for at least 24 hours before mounting in OCT compound and freezing on dry ice. Mounted samples were stored at -80°C until use.

2.3 Cryosection

All tissues to be cryosectioned were acclimatized to -16°C before being cut using a Bright cryostat to 10-30 µm thick sections. The sections were collected onto

poly-lysine-treated glass microscope slides and allowed to air-dry at room temperature for 2 hours before storage at -20°C until immunohistochemical staining was performed (see Section 2.6.2).

2.4 Cell Culture

2.4.1 Primary mixed ventral horn culture

Spinal cord ventral horn cultures were acquired from E12.5-13.5 embryos. Pregnant females were euthanized by intraperitoneal injection of a lethal overdose (>150 mg/kg) of sodium pentobarbital (Euthatal, Merial). The embryos were removed and placed into Hank's Balanced Salt Solution (HBSS, Gibco, 14175-053). Embryos were decapitated and the tails removed. The skin overlying the spine was removed with blunt dissection to expose the spinal cord. This was then separated from the underlying tissue, and the meninges removed. The spinal cord was flattened and the dorsal regions cut away to leave only the ventral spinal cord. This was then roughly chopped and added to 1 ml of HBSS with 0.025% trypsin (Gibco, 1509-046) for enzymatic digestion for 10 minutes at 37°C. Half-way (at 5 minutes) the spinal cord was mechanically dissociated by trituration with a 1 ml pipette. After trypsin incubation, the cords were mechanically dissociated further in decreasing concentrations of DNase: 1 ml Leibovitz's L-15 media + 0.4% bovine serum albumin (BSA) + 0.1 mg/ml DNase I (Thermo Scientific, 89836), then 1 ml Leibovitz's L-15 media + 0.4% bovine serum albumin (BSA) + 0.02 mg/ml DNase I. A BSA cushion of 4% BSA-L15 was gently applied to the bottom of the tube containing dissociated cord. The cells were centrifuged at room temperature for 5 minutes at 380 *g*. The supernatant was aspirated, and the cell pellet resuspended in primary motor neuron medium before seeding onto glass coverslips coated with poly-L-ornithine (15 µg/ml in sterile H_2O, 5 hours, Sigma, P4538) and laminin (3 µg/ml in Neurobasal, overnight, Sigma, L2020). Neuronal cultures were maintained in primary motor neuron medium (see Section 2.7) at 37°C, 5% CO_2 until experiments were performed between 5 and 7 days *in vitro* (DIV).

2.5 Western blotting

See Table 2.1 for solution recipes and Table 2.2 for antibodies used.

2.5.1 Sample preparation

Tissue samples were homogenised in chilled RIPA lysis buffer (see Section 2.8) on ice using an electrical homogeniser. Lysates were incubated on ice for 2 hours before centrifugation (14,000 *g*, 4°C) to pellet insoluble debris. The supernatant was collected and Laemmli 4x sample buffer (see Section 2.8) was added before denaturing at 95°C for 5 minutes.

Cell cultures were washed 3 times in cold PBS before adding chilled RIPA buffer to the culture plates on ice. Cells were scraped in the buffer and collected into Eppendorf tubes before incubating at 4°C for 1 hour on a rotating wheel. Samples were centrifuged, supernatants collected and denatured as for tissue samples above.

2.5.2 SDS-PAGE and western blotting

Samples were loaded into precast 4–15% Mini-PROTEAN™ TGX Stain-Free™ Protein Gels (BioRad) and electrophoresed at 100 V for 5 minutes and then 150 V for 45 minutes. Gels were activated for total protein content using the BioRad Stain-Free Technology prior to transfer onto polyvinylidene fluoride (PVDF) membrane using the Trans-Blot® Turbo™ Transfer System (Bio-Rad). PVDF membranes were blocked for 1 hour in TBS-T (see Section 2.8) with either 5% semi-skimmed milk or 5% BSA depending on primary antibody to be used. Membranes were then incubated overnight at 4°C with primary antibody diluted in blocking solution. The following day, the membranes were washed three times for 10 minutes with TBS-T before incubating in horseradish peroxidase (HRP)-conjugated secondary antibodies diluted in blocking solution for 1 hour. Membranes were washed 4 times for 10 minutes with TBS-T before imaging total protein. Chemiluminescence substrate was then added to the membranes and incubated for 1 minute at room temperature before imaging. Western blots were analysed using Image Lab™ Software 5.2.1 (BioRad). Protein bands were quantified using volume measurements (the sum of all intensities within the band boundaries) and were then normalised to total protein in each lane.

2.6 Immunocytochemistry and Immunohistochemistry

See Table 2.1 for solution recipes and Table 2.2 for antibodies used.

2.6.1 Cultured cells

Cells were fixed for 10 minutes at room temperature with 4% PFA-PBS prewarmed to 37°C. Cells were then washed 6 times in PBS before incubating in immunocytochemistry (ICC) blocking solution (see Section 2.8) for 15 minutes. Primary antibodies were diluted in blocking solution and incubated for 1 hour. Cells were washed six times before incubating with secondary antibodies diluted in blocking solution for 1 hour in the dark. Cell nuclei were stained with DAPI (diluted 1/5000) in PBS for 15 minutes before a final six washes in PBS and mounting onto microscope slides with fluorescence mounting media (Dako, S3023).

Some cells were acid washed to remove surface-bound proteins prior to fixation. Cells were incubated on ice for 1 minute before aspirating cell media and replacing with ice-cold acid wash buffer (see Section 2.8). Cells were incubated on ice for 1 minute before washing thoroughly with large volumes of PBS. Cells were then fixed and stained as above.

2.6.2 Tissue sections

Frozen tissue sections were thawed and allowed to air dry for 1 hour before rehydrating with TBS for 30 minutes. Sections were washed three times by flooding and aspirating slides with TBS + 0.3% Triton-X100. Tissue was blocked with cryosection immunohistochemistry (IHC) blocking solution (see Section 2.8) for 30 minutes at room temperature. Primary antibodies were diluted in IHC blocking solution and sections were incubated overnight at 4°C in a humidified chamber. The next day, sections were washed 3 times in TBS + 0.3% Triton X-100 before incubating with secondary antibodies diluted in IHC blocking solution for 1 hour in the dark. Sections were washed 3 times before adding fluorescence mounting media and sealing with microscope coverslips.

2.6.3 Whole mount lumbrical muscles

Muscles were fixed in 4% PFA-PBS before incubating with whole-mount-immunohistochemistry (WM-IHC) permeabilisation solution (see Section 2.8) for 30 minutes and then WM-IHC blocking solution (see Section 2.8) for 30 minutes.

Muscles were then incubated with primary antibodies diluted in blocking solution overnight at 4°C. Muscles were washed with PBS before staining with secondary antibodies for 2 hours. Acetylcholine receptors were stained with α-BTX-555 (see Section 2.9, Invitrogen) for 10 minutes before washing in PBS and mounting of whole muscles onto glass microscope slides with fluorescence mounting medium.

2.6.4 Imaging

Images were taken on an inverted Zeiss LSM 780 NLO scanning confocal microscope with either oil immersion objectives (Plan-Apochromat 40x/1.3 Oil DIC M27, Plan-Apochromat 63x/1.4 Oil DIC M27) or a Plan-Apochromat 20x/0.8 M27 objective. Images were analysed using Zen LSM software or FIJI (Schindelin et al., 2012).

2.7 Proximity Ligation Assay

DIV6 primary mixed ventral horn cultures on glass coverslips were fixed and incubated with primary antibodies as for ICC (see Section 2.6.1). Proximity Ligation Assays (Duolink® In Situ PLA®, Sigma) were subsequently performed as follows.

PLA probes (Duolink® In Situ PLA® Probe Anti-Rabbit PLUS, DUO92002; Duolink® In Situ PLA® Probe Anti-Mouse MINUS, DUO92004) were mixed and diluted 1:5 in ICC blocking buffer (see Section 2.8), along with any secondary antibodies required for counterstaining, and incubated at room temperature for 20 minutes. Cells were removed from primary antibody solution and washed in PBS. Cells were then placed in a pre-heated humidity chamber, probe solution added, and cells incubated at 37°C for 1 hour. Ligation solution was prepared by dilution (1:5) of the ligation stock with Milli-Q® H_2O. Ligase was added to the solution (1:40 dilution) just before application. Cells were thoroughly washed in PLA *in situ* wash buffer A (see Section 2.8) before returning to humidity chamber and applying ligation solution. Cells were incubated at 37°C for 30 minutes. Amplification solution was prepared by dilution (1:5) of amplification stock in Milli-Q® H_2O. Polymerase was added to the solution (1:80 dilution) just before applying to cells. Cells were thoroughly washed in PLA *in situ* wash buffer A (see Section 2.8) before returning to humidity chamber and applying amplification solution. Cells were incubated at 37°C for 90 or 100 minutes, depending upon experiment.

At the end of amplification time cells were washed thoroughly, first in 1x PLA *in situ* wash buffer B (see Section 2.8) and then in 0.01x PLA *in situ* wash buffer B. Cells were allowed to air dry for 30 minutes at room temperature before mounting onto glass microscope slides with Duolink® In Situ Mounting Medium with DAPI (Sigma, DUO82040). Imaging of fluorescence was performed as described previously (see Section 2.6.4).

2.8 Media and Reagents

Table 2.1 Recipes of solutions used in this thesis.

Solution	Recipe
Primary motor neuron medium (MNM)	Neurobasal™ (Gibco, 21103049) 1% B27™ supplement (ThermoFisher Scientific, 17504044) 2% heat inactivated horse serum (Gibco, 26050-088) 1% GlutaMAX™ supplement (ThermoFisher Scientific, 35050061) 24.8 µM 2-mercaptoethanol (Gibco, 31350-010) 10 ng/ml ciliary neurotrophic factor (CNTF, Peprotech, 450-50) 0.1 ng/ml glial-derived neurotrophic factor (GDNF, Peprotech, 450-10) 1 ng/ml bone-derived neurotrophic factor (BDNF, Peprotech, 450-02-50) 1% penicillin/streptomycin Filtered (0.22 µm pore size)
N2a medium	DMEM (Gibco, 41966-029) 1% GlutaMAX™ supplement (ThermoFisher Scientific, 35050061) 10% fetal bovine serum (FBS, Labtech International, FCS-SA/500) Filtered (0.22 µm pore size)
Phosphate buffered saline (PBS), pH 7.3	PBS (Dulbecco A) tablets (Oxoid Ltd., BR0014G) Typical formula: 137 mM NaCl, 2.7 mM KCl, 7.98 mM Na_2HPO_4, 1.5 mM KH_2PO_4
Tris buffered saline (TBS), pH 7.4	50 mM Tris base 150 mM NaCl
TBS-T	TBS 0.01% Tween-20.

Immunocytochemistry (ICC) blocking solution	PBS 10% heat inactivated horse serum (Gibco, 26050-088) 0.5% BSA (Fraction V, Sigma, 10735094001) 0.2% Triton X-100
Muscle whole-mount immunohistochemistry (WM-IHC) blocking solution	PBS 1% Triton X-100 4% BSA (Fraction V, Sigma, 10735094001)
WM-IHC permeabilisation solution	PBS 2% Triton-X100
Cryosection immunohistochemistry (IHC) blocking solution	TBS 0.3% Triton X-100 5% normal goat serum (Vector Labs, S-1000) or donkey serum (Sigma, D9663)
RIPA tissue lysis buffer	50 mM Tris-HCl pH 7.5 150 mM NaCl 1% NP-40 0.5% sodium deoxycholate 0.1% sodium dodecyl sulfate (SDS) 1 mM EDTA 1 mM EGTA 1% Halt protease and phosphatase inhibitor cocktail (Thermo Scientific, 78445).
Laemmli 4x sample buffer	250 mM Tris-HCl pH 6.8 8% SDS 40% glycerol 0.02% bromophenol blue 1.43 M 2-mercaptoethanol
Western blot blocking solution	TBS-T 5% skimmed milk powder or 5% BSA (Fraction V, Sigma, 10735094001)
Acid wash buffer, pH 2	0.2 M acetic acid 0.5 M NaCl
PLA *in situ* wash buffer A, pH 7.4	0.01 M Tris 0.15 M NaCl 0.05% Tween-20 Filtered (0.22 µm pore size)
PLA *in situ* wash buffer B, pH 7.5	0.2 M Tris 0.1 M NaCl Filtered (0.22 µm pore size)

Solutions were made up in Milli-Q® ultrapure H_2O (resistivity of 18.2 MΩ.cm) unless stated otherwise.

2.9 Antibodies and Molecular Probes

Table 2.2 Antibodies and labelled molecular probes used in this thesis

Antibody target	Species	Supplier	Dilution (application)
Primary antibodies			
Agrin	goat	R&D Systems, AF550	1/200 (IHC)
AKT	rabbit	Cell Signalling Technology, #9272	1/1000 (WB)
phospho-AKT (Ser473)	rabbit	Cell Signalling Technology, #9272	1/100 (WB)
BDNF	rabbit	Alomone, ANT-010	1/1000 (WB)
βIII tubulin	chicken	Synaptic Systems, 302-306s	1/500 (ICC)
βIII tubulin	rabbit	Sigma, T2200	1/1000 (ICC)
βIII tubulin	mouse	Covance, MMS-435P	1/1000 (ICC)
βIII tubulin	rabbit	Covance, PRB-435P	1/1000 (ICC)
ChAT	goat	Merck, AB144P	1/100 (IHC)
ERK1/2	rabbit	Cell Signalling Technology, #9102	1/1000 (WB)
phospho-ERK1/2 (Thr202/Tyr204)	rabbit	Cell Signalling Technology, #9101	1/500 (WB)
GAPDH	mouse	Millipore. MAB374	1/5000 (WB)
GDNF	rabbit	Alomone, ANT-014	1/1000 (WB)
GFAP	chicken IgY	Abcam, Ab4674	1/1000 (ICC)
GFRα1 (E-11)	mouse	Santa Cruz, sc-271546	1/100 (ICC) 1/1000 (WB)
HA (clone 12A5)	mouse	Cancer Research UK	1/200 (ICC)
Laminin	rabbit	Sigma, L9393	1/1000 (ICC, IHC)
MAP2	guinea pig	Synaptic Systems, 188-004	1/500 (ICC)
Neurofilament (NF-M)	mouse	DSHB, 2H3-s	1/100 (IHC)
Nidogen 1	rabbit	Abcam, Ab14511	1/250 (ICC) 1/500 (IHC) 1/1000 (WB)
Nidogen 2	rabbit	Abcam, Ab14513	1/250 (ICC) 1/500 (IHC) 1/1000 (WB)
Nidogen 2	sheep	R&D Systems, AF6760	1/1000 (WB)
Olig2	mouse	Kind gift from Prof W. Richardson (UCL)	1/500 (ICC)
$p75^{NTR}$	rabbit	Kind gift from Prof M. Chao (New York University)	1/1000 (ICC)
PECAM1 (M-20)	goat	Santa Cruz, sc-1506	1/100 (ICC)
Sox10	guinea pig	Kind gift from Prof W. Richardson (UCL)	1/5000 (ICC)
SV2-c	mouse	DSHB	1/50 (IHC)
pan-Trk (B-3)	mouse	Santa Cruz, sc-7268	1/100 (ICC)
pan-Trk	mouse	Zymed, 13-6500	1/1000 (ICC)

TrkB	rabbit	Millipore Upstate, 07-225	1/1000 (WB)
TrkB	rabbit	Millipore, Ab9872	1/1000 (ICC) 1/1000 (WB)
TrkB	goat	R&D Systems, AF1494	1/100 (ICC)
phospho-TrkB (Tyr515)	rabbit	Abcam, Ab109684	1/500 (WB)
Vimentin	chicken	Novus Biological, NB300-233	1/2000 (ICC)
Secondary antibodies HRP-conjugated			
Mouse Ig	Rabbit	Dako, P0161	1/3000
Rabbit Ig	Swine	Dako, P0399	1/3000
Sheep Ig	Rabbit	Dako, P0163	1/3000
Secondary antibodies fluorophore-conjugated			
All species	*n/a*	Invitrogen	1/1000
Fluorescently-labelled probes			
α-BTX-Alexa Fluor™ 555	*n/a*	Invitrogen, B35451	1/2000 (IHC)
Tetanus toxin C-terminal fragment-Alexa Fluor™ 647	*n/a*	In house	40 nM (ICC)
Fluoro-myelin Texas Red	*n/a*	Invitrogen, F34652	1/300 (IHC)
DAPI	*n/a*	Sigma, D8417	1/2000 (ICC, IHC)

Chapter 3. Nidogen Expression in the Neuromuscular System

3.1 Specific Aims

To begin investigating the role of nidogens at the neuromuscular junction, it was important to first understand the protein expression profile of the two nidogen isoforms throughout the mouse neuromuscular system. Differences in the expression levels or patterns in these tissues could suggest significant and distinct physiological roles of these extracellular proteins.

Accordingly, my specific aims were as follows;

a) To assess relative protein expression levels of nidogen-1 and nidogen-2 in tissues of the mouse neuromuscular system, including the brain, spinal cord, sciatic nerve and hindlimb skeletal muscles.
b) To investigate the protein localisation of nidogen-1 and nidogen-2 in these tissues via immunohistochemical analysis.

These experiments were performed on tissue from wild type mice of the C57BL/6J – SJL mixed background from both genders.

3.2 Nidogens in the nervous system

Protein expression of nidogen-1 and nidogen-2 was first investigated via western blotting (Figure 3.1A) to assess the relative levels in neuromuscular tissues. The central nervous system (CNS) tissues (brain and spinal cord) and a peripheral nervous system (PNS) tissue (the sciatic nerve, which innervates the hindlimb muscles) were compared. Protein levels were normalised to the total protein loaded, as measured by stain-free technology (BioRad) and presented relative to expression in the brain (Figure 3.1B). Nidogen-1 was identified by the presence of a clear band at approximately 150 kDa (Figure 3.1A). Nidogen-2 was observed as two bands at approximately 140-160 kDa. These are expected to represent the full length protein (140 kDa) and a post-translationally glycosylated form (160 kDa; Kohfeldt et al., 1998). Nidogen-2 quantification comprised the summation of both these bands. Both nidogen-1 and -2 were expressed at much lower levels in the brain than in the spinal cord. Expression of both nidogens appeared to be

highest in the sciatic nerve compared to the brain and spinal cord (Figure 3.1), with nidogen-1 expressed approximately 200-fold higher and nidogen-2 expressed approximately 150-fold higher in the sciatic nerve than the brain. It is interesting that the difference in expression between the sciatic nerve and the CNS was much greater for nidogen-2 than nidogen-1. This may suggest a redundancy in function between nidogen-1 and nidogen-2 in the CNS, whereas they may play distinct roles in the sciatic nerve requiring high expression of both isoforms in this tissue.

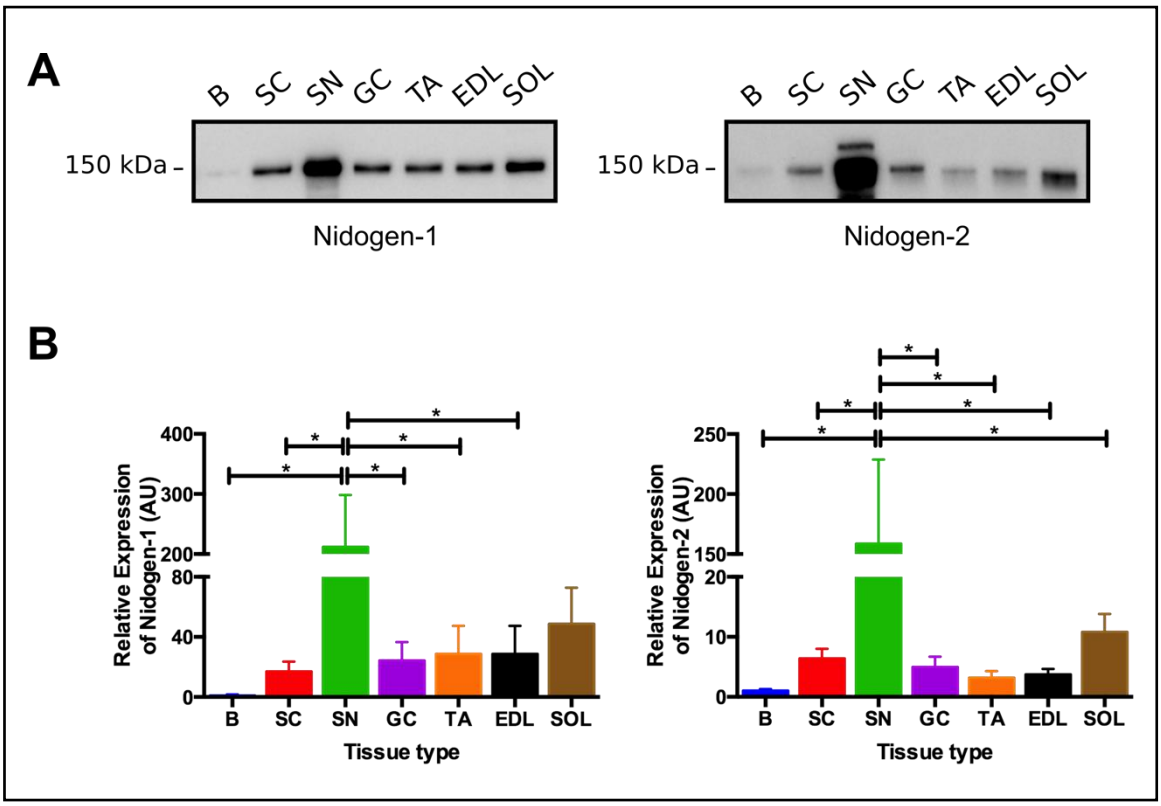

Figure 3.1 Nidogen protein expression in the neuromuscular system.

(A) Western blots showing the protein expression of nidogen-1 and nidogen-2 in tissues of the mouse neuromuscular system; brain (B), spinal cord (SC), sciatic nerve (SN), and the hindlimb muscles gastrocnemius (GC), tibialis anterior (TA), extensor digitorum longus (EDL), soleus (SOL). 10 µg of total protein was loaded in each lane except for the sciatic nerve, for which 5 ug was loaded to prevent oversaturation and masking of signal from the other tissue types. **(B)** Quantification of protein expression in **(A)**. Expression was normalised to total protein and expressed as relative to expression in the brain. Data expressed as mean ±SEM; N=3; One-way ANOVA was performed and statistical significance between tissue types assessed using Tukey's multiple comparisons test (* $p < 0.05$).

To gain further insights into the expression pattern of nidogens in the PNS, immunohistochemistry was performed on transverse sections of the mouse sciatic nerve (Figure 3.2). Previously, cultured Schwann cells have been shown to synthesise and secrete nidogens (Dziadek et al., 1986). In rat sciatic nerves, nidogen-1 is found in the basement membrane (BM) surrounding all axons, but nidogen-2 expression is restricted to unmyelinated axons (Lee et al., 2007). As we are using mice, we investigated whether this differential expression was also apparent in the adult mouse sciatic nerve. In transverse sections, Nidogen-1 displayed a uniform expression pattern throughout the basement membranes of the mouse sciatic nerve (see Figure 3.2A). Nidogen-1 can be seen in the perineurium surrounding the axon bundles within the nerve (see filled arrowheads in upper panels of (Figure 3.2A) at a comparable intensity to the basement membrane of the endoneurium which ensheaths individual axons (see lower panels of (Figure 3.2A). Counterstaining with a fluorescence myelin stain indicated that nidogen-1 surrounds myelinated axons, external to the myelin sheath, as well as smaller structures which could be unmyelinated axons or capillaries (see empty arrowheads Figure 3.2A). In contrast, nidogen-2 appeared to be expressed at lower levels surrounding individual axons despite remaining high in the perineurium (see filled arrowhead Figure 3.2B). Nidogen-2 was also highly expressed in the vasculature, and smaller structures which again could be unmyelinated axons (empty arrowheads Fig. 2B). No obvious immunoreactivity was observed for either of the nidogens within axons themselves. Combined with the protein quantification, it is clear that nidogens comprise a large proportion of the protein content of the sciatic nerve compared to brain.

While cross-sections of the sciatic nerve provide a clear view of nidogen distribution in the transverse axis, it is difficult to completely and clearly follow single axons in longitudinal sections. Therefore, to look at the distribution of nidogens along their surface, individual axons were teased from the sciatic nerve, mounted onto microscope slides and stained for the nidogen isoforms (Figure 3.3).

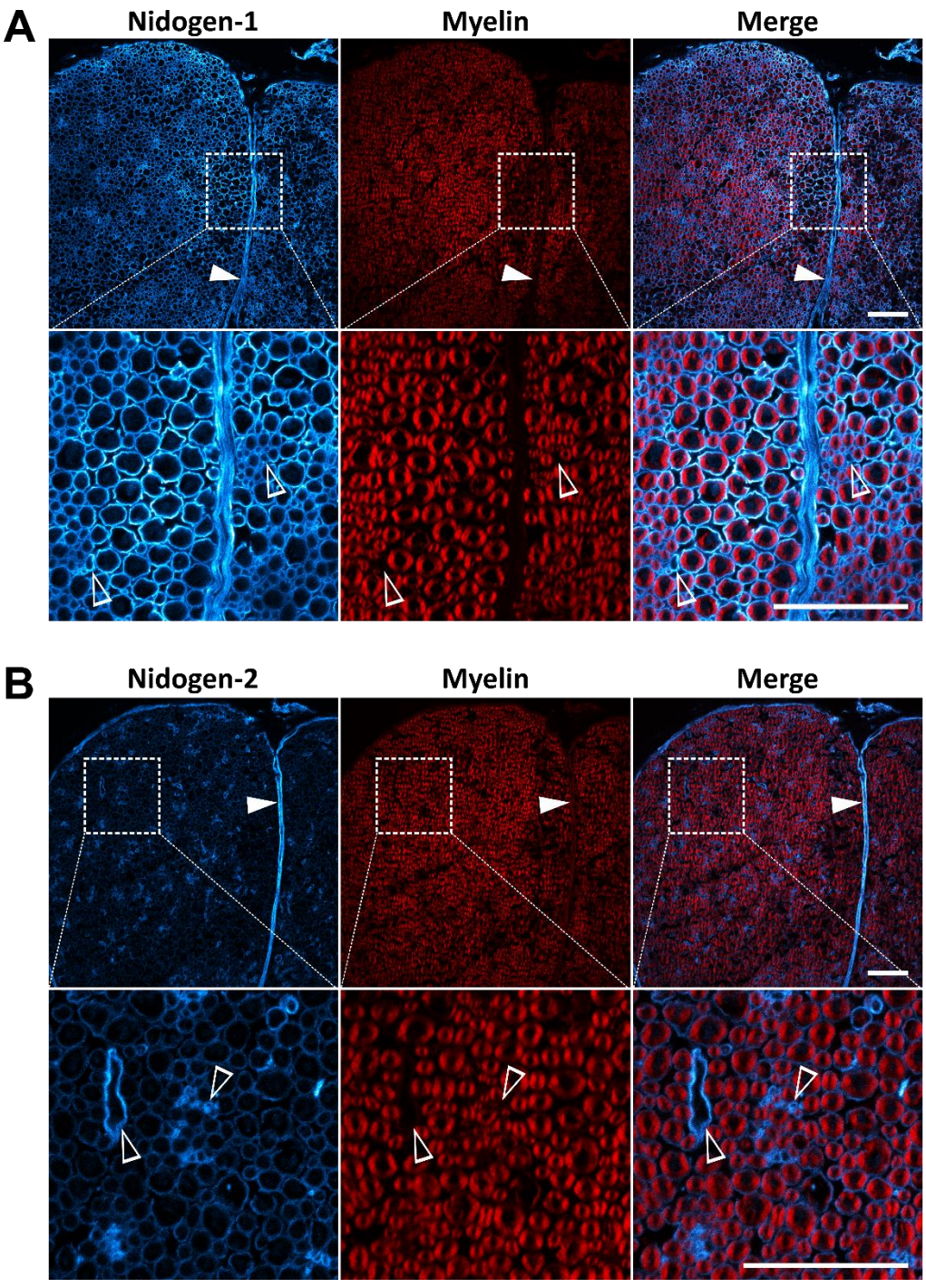

Figure 3.2 Nidogen protein expression in the sciatic nerve.

Transverse (10 µm) sections of the mouse sciatic nerve immunostained for nidogen protein expression and counter stained with FluoroMyelin™ Red. Dashed boxes indicated region cropped in lower panels. **(A)** Nidogen-1 is expressed with uniform intensity throughout basement membranes of the sciatic nerve. Filled arrowhead indicates perineurium surrounding axons bundles. Empty arrowhead indicates unmyelinated axons or small capillaries. **(B)** Nidogen-2 is more highly expressed in the perineurium (filled arrowhead) and vasculature (empty arrowheads) than in the basement membrane surrounding individual axons. Scale bars equal to 50 µm. Images representative of a minimum of three independent preparations.

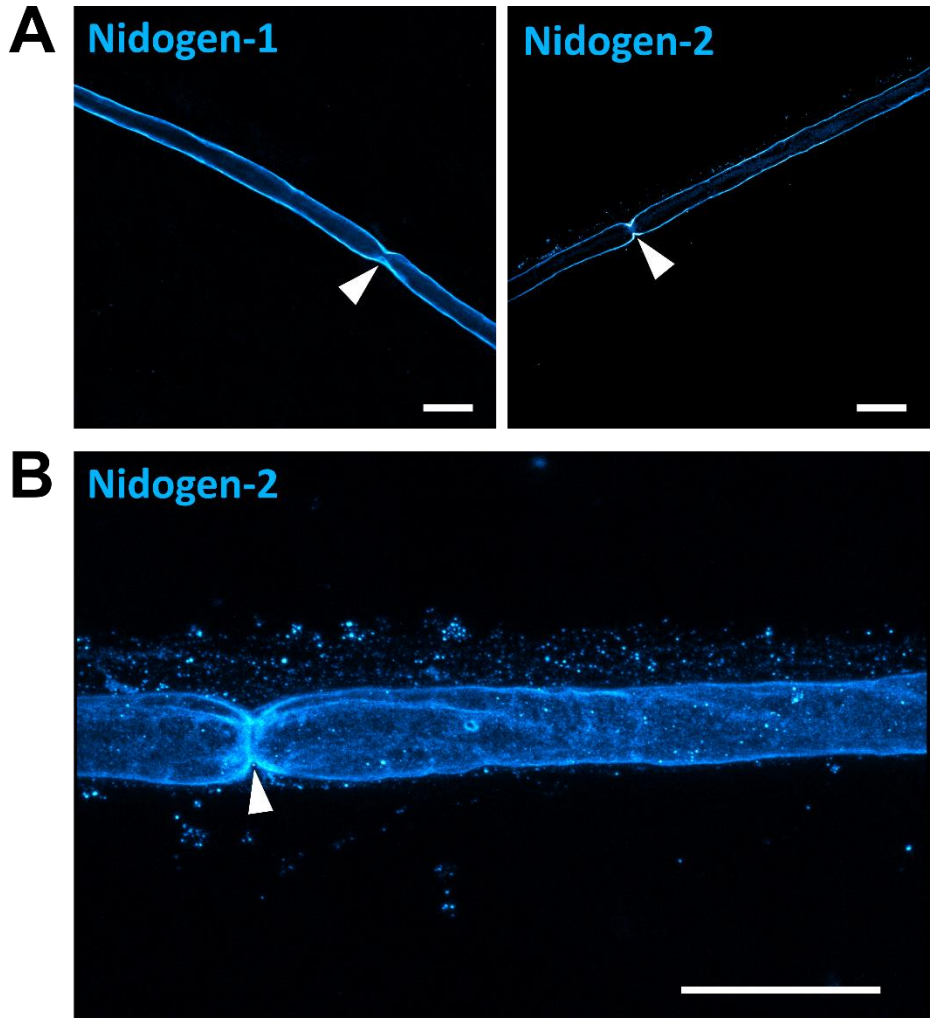

Figure 3.3 Nidogen protein expression in individual axons of the sciatic nerve.

Single axons were teased from the sciatic nerve and isolated before staining for nidogen protein expression. **(A)** Nidogen-1 and nidogen-2 surround the axons and are both present at the nodes of Ranvier (arrowheads). Nidogen-2 appears enriched at the node, compared to the nidogen-1. **(B)** Three-dimensional projections of confocal Z-stacks reveal the tight association of the nidogen basement membrane with the surface of the myelinated axon. A greater intensity of nidogen-2 staining can again be seen at the node of Ranvier (arrowhead). Scale bar equal to 50 µm. Images representative of a minimum of three independent preparations.

Nidogen-1 appears to be uniformly distributed along the surface of axons, with equal intensities recorded along the axon shaft, and at the nodes of Ranvier (Figure 3.3A, see arrowheads for node). However, nidogen-2 shows an enrichment at the node of Ranvier relative to the distribution along the rest of the axon. Three-dimensional projections of confocal Z-stacks clearly show this enrichment at the node, in addition to revealing the tight association of the nidogen basement membrane with the myelin sheath surrounding the axon (Figure 3.3B). Nodal enrichment of nidogen-2 is therefore another example of differential expression between the nidogen isoforms. This enrichment at the nodes of Ranvier has not previously been shown for nidogens.

I next performed immunohistochemistry on transverse sections of the mouse spinal cord to better understand the protein expression pattern in the CNS. Different regions of the spinal cord were examined to assess whether nidogens were expressed in certain cell types or structures within the spinal cord (Figure 3.4A). The key basement membranes within the spinal cord are the vascular basement membrane, which surrounds the blood vessels comprising the blood-brain barrier, and the pial basement membrane, which is tightly associated with the pia mater meninges and surrounds the entire CNS (Halfter and Yip, 2014). Both nidogen-1 and nidogen-2 were found to be highly expressed in the pial basement membrane surrounding the cord and with the anterior spinal artery (arrowhead and asterisk respectively, Figure 3.4B). Counterstaining for choline acetyltransferase (ChAT)-positive motor neurons in the ventral horn and GFAP-positive glia in the white matter indicated no overt expression of the nidogen isoforms within neuronal cell bodies or in glia (Figure 3.4C and D). The most robust expression of nidogen-1 and nidogen-2 was seen in structures identical to those positive for the endothelial cell marker PECAM1, representing the spinal cord vasculature. No major differences in localisation of nidogen-1 compared to nidogen-2 were observed in the spinal cord.

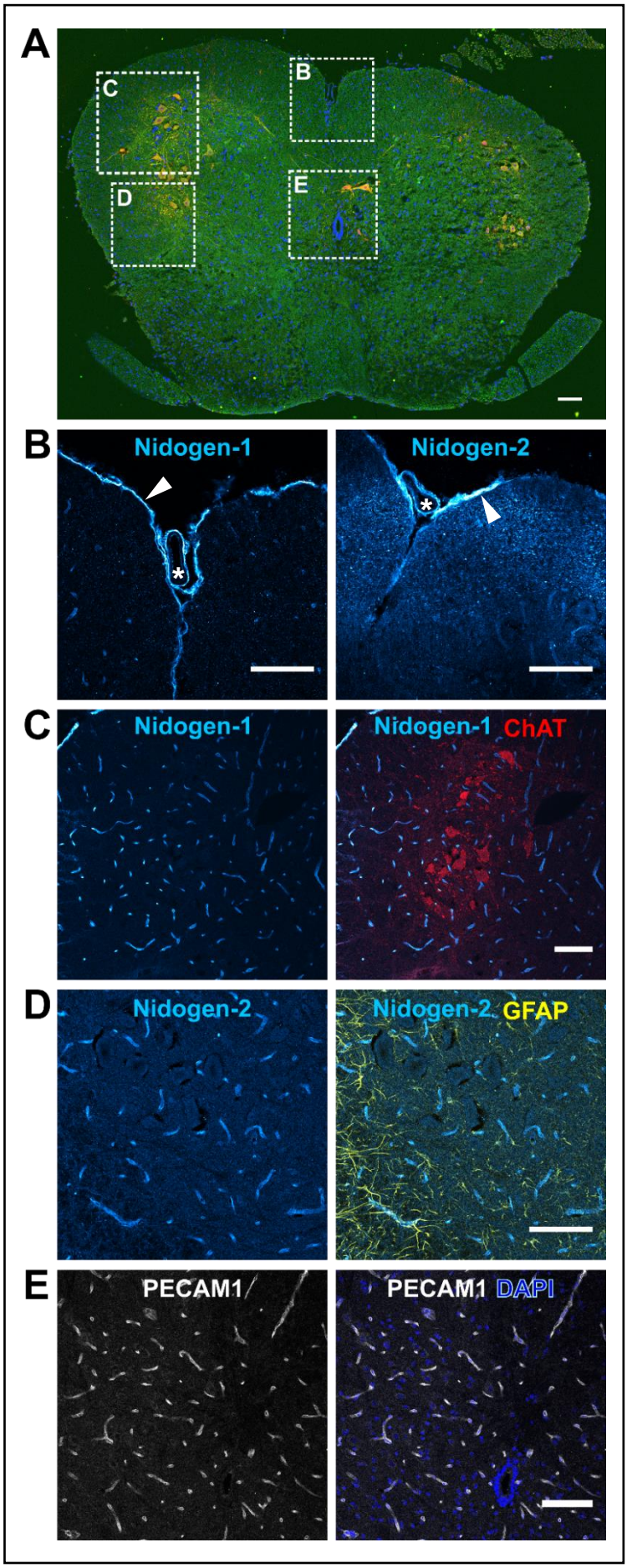

Figure 3.4 Nidogen protein expression in the mouse spinal cord.

Figure 3.4 Nidogen protein expression in the mouse spinal cord.

Transverse sections of adult mouse spinal cord were stained for nidogen-1 and nidogen-2 protein expression patterns. **(A)** A representative section through the lumbar spinal cord indicates the regions examined and magnified in (B) – (E). Orange indicates ChAT-positive motor neurons and blue indicates DAPI-stained nuclei. **(B)** Magnification of the anterior median fissure shows expression of both nidogens in the basement membrane underlying the pia mater (arrowhead) and surrounding the anterior spinal artery (asterisk). **(C) – (E)** Magnification of the ventral horn and nearby white matter show nidogen expression is localised to structures positive for the endothelial cell marker PECAM1. No obvious expression was detected in motor neuron cell bodies (ChAT-positive) or glial cells (GFAP-positive). Scale bar equal to 100 µm. Images representative of a minimum of three independent preparations.

3.3 Nidogens in skeletal muscle

To increase our understanding of nidogen expression throughout the neuromuscular system, the presence of nidogen at the neuromuscular junction (NMJ) was investigated. Imaging NMJs and their associated neural counterparts in tissue sections is challenging as a result of tissue processing and the thin sectioning required for antibody penetration. I therefore dissected and performed whole mount staining of mouse lumbrical muscles of the hind paw, as previously described (Sleigh et al., 2014). This preparation involved fixing and staining of whole, isolated muscles in suspension before mounting and imaging. There is no need to divide the muscle, as it is only a few fibres thick. This has the advantage of not only allowing sufficient antibody penetration, but also visualisation of the entire neuromuscular network of the muscle without serial sectioning and 3D reconstruction. Taking confocal image stacks through multiple planes builds up a view of the neuronal innervation and the NMJ to a degree of detail where changes in the structure over postnatal development can be observed in health and disease (Sleigh et al., 2014). Mouse lumbrical muscles were isolated and stained for neurofilament (NF) and synaptic vesicle protein 2 (SV2) to visualise the neuronal axons and the presynaptic terminals, and alpha-bungarotoxin (BTX) which binds to nicotinic acetylcholine receptors (AChRs) in the muscle thereby marking the postsynaptic membrane. Together these markers allow visualisation of the neuromuscular junction and the innervating neurons. Co-staining for the nidogen isoforms revealed both nidogen-1 and nidogen-2 surrounding the innervating axons as well as the synaptic terminals (Figure 3.5A and B). Blood

vessels were marked using the isolectin IB4 (Ernst and Christie, 2006). Nidogens were found associated with the muscle vasculature, similar to that seen in the sciatic nerve and spinal cord (empty arrowheads, Figure 3.5A and B). Interestingly, both isoforms were also observed in a distinct pattern interweaving with the presynaptic terminals (filled arrowhead, Figure 3.5A and B, C). This pattern overlapped with that of BTX (Figure 3.5B) and was reminiscent of that seen when staining for agrin, an extracellular heparan sulfate proteoglycan involved in clustering of AChRs and maturation of the NMJ (Figure 3.5E). This pattern of nidogen immunoreactivity in the muscle suggests a specific role for nidogen at the NMJ, distinct to its role in other basement membranes. To clarify the localisation of nidogen surrounding the innervating axons, muscles were co-stained with myelin basic protein (MBP) to reveal the myelin sheath. Consistent with the transverse sections of the sciatic nerve, nidogens were observed to be external to the myelin sheath (arrowheads Figure 3.5D).

It has been previously shown that muscles differ in contractile properties, metabolic demands, patterns of innervation, and development of neuromuscular junctions (NMJs) (Donoghue and Sanes, 1994; Pun et al., 2002). Additionally, one study has reported abnormalities in the structure of NMJs in nidogen-2 knock out mice, the extent of which appeared to vary with the type of muscle (Fox et al., 2008). We investigated expression of nidogens by SDS-PAGE and western blot in the mouse soleus (SOL, a slow twitch muscle), the extensor digitorum longus and tibialis anterior (EDL and TA, predominantly fast twitch muscles), and the gastrocnemius (GC, a mixed muscle) (Figure 3.1). Expression of nidogen-1 in the GC, TA and EDL appeared relatively consistent. However, the SOL showed a trend towards an increased expression of nidogen-1. While nidogen-1 expression levels in the GC, TA and EDL were all significantly lower than those in the sciatic nerve, the expression in the SOL was not significantly different (Figure 3.1B). Nidogen-2 also showed a trend towards higher expression in the SOL than in the other muscle types, but this lacked statistical significance (Fig. 1B).

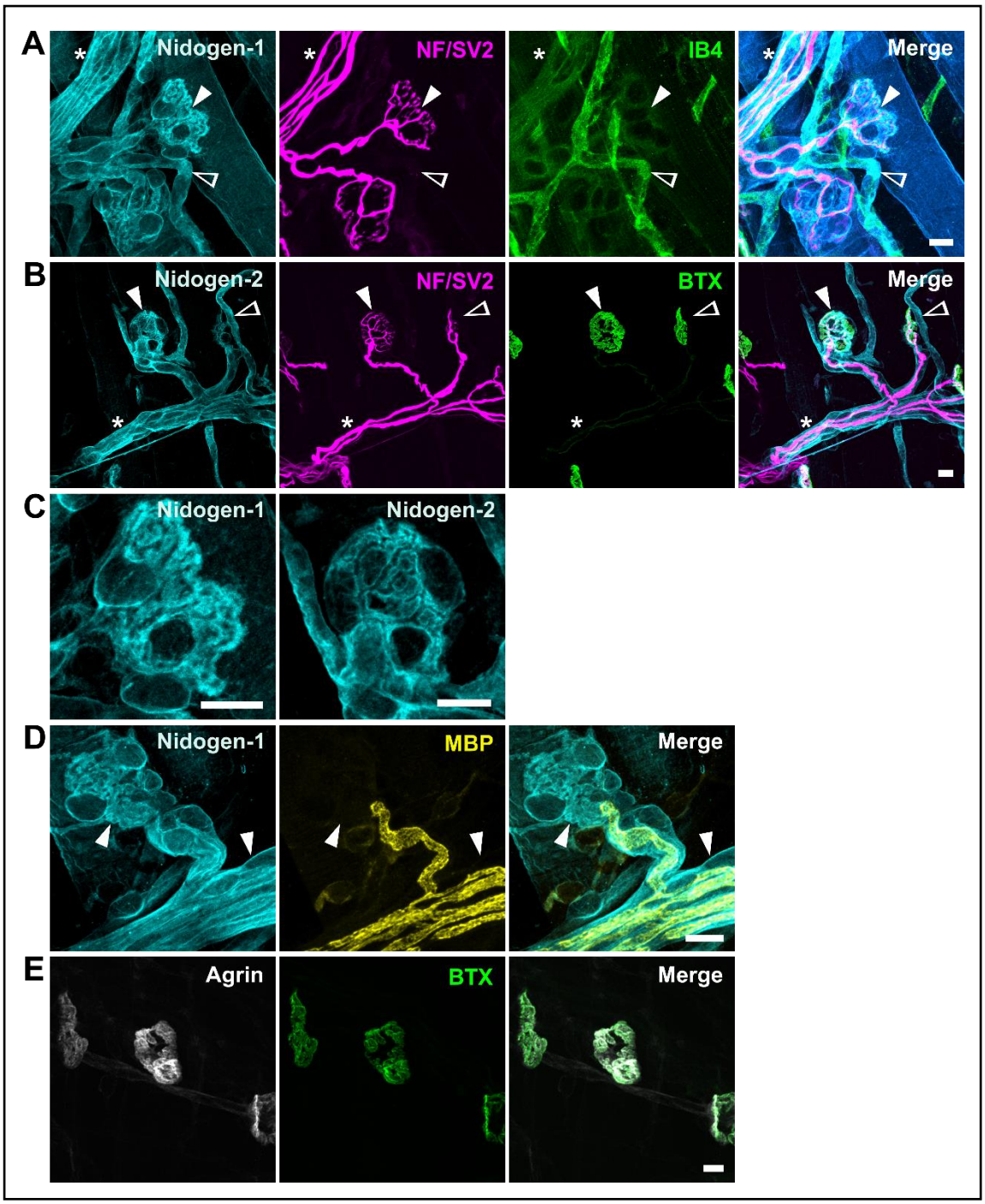

Figure 3.5 Nidogen protein expression in mouse lumbrical muscles.

The mouse hind paw lumbrical muscles were whole-mounted and stained to visualise complete neuromuscular connections. **(A)** and **(B)** Nidogen-1 and nidogen-2 show similar expression patterns within lumbricals, surrounding innervating axons (asterisk), muscle vasculature (empty arrowheads) and neuromuscular junctions (filled arrowheads). Neurofilament (NF) and synaptic vesical protein (SV2) were used to indicate the innervating axons and presynaptic terminals. The isolectin IB4 was used to mark endothelial cell walls, and postsynaptic acetylcholine receptors were stained with fluorophore-conjugated alpha-bungarotoxin (BTX) to mark the postsynaptic membrane. **(C)** Higher magnification of NMJs in (A) and (B). **(D)** Counterstaining for myelin basic protein (MBP) shows that nidogens surround the innervating axons external to the myelin sheath (arrowheads). **(E)** Synaptic agrin and BTX show similar patterns to the nidogen found at the NMJ. Scale bars equal to 10 µm. Images representative of a minimum of three independent preparations.

3.4 Conclusions

My aims were to assess the protein expression levels and localisation of the nidogen isoforms in tissues of the neuromuscular system. Relative levels of nidogen expression were quantified in the brain, spinal cord, sciatic nerve, and four different muscles; the gastrocnemius (GC), tibialis anterior (TA), extensor digitorum longus (EDL) and soleus (SOL). Both nidogens showed the lowest expression levels in the brain compared to the other tissues investigated, while spinal cord expression was within a range comparable to that seen in muscles. Immunohistochemical analysis of the spinal cord revealed that nidogens were associated with the vasculature and meninges, with no immunoreactivity observed in neuronal or glial cell bodies. The highest expression of both isoforms was observed in the sciatic nerve. Immunohistochemistry of transverse sections of the nerve, showed that nidogens were robustly expressed throughout the basement membranes of this peripheral nerve. As the sciatic nerve is a relatively simple tissue, it is perhaps unsurprising that nidogens, as a key component of the basement membrane, comprise such a significant proportion of the protein content, in comparison to the complex proteinaceous composition of the brain and spinal cord.

Interestingly, when teased axons from the sciatic nerve were examined, nidogen-2 appeared to be enriched at the nodes of Ranvier. Nodes of Ranvier are gaps of approximately 1 µm between myelin segments at which clusters of Na+ channels are positioned for the regeneration and rapid propagation of the action potential down the axon (Susuki and Rasband, 2008). Establishment of these channel clusters has been shown to depend upon interactions between cell adhesion molecules on the axon, the neuronal cytoskeleton, and components of the extracellular matrix (ECM) surrounding the node. Ligands of the transmembrane protein dystroglycan include the ECM proteins laminin and perlecan, and these interactions are involved in nodal component clustering (Colombelli et al., 2015). Nodal enrichment of perlecan was shown to be independent of its presence in the Schwann cell basement membrane, and dependent upon the expression of dystroglycan (ibid.). Immunostaining of perlecan at the nodes of Ranvier in that study was reminiscent of my observation for nidogen-2. As the extent of this enrichment was not observed for nidogen-1,

it is possible that there is a specific role for nidogen-2 at this site, distinct from its role in the Schwann cell basement membrane.

Expression of nidogen-1 and nidogen-2 was robust in all muscles examined. Interestingly, although the difference was not significant, there was a trend for a higher expression level of both nidogens in the SOL. The SOL was the only slow twitch muscle investigated, with the GC being comprised of a mixed of fast and slow twitch fibres, and the TA and EDL being predominantly fast twitch. While different fibre types are characterised by their metabolic demands and neuronal firing patterns, differences in their synapses have also been described. Pun and colleagues described a difference in the initial stages of neuromuscular junction (NMJ) development in different muscles (Pun et al., 2002). The NMJs of the SOL were shown to develop at a slower rate compared to those of the other muscles, with a diffuse clustering of AChRs prior to neural innervation. In contrast, the TA and EDL showed robust and specific clustering of AChRs with less dependence on the presence of innervating neurons for postsynaptic specialisation. The GC was found to be an intermediate muscle with characteristics of both synapse types. The slower organising NMJs were termed ‘Delayed Synapsing’ (DeSyn) while the faster were called ‘Fast Synapsing’ (FaSyn). In addition to a greater dependence on neural innervation, the DeSyn muscles were also more sensitive to the absence of agrin in *z-agrin*$^{-/-}$ mice, failing to form AChR clusters, while in FaSyn muscles AChRs coalesced apparently normally but failed to maintain clusters. This provides evidence for a differential requirement or downstream signalling of an ECM component at the NMJ, in this case agrin. It is therefore possible that nidogen represents another extracellular molecule with a specific role in certain muscle types. Immunohistochemistry of whole-mounted muscles revealed that nidogen-1 and nidogen-2 are both present at the NMJ in a distinct pattern that overlaps that of AChRs (marked by BTX) and agrin. This is consistent with a specific role at the NMJ which warrants further investigation.

In summary, both nidogens are highly expressed in the peripheral nervous system and in muscles. While nidogens were consistently found in basement membranes associated with the vasculature and supportive connective tissue, a significant localisation of nidogens to the synaptic cleft of NMJs was also observed. As different synapse types in muscles (FaSyn and DeSyn) have

displayed differences in development and maintenance of the NMJ postsynapse, the role of nidogen at the neuromuscular system was further investigated by examining expression of the nidogen isoforms over post-synaptic development and in a scenario where neural innervation is withdrawn; in a model of neurodegeneration.

Chapter 4. Nidogens in postnatal development and disease

4.1 Specific Aims

As shown in Chapter 3, nidogens are highly expressed throughout the neuromuscular tissue, but particularly at the NMJ. A previous PhD student in our laboratory showed that nidogens are essential for the endocytosis of the binding fragment of the tetanus neurotoxin (HcT) into NMJs and its internalisation into motor neurons (Bercsenyi et al., 2014). When combined with the high expression of nidogens at the NMJ, this suggests that HcT hijacks an endogenous pathway which involves nidogen internalisation from the basement membrane of the NMJ into motor neuron synaptic terminals. My aim was therefore to investigate an endogenous signalling role for nidogens in muscle, distinct from their role in basement membrane stabilisation.

Changes in protein expression levels can indicate potential signalling roles if significant alterations are observed concomitant with known physiological events. To begin understanding the role of nidogens in muscle, observing expression over postnatal ages where the NMJ is still maturing could reveal if nidogen plays a role in this developmental process. In addition, modulation of nidogen expression in models of NMJ denervation and motor neuron death could indicate a role of nidogens in degeneration, regeneration or remodelling. Knock out models can also provide significant insight into the function of proteins and the level of redundancy within specific tissues.

Thus far, only one group has specifically investigated the muscle architecture of a nidogen-1 knock out mouse model. Fox and colleagues demonstrated abnormal topology of NMJs in the diaphragm muscle of nidogen-2 mutants and differential burden of abnormalities in different limb muscles, whereby the soleus and diaphragm were more affected than the extensor digitorum longus and the tibialis anterior (Fox et al., 2008). This group also showed that nidogen-2 may become restricted to the basement membrane of the NMJ shortly after birth, while nidogen-1 remains expressed throughout the synaptic and extrasynaptic basement membrane. However, these experiments did not include quantitative analysis of nidogen protein expression levels.

Outstanding questions therefore remain. Do expression levels of nidogens change over the course of development in addition to their altered localisation? Is NMJ denervation associated with changes in nidogen expression? Does knock out of the more ubiquitous nidogen-1 isoform affect expression of nidogen-2 in muscles?

To investigate these questions, my specific aims were as follows.

a) Examine expression levels of the nidogen isoforms in muscle over different stages of postnatal NMJ development;

b) Compare expression of nidogens between wild type and $SOD1^{G93A}$ mice. The latter mice express a human mutant (G93A) of superoxide dismutase 1 (SOD1) which is associated with amyotrophic lateral sclerosis (ALS). This mouse is an established model of ALS and neuromuscular degeneration;

c) Investigate nidogen expression in a nidogen-1 knock out mouse model.

4.2 Nidogens over postnatal muscle development and neuromuscular disease progression

Skeletal muscle is highly plastic and expression profiles of proteins can change drastically over muscle development as muscle fibres differentiate and the NMJ matures, as well as in response to environmental pressures, such as resistance exercise training, or during remodelling and synaptic maintenance in degenerative states (Denies et al., 2014; Hoppeler, 2016; Potthoff et al., 2007). Different muscle types may also display different expression profiles as a result of their varied physiological roles. For example, slow-twitch muscle fibres display higher levels of myogenin compared to fast-twitch fibres (Hughes et al., 1999). Interestingly, this protein (myogenin) is a transcription factor involved in increasing oxidative metabolism, the predominant energy supply for slow muscles. Therefore, investigating the expression profile of nidogens in different muscles types and over different ages may reveal if a change in expression occurs at a physiologically relevant age or is different in muscles with different metabolic demands.

I and others have shown that nidogens are present at the NMJ (Chapter 3; Fox et al., 2008). In early postnatal ages, the NMJ is still maturing. At birth, the

postsynaptic acetylcholine receptors (AChR) exist in diffuse clusters and synapses have not fully formed between the end plate and the innervating motor neurons. As postnatal development progresses, the NMJs are polyinnervated, with each synapse being contacted by multiple nerve terminals. Within the first three postnatal weeks, mouse NMJs undergo terminal pruning, synapse elimination and stabilisation of AChR clustering (Walsh and Lichtman, 2003) to produce distinct, monoinnervated 'pretzel' shaped NMJs with tightly apposed pre- and post-synaptic elements for efficient signal transduction. Extracellular proteins associated with the basement membrane have been implicated in NMJ maturation. Therefore, to understand whether nidogen may play a role, I selected two time points either side of this period of NMJ formation, postnatal day (PND) 15 and PND 36, to observe any altered regulation of nidogen protein expression during neuromuscular development.

To assess whether nidogen expression is altered in pathological conditions in which NMJ integrity is disrupted, I also collected muscles from a model of ALS, the $SOD1^{G93A}$ mouse (Kalmar et al., 2008). ALS is a neurodegenerative disease characterised by the loss of upper and lower motor neurons, which results in progressive muscle weakness and eventual paralysis. The causative event for this neuronal loss remains unclear, despite a range of pathological mechanisms being proposed. In the $SOD1^{G93A}$ mouse model, impaired axonal transport of mitochondria and signalling endosomes has been reported, suggesting that insufficient energy supply and a lack of trophic support may be responsible for the death of motor neurons (Bilsland et al., 2010; De Vos et al., 2007; Kieran et al., 2005). The formation of insoluble protein inclusions within the cytoplasm of motor neurons has also been reported, although it is unclear if these are themselves toxic or an attempt at cellular self-preservation (Ayers et al., 2017; Farrawell et al., 2015). In contrast to these relatively neuro-centric observations, muscle atrophy and NMJ alterations are some of the earliest degenerative events, preceding motor neuron loss (Fischer et al., 2004). However, the initiating event in NMJ denervation has not yet been identified. A greater understanding of the alterations occurring at this peripheral synapse over disease progression may therefore reveal early, and perhaps causative, pathological mechanisms of muscular degeneration.

In this investigation, samples were collected from a range of ages chosen to cover the disease progression from presymptomatic (PND 52), to early and late symptomatic (PND 76 and PND 92) and finally to end-stage disease in the SOD1^{G93A} mouse (PND 121), where NMJ are denervated (Bilsland et al., 2010; Tremblay et al., 2017). As different muscle types are composed of different fibre types with various metabolic demands and differential protein expression, I also investigated expression of nidogens in the mouse soleus (SOL); a slow twitch muscle, the extensor digitorum longus (EDL) and tibialis anterior (TA); predominantly fast twitch muscles, and the gastrocnemius (GC); a mixed muscle. These muscles have been reported to show differing susceptibilities to disease, including degeneration in the SOD1^{G93A} mouse (Tremblay et al., 2017). The mechanisms behind the relative resistance of slow muscles to degeneration remain unclear so investigating differences between the muscle types could reveal potential therapeutic targets for neuromuscular diseases.

To understand the expression profile of nidogens over postnatal development and neuromuscular degeneration, relative protein expression was measured by western blotting of whole muscle lysates. Proteins quantified in this way are usually normalised to a loading control which is typically a 'housekeeping' protein that is expressed at the same level throughout the different samples. Classical examples are the proteins GAPDH and alpha-tubulin. However, my study involved comparison of different tissues and ages in disease states. Different muscle types have been shown to express different levels of GAPDH as it is a metabolic enzyme, with the mainly oxidative slow-twitch muscle fibres containing less GAPDH than the fast-twitch fibres (Galpin et al., 2012). In agreement with this, I found GAPDH to be more highly expressed in the highly glycolytic TA, than in the EDL or slow-twitch SOL muscles (Figure 4.1A). In addition, alpha-tubulin showed lower expression levels in the SOL than in the TA, GC and diaphragm muscles, as well an increase in the number of observed bands suggesting additional post-translational or splicing modifications in different tissue types (Figure 4.1B). GAPDH, beta-actin and alpha-tubulin have all been shown to decrease with age so are not suitable to normalise samples of different ages (Vigelsø et al., 2015). Single proteins were therefore determined to be too unreliable as loading controls in this analysis and so total protein was used. This was measured using a stain-free technology (BioRad) which covalently bonds a

trihalo compound to the tryptophan residues in the proteins separated by SDS-PAGE. When activated by exposure to UV light, these residues fluoresce allowing proteins to be detected, imaged and quantified. The total protein loaded in a lane was then used to normalise the experimental band.

Figure 4.1 Expression of standard loading controls in different muscle types.

Tissue lysates of the tibialis anterior (TA), soleus (SOL), extensor digitorum longus (EDL), diaphragm (DIA) and gastrocnemius (GC) were probed for expression of the widely used western blot loading controls GAPDH **(A)** and alpha-tubulin **(B)**. The same amount of protein (10 µg) was loaded in each lane but expression levels of both proteins clearly vary with muscle type.

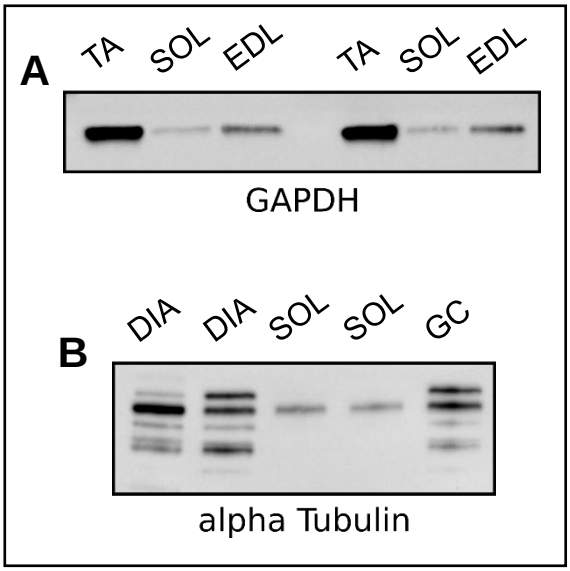

Expression of nidogen-1 was first investigated. Expression was presented as relative to the mean expression in wild type animals of 122 days old (PND 122), as representative of an adult mouse. In the GC, nidogen-1 expression in both wild type and SOD1^{G93A} animals was significantly higher at PND 17 than adult ages ($P \leq 0.05$, Figure 4.2). Nidogen-1 levels were very closely matched in wild type and SOD1^{G93A} GC with no significant difference observed between genotypes. In the TA, nidogen-1 expression of both genotypes was very closely matched from PND 17 – 91, showing relatively steady levels (Figure 4.2). However, at PND 122 nidogen-1 was significantly higher in SOD1^{G93A} TA compared to younger ages of the same genotype and compared to P122 wild type (P122 vs. P77 $P \leq 0.01$; P122 vs. P52 $P \leq 0.05$; P122 vs. P36 $P \leq 0.05$; P122 SOD1^{G93A} vs. P122 WT $P \leq 0.01$, Figure 4.2B). Wild type EDL showed a significant and steady decline in nidogen-1 expression over age ($P \leq 0.05$, Figure 4.2). SOD1^{G93A} EDL showed more fluctuations and no significant change over age, or compared to age-matched wild type. A similar decline in nidogen-1 was observed in the SOL muscle in both genotypes, although this was less consistent (Figure 4.2). Again, there was no significant difference between nidogen-1 expression levels in wild type and SOD1^{G93A} in the SOL.

Nidogen-2 expression was then investigated. In contrast to nidogen-1 where a single band representing the full-length protein was consistently observed in all samples, nidogen-2 appeared as three bands ranging from 100 kDa to approximately 200 kDa (Figure 4.3A). These are understood to represent the full-length protein and the major proteolytic fragments which are endogenously cleaved (Kohfeldt et al., 1998; Schymeinsky et al., 2002). The biological relevance of these cleaved fragments is unclear, but it has been shown for other components of the basement membrane that proteolytic degradation can reveal novel interaction sites perhaps potentiating alternative functional roles (Dziadek et al., 1988; Xu et al., 2001). Interestingly, in samples where the lowest band was observed, the full-length band was largely absent. In addition, this lower band was more prevalent in samples prepared from the youngest mice, particularly in the GC, TA and EDL muscles, perhaps suggesting a different binding repertoire for nidogen-2 at these ages. This age also correlates temporally with when Fox and colleagues observed restriction of nidogen-2 to synaptic sites (Fox et al., 2008).

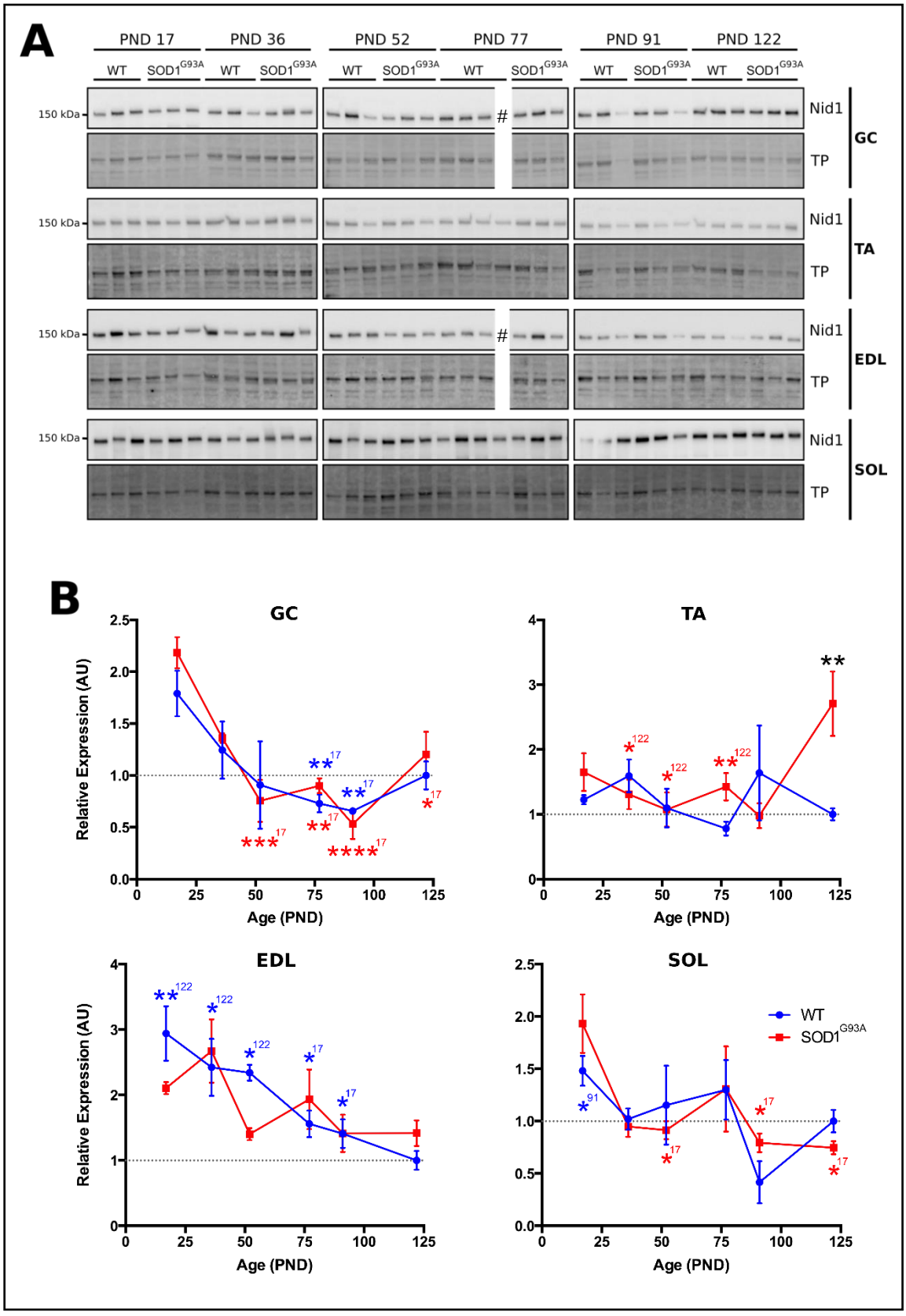

Figure 4.2 Expression of nidogen-1 in wild type and SOD1^{G93A} muscles.

Figure 4.2 Expression of nidogen-1 in wild type and SOD1^{G93A} muscles.

(A) Tissue lysates of the GC, TA, EDL and SOL from wild type and SOD1^{G93A} mice were probed for expression of nidogen-1. Muscles were examined at ages where NMJs were still maturing (PND 17–36) as well as ages representing progression of disease in the SOD1^{G93A} model of ALS; PND 52 (pre-symptomatic), PND 77 (early symptomatic), PND 91 (symptomatic), PND 122 (end stage). For one PND 77 wild type mouse, only TA and SOL samples were collected (#). **(B)** Nidogen-1 bands from the western blots in (A) were quantified, normalised to total protein and expressed as relative to wild type PND 122 levels. Grey dashed lines represent the wild type PND 122 expression level. Data are expressed as mean ± SEM and were analysed by two-way ANOVA with Tukey's multiple comparison test. Statistical significance is presented as significance compared to the superscripted age within the same coloured genotype. Differences between genotypes of the same age are indicated in black. * *P ≤ 0.05,* ** *P ≤ 0.01*; *** *P ≤ 0.005;* **** *P ≤ 0.001*. N=3 biological replicates (N=4 biological replicates for WT PND77 TA and SOL)

WT – wild type; GC – gastrocnemius; TA – tibialis anterior; EDL – extensor digitorum longus; SOL – soleus; NMJ – neuromuscular junction; PND - postnatal day; TP - total protein.

Nidogen-2 expression was quantified as the sum of the three observed bands for consistency between ages (Figure 4.3B). In wild type GC, there was a significant peak in nidogen-2 expression at PND 17 (*P ≤ 0.05* compared to WT P77 and P91, Figure 4.2). Interestingly, there was a significant upregulation of nidogen-2 expression in SOD1^{G93A} GC at PND 122 (*P ≤ 0.05*). In the TA, significantly higher nidogen-2 expression was seen in both wild type and SOD1^{G93A} at earlier ages, with a more robust decline observed in wild type tissue (*P ≤ 0.01*, Figure 4.3B). Expression of nidogen-2 in wild type TA was significantly greater than in SOD1^{G93A} at PND 17 (*P ≤ 0.05*). In the EDL muscle, nidogen-2 expression is very closely matched in the two genotypes and shows a highly significant steady reduction from early postnatal ages to adult (Figure 4.3). On the other hand, in the SOL, both wild type and SOD1^{G93A} showed a trend in reducing nidogen-2 over age, but this was only significant between wild type PND 17 and PND 91. The large variation in nidogen-2 expression in PND 17 SOL samples makes it difficult to draw any conclusions.

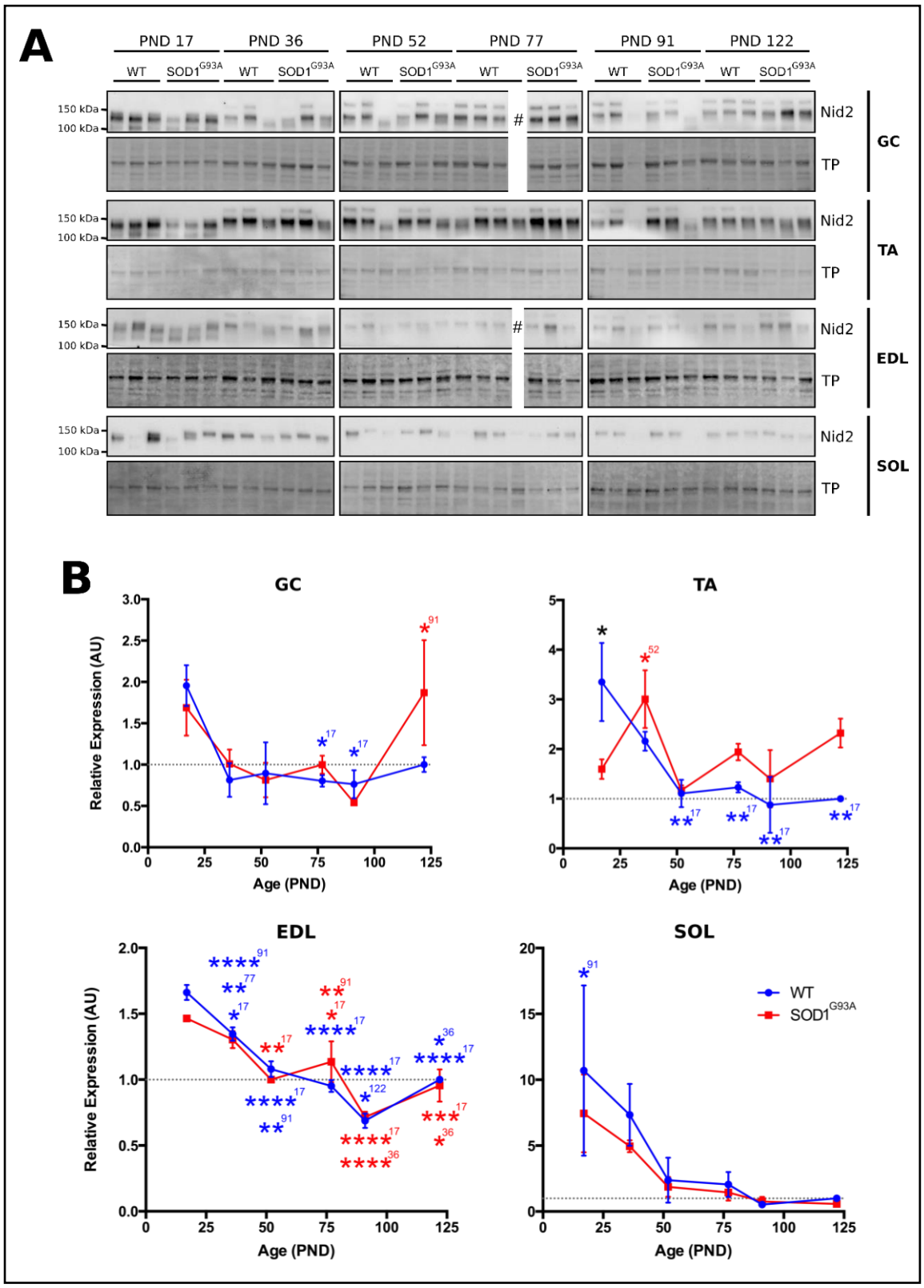

Figure 4.3 Expression of nidogen-2 in wild type and SOD1^{G93A}

Figure 4.3 Expression of nidogen-2 in wild type and SOD1^{G93A} muscles.

(A) Tissue lysates of the GC, TA, EDL and SOL from wild type and SOD1^{G93A} mice were probed for expression of nidogen-2. Muscles were examined at ages where NMJs were still maturing (PND 17–36) as well as ages representing progression of disease in the SOD1^{G93A} model of ALS; PND 52 (pre-symptomatic), PND 77 (early symptomatic), PND 91 (symptomatic), PND 122 (end stage). For one PND 77 wild type mouse, only TA and SOL samples were collected (#). **(B)** Nidogen-2 bands from the western blots in (A) were quantified, normalised to total protein and expressed as relative to wild type PND 122 levels. Grey dashed lines represent the wild type PND 122 expression level. Data are expressed as mean ± SEM and were analysed by two-way ANOVA with Tukey's multiple comparison test. Statistical significance is presented as significance compared to the superscripted age within the same genotype. * $P \leq 0.05$; ** $P \leq 0.01$; *** $P \leq 0.005$. Differences between genotypes of the same age were not significant. N=3 biological replicates (N=4 biological replicates for WT PND77 TA and SOL)

WT – wild type; GC – gastrocnemius; TA – tibialis anterior; EDL – extensor digitorum longus; SOL – soleus; NMJ – neuromuscular junction; PND - postnatal day; TP - total protein.

Overall, expression of both nidogens appeared variable throughout age and different samples. Peaks in expression did not seem to correlate specifically with any age representing periods of disease onset and progression. Higher expression levels for both nidogens were consistently observed at PND 17 in all muscle types investigated. As basement membrane components have been shown to play roles in tissue remodelling and development, this is perhaps unsurprising as nidogens are key components of the extracellular matrix, and skeletal muscle is still adapting during the first postnatal weeks. Investigation of even earlier postnatal ages may have revealed more significant upregulation of nidogen expression. Alterations in nidogen expression as a result of disease progression and muscle denervation may also have been masked due to the small sample sizes of the age groups. Not all mice demonstrate the same severity of symptoms so those that are less affected may have represented a larger proportion of the sample than those who may have had more significant muscle denervation.

4.3 Neurotrophin expression over postnatal muscle development and neuromuscular disease progression

Different nidogen-2 fragments were observed in earlier ages compared to more mature muscles (PND 17 and 36 vs. PND 52-122, Figure 4.3), and it is possible that the role of this matrix protein changes over age or disease. These fragments may have different physiological roles or binding partners. As previously mentioned, the heavy chain fragment of the tetanus neurotoxin (HcT) was shown to colocalise with nidogen-2 in signalling endosomes within primary motor neurons (Bercsenyi et al., 2014). HcT has also been shown to colocalise with the neurotrophin receptors $p75^{NTR}$ and TrkB (Deinhardt et al., 2006). It is therefore possible that nidogens may endogenously bind to either neurotrophins or their receptors and act as mediators in their concentration or signalling at the NMJ, and that HcT hijacks this pathway. I therefore decided to investigate the expression of trophic molecules in the same samples probed for nidogen expression, to assess if there was a correlation in expression patterns.

BDNF expression in the muscle is contentious as variable amounts of mRNA and protein have been reported throughout the literature (Sakuma and Yamaguchi, 2011). The majority of reports suggest that muscle expression of neurotrophins is extremely low (Pitts et al., 2006). In my own samples, BDNF protein expression was undetectable via western blotting (data not shown). GDNF on the other hand has been reported to be robustly expressed in skeletal muscle and Schwann cells and is involved in myogenesis and maturation of singly innervated NMJs (Henderson et al., 1994; Nguyen et al., 1998). High levels of GDNF mRNA was found in intramuscular nerves and mRNA expression of the GDNF receptors GFRα1 and RET was upregulated in motor neurons (Kami et al., 1999). GDNF can bind to heparan sulfate and recent data suggest that heparan sulfates are required for GFRα1- and RET-mediated GDNF signalling (Saarma, 2009). In addition, GDNF binds with high affinity to syndecan, which allows matrix-bound GDNF to signal via delivery to GFRα1/RET or direct activation of Src signalling pathway (ibid.). This is therefore an example of matrix-bound and soluble forms of a trophic molecule being targeted to different signalling pathways – a concept that may be relevant to the nidogen-2 fragments observed previously. GDNF has

also been reported at NMJs and surrounding the axons of peripheral nerves (Suzuki et al., 1998), showing in principle a pattern similar to that demonstrated by nidogens (see Chapter 3).

To determine the expression of GDNF in wild type and SOD1^{G93A} mice during disease progression, I tested the samples probed for nidogen-1 and -2 for GDNF. GDNF expression in wild type GC did not change significantly over the ages investigated (Figure 4.4). However, while in earlier ages wild type and SOD1^{G93A} GDNF expression levels were similar, SOD1^{G93A} PND 122 showed a significant increase in GDNF expression ($P \leq 0.05$, Figure 4.4B). In the TA, both genotypes showed relatively stable GDNF expression which was not significantly different between genotypes. Wild type EDL showed a significant peak in GDNF expression at PND 17 ($P \leq 0.05$), while SOD1^{G93A} TA was relatively stable. Conversely, both wild type and SOD1^{G93A} SOL showed the lowest GDNF expression at PND 17, which was significantly lower than older ages in wild type samples ($P \leq 0.05$, Figure 4.4B). No significant differences were observed between the genotypes in any of the muscle samples and ages investigated (Figure 4.4).

The expression of the GDNF co-receptor GFRα1 was also examined in these samples (Figure 4.5). In the GC, both genotypes showed relatively steady levels of GFRα1 expression (Figure 4.5B). The TA displayed a sharp and significant drop in the levels of GFRα1 in both genotypes after PND 17 ($P \leq 0.05$, Figure 4.5B). In the EDL, a less dramatic, but still significant, reduction in GFRα1 expression was observed in both genotypes over age ($P \leq 0.05$, Figure 4.5B). GFRα1 expression in the SOL was closely matched between genotypes at all ages except PND 36. In the wild type there was a peak in GFRα1 expression significantly different to the levels seen in older samples ($P \leq 0.05$). This was not observed in SOD1^{G93A} PND 36 SOL, but the difference between genotypes was not statistically significant.

Expression profiles of GDNF and its co-receptor GFRα1 did not follow the same or complementary patterns. There was a tendency for a reduction in GFRα1 expression over age. I also did not detect shared patterns between the expression of GDNF/GFRα1 and nidogens.

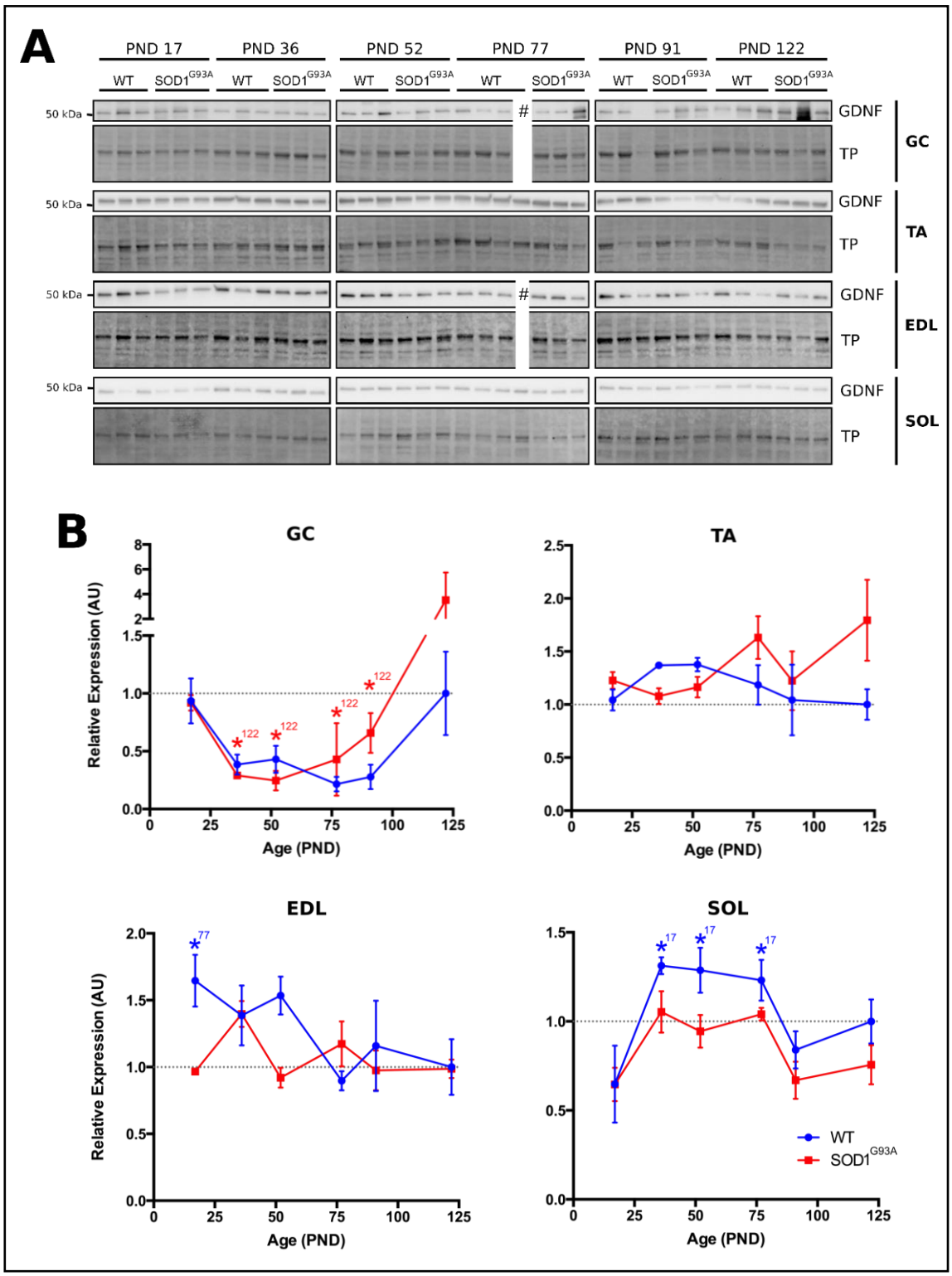

Figure 4.4 Expression of GDNF in wild type and SOD1^{G93A}

Figure 4.4 Expression of GDNF in wild type and SOD1^{G93A} muscles.

(A) Tissue lysates of the GC, TA, EDL and SOL from wild type and SOD1^{G93A} mice were probed for expression of GDNF. Muscles were examined at ages where NMJs were still maturing (PND 17–36) as well as ages representing progression of disease in the SOD1^{G93A} model of ALS; PND 52 (pre-symptomatic), PND 77 (early symptomatic), PND 91 (symptomatic), PND 122 (end stage). For one PND 77 wild type mouse, only TA and SOL samples were collected (#). **(B)** GDNF bands from the western blots in (A) were quantified, normalised to total protein and expressed as relative to wild type PND 122 levels. Grey dashed lines represent the wild type PND 122 expression level. Data are expressed as mean ± SEM and were analysed by two-way ANOVA with Tukey's multiple comparison test. Statistical significance is presented as significance compared to the superscripted age within the same genotype. * $P \leq 0.05$. Differences between genotypes of the same age were not significant. N=3 biological replicates (N=4 biological replicates for WT PND77 TA and SOL)

WT – wild type; GC – gastrocnemius; TA – tibialis anterior; EDL – extensor digitorum longus; SOL – soleus; NMJ – neuromuscular junction; PND - postnatal day; TP - total protein.

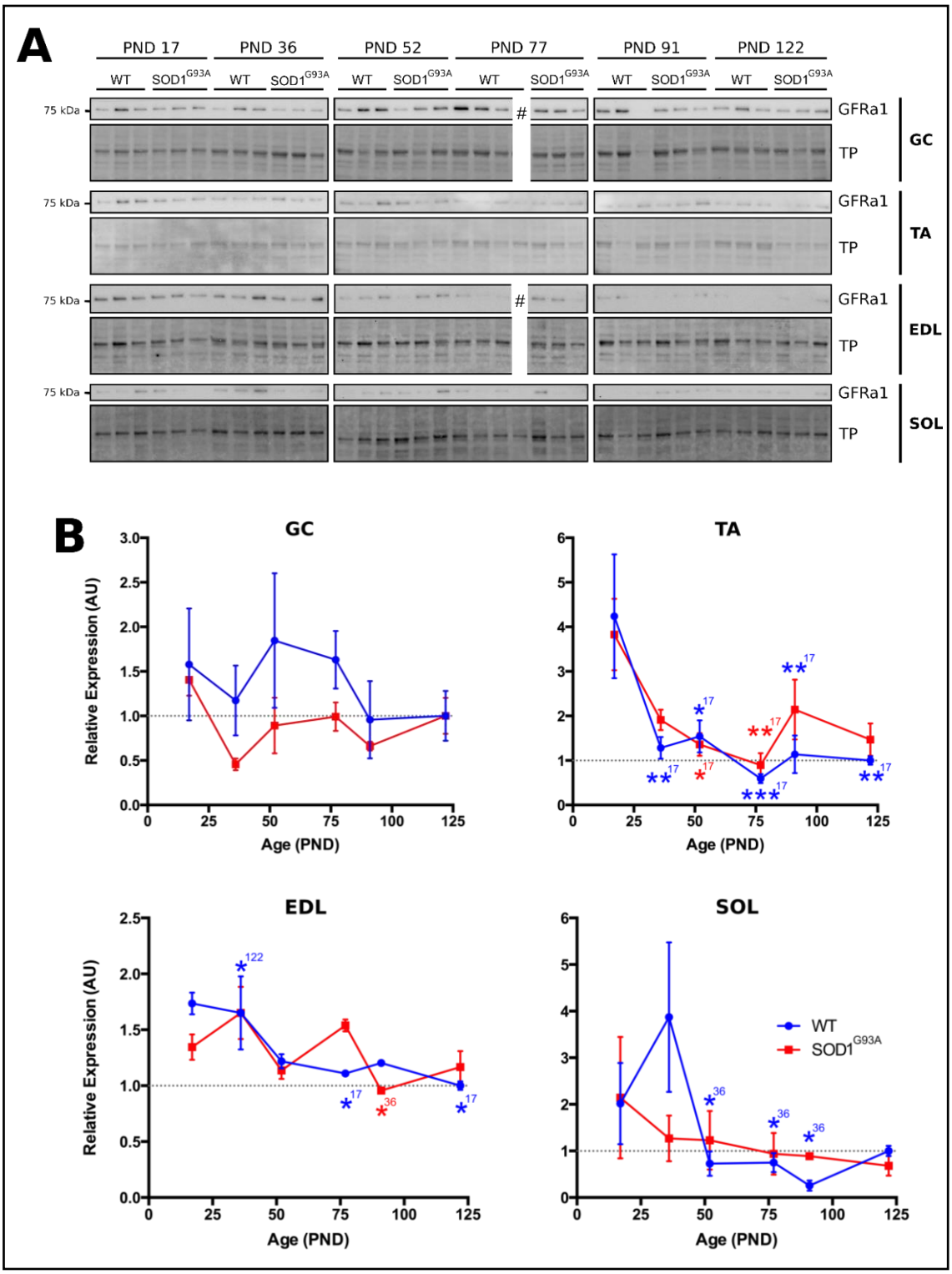

Figure 4.5 Expression of GFRα1 in wild type and SOD1^{G93A}

Figure 4.5 Expression of GFRα1 in wild type and SOD1^{G93A} muscles.

(A) Tissue lysates of the GC, TA, EDL and SOL from wild type and SOD1^{G93A} mice were probed for expression of GFRα1. Muscles were examined at ages where NMJs were still maturing (PND 17–36) as well as ages representing progression of disease in the SOD1^{G93A} model of ALS; PND 52 (pre-symptomatic), PND 77 (early symptomatic), PND 91 (symptomatic), PND 122 (end stage). For one PND 77 wild type mouse, only TA and SOL samples were collected (#). **(B)** GFRα1 bands from the western blots in (A) were quantified, normalised to total protein and expressed as relative to wild type PND 122 levels. Grey dashed lines represent the wild type PND 122 expression level. Data are expressed as mean ± SEM and were analysed by two-way ANOVA with Tukey's multiple comparison test. Statistical significance is presented as significance compared to the superscripted age within the same genotype. * $P \leq 0.05$. Differences between genotypes of the same age were not significant. N=3 biological replicates (N=4 biological replicates for WT PND77 TA and SOL)

WT – wild type; GC – gastrocnemius; TA – tibialis anterior; EDL – extensor digitorum longus; SOL – soleus; NMJ – neuromuscular junction; PND - postnatal day; TP - total protein.

4.4 Nidogen-1 knock out mouse model

To further investigate the role of nidogen in the muscle, our collaborators at MRC Harwell have generated a nidogen-1 knock out mouse model. The nidogen-1 allele has been generated to target an essential exon for loxP recombination thereby generating a genetic null when crossed with a Cre-expression mouse. The line investigated here is a ubiquitous knock out developed by crossing the floxed nidogen-1 mice to Cre-actin mice. These mice have been observed to display a mild hindlimb ataxia phenotype in addition to a stress-induced seizure activity (T. Cunningham, personal communication). This is consistent with reports from previous nidogen-1 knock out models (Bader et al., 2005; Halfter et al., 2002; Murshed et al., 2000). Considering this phenotype, hindlimb muscles (quadriceps femoris and triceps surae) and brain tissue were sampled from mice homozygous and heterozygous for the knock out allele, as well as their wild type littermates (*Nid1*$^{-/-}$, *Nid1*$^{-/+}$. *Nid1*$^{+/+}$ respectively). Tissue was then examined for nidogen-1 expression to confirm the penetrance of the knock out as well as nidogen-2 expression to investigate possible compensatory upregulation.

The first muscle examined was the triceps surae mixed muscle group. This is comprised of the soleus, gastrocnemius and plantaris muscles in the mouse hindlimb. Whole muscle lysates were probed for expression of nidogen-1 and showed complete lack of detectable nidogen-1 protein in the homozygous knock out tissues (*Nid1*$^{-/-}$, Figure 4.6A). Quantification of these samples indicated a

slight trend in lower expression of nidogen-1 in *Nid1*$^{-/+}$ compared to *Nid1*$^{+/+}$, however this was not significant (Figure 4.6B). Thus, a single functioning allele of the nidogen-1 gene appears to be sufficient for maintenance of normal nidogen-1 protein expression levels in the triceps surae muscle.

Investigation of nidogen-2 in the triceps surae revealed a striking increase in protein expression in *Nid1*$^{-/-}$ muscles compared to both *Nid1*$^{-/+}$ and *Nid1*$^{+/+}$ ($P \leq 0.05$, Figure 4.6C, D). As no significant difference in nidogen-2 expression was observed between *Nid1*$^{-/+}$ and *Nid1*$^{+/+}$, where nidogen-1 expression is unaltered, this suggests an upregulation in nidogen-2 may serve to compensate for the lack of nidogen-1 in knock out muscle. Interestingly, the scale of nidogen-2 upregulation far exceeds that of nidogen-1 downregulation. This is likely to reflect the more ubiquitous expression pattern of nidogen-1 compared to basal nidogen-2, and the need for a huge increase in nidogen-2 expression to fully occupy the niche usually dominated by nidogen-1. Alternatively, this may represent the ability of nidogen-2 to replace nidogen-1 but incompletely.

GDNF expression was also investigated in these animals as GDNF is an important neurotropic factor in muscle, as previously described, in addition to being implicated in epileptic activity. Upregulation of GDNF mRNA and protein in the dentate gyrus and hippocampus and upregulation of GFRα1 and RET mRNA in the hippocampus has been found in response to kainic acid-induced seizures (Mikuni et al., 1999; Reeben et al., 1998). The delivery of a GDNF transgene via an rAAV-vector was also shown to ameliorate seizure activity in models of temporal lobe epilepsy (Kanter-Schlifke et al., 2007). Analysis of GDNF expression in the triceps surae indicated no significant differences between the genotypes (Figure 4.6E, F). This is consistent with the lack of obvious associations between nidogen-1 and GDNF expression patterns in the individual GC, SOL, TA and EDL muscles previously examined (Figure 4.2 and Figure 4.4).

An alternative muscle group was also investigated to check consistency in expression patterns between muscles. The quadriceps muscle group comprises of four individual muscles: rectus femoris, vastus intermedius, vastus lateralis, and the vastus medialis. Together this mixed group of muscles are the major extensors of the knee joint. Nidogen-1 expression analysis confirmed the knock out in *Nid1*$^{-/-}$ quadriceps tissue, and also the lack of haploinsufficiency for the *Nid1* gene (Figure 4.7A, B). Nidogen-2 showed the same pattern as found in the triceps

surae; a significant increase in nidogen-2 expression in *Nid1*$^{-/-}$ muscle compared to *Nid1*$^{-/+}$ and *Nid1*$^{+/+}$ (*P ≤ 0.05*, Figure 4.7B). However, this increase was not as dramatic as in the triceps, perhaps suggesting a greater need for compensation in the muscles or one of the muscles of the triceps group compared to those in the quadriceps. Expression of GDNF in the quadriceps was not significantly different between genotypes, again consistent with expression in the triceps surae.

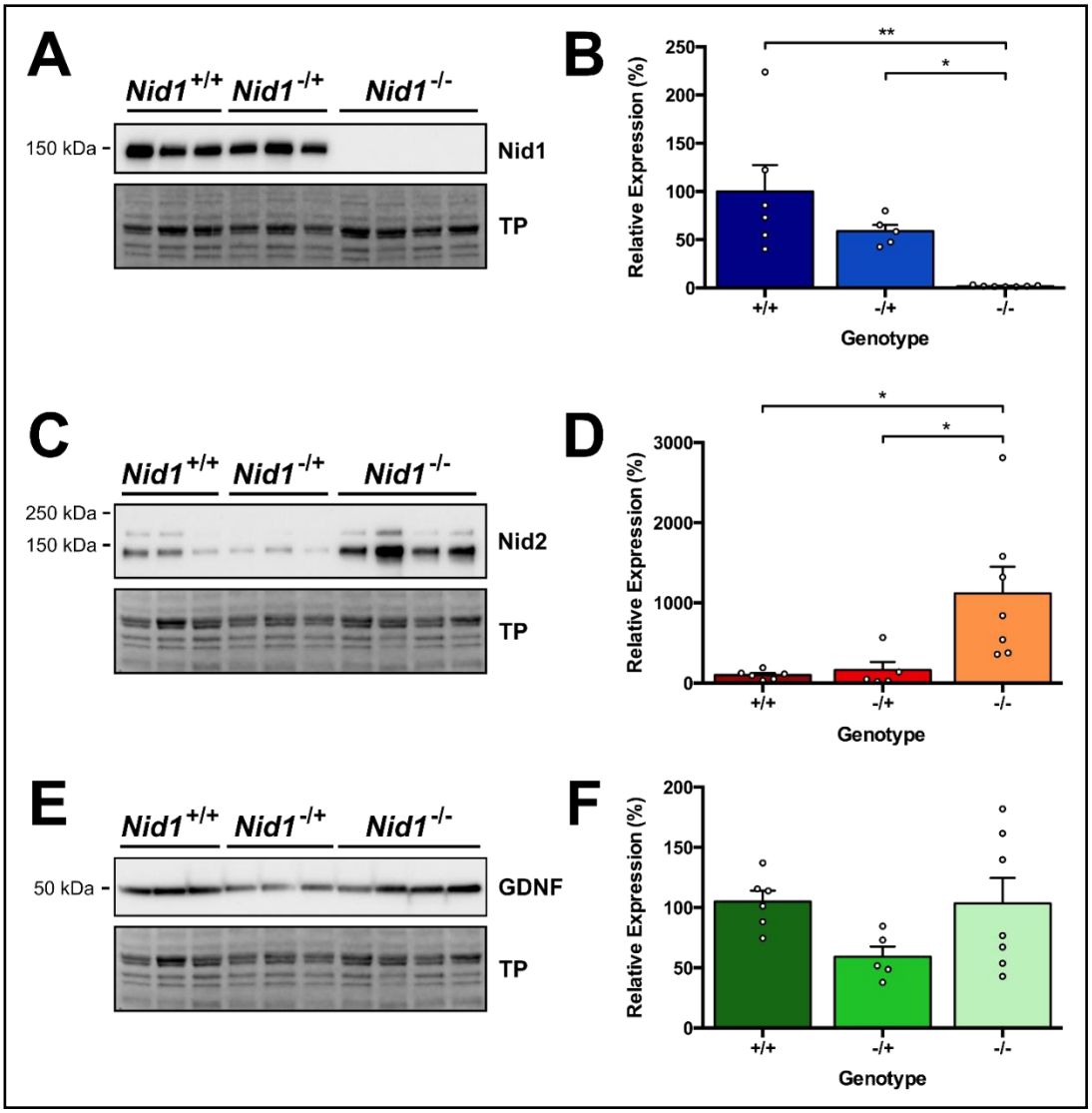

Figure 4.6 Expression of nidogens and GDNF in triceps surae muscle from nidogen-1 knock out mice.

(A) Triceps surae muscle from wild type (*Nid1*$^{+/+}$), heterozygous (*Nid1*$^{-/+}$) and homozygous null (*Nid1*$^{-/-}$) mice were probed for nidogen-1 protein expression via western blot. A blot of representative tissue samples is shown. **(B)** Nidogen-1 bands were quantified, normalised to total protein and expressed as a percentage of the mean of wild type levels. **(C, D)** Triceps were also probed for nidogen-2 expression and **(E, F)** GDNF expression. Data are expressed as mean ± SEM and were analysed using the Kruskal-Wallis test with Dunn's multiple comparisons test (* *P ≤ 0.05*; ** *P ≤ 0.01*). Data points on graphs indicate number of biological replicates for each group. *TP - total protein.*

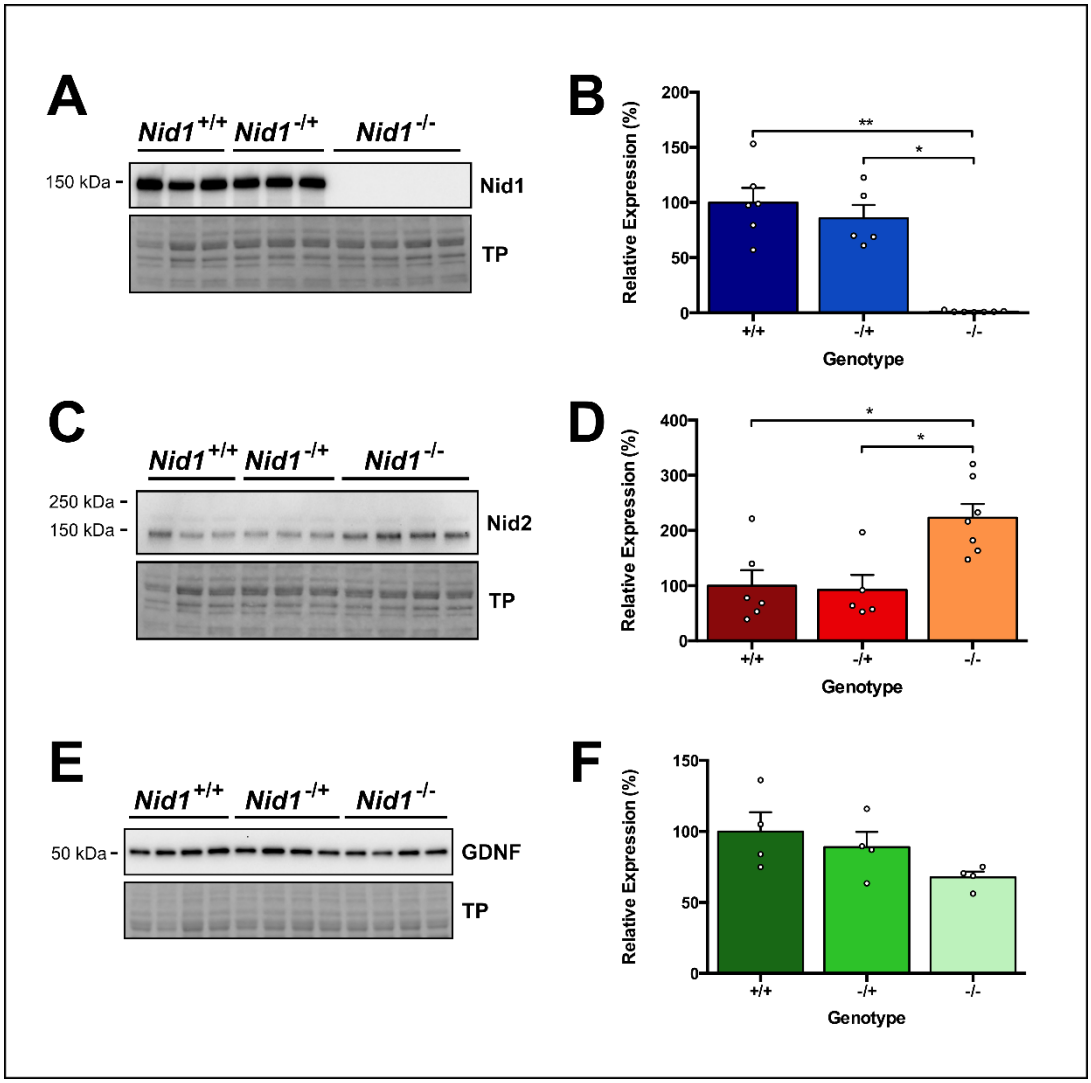

Figure 4.7 Expression of nidogens and GDNF in quadriceps muscle from nidogen-1 knock out mice.

(A) Quadriceps muscle from wild type (*Nid1*$^{+/+}$), heterozygous null (*Nid1*$^{-/+}$) and homozygous null (*Nid1*$^{-/-}$) mice were probed for nidogen-1 protein expression via western blot. A blot of representative tissue samples is shown. **(B)** Nidogen-1 bands were quantified, normalised to total protein and expressed as a percentage of the mean of wild type levels. **(C, D)** Quadriceps were also probed for nidogen-2 expression and **(E, F)** GDNF expression. Data are expressed as mean ± SEM and were analysed using the Kruskal-Wallis test with Dunn's multiple comparisons test (* $P \leq 0.05$; ** $P \leq 0.01$). Data points on graphs indicate number of biological replicates for each group. *TP - total protein.*

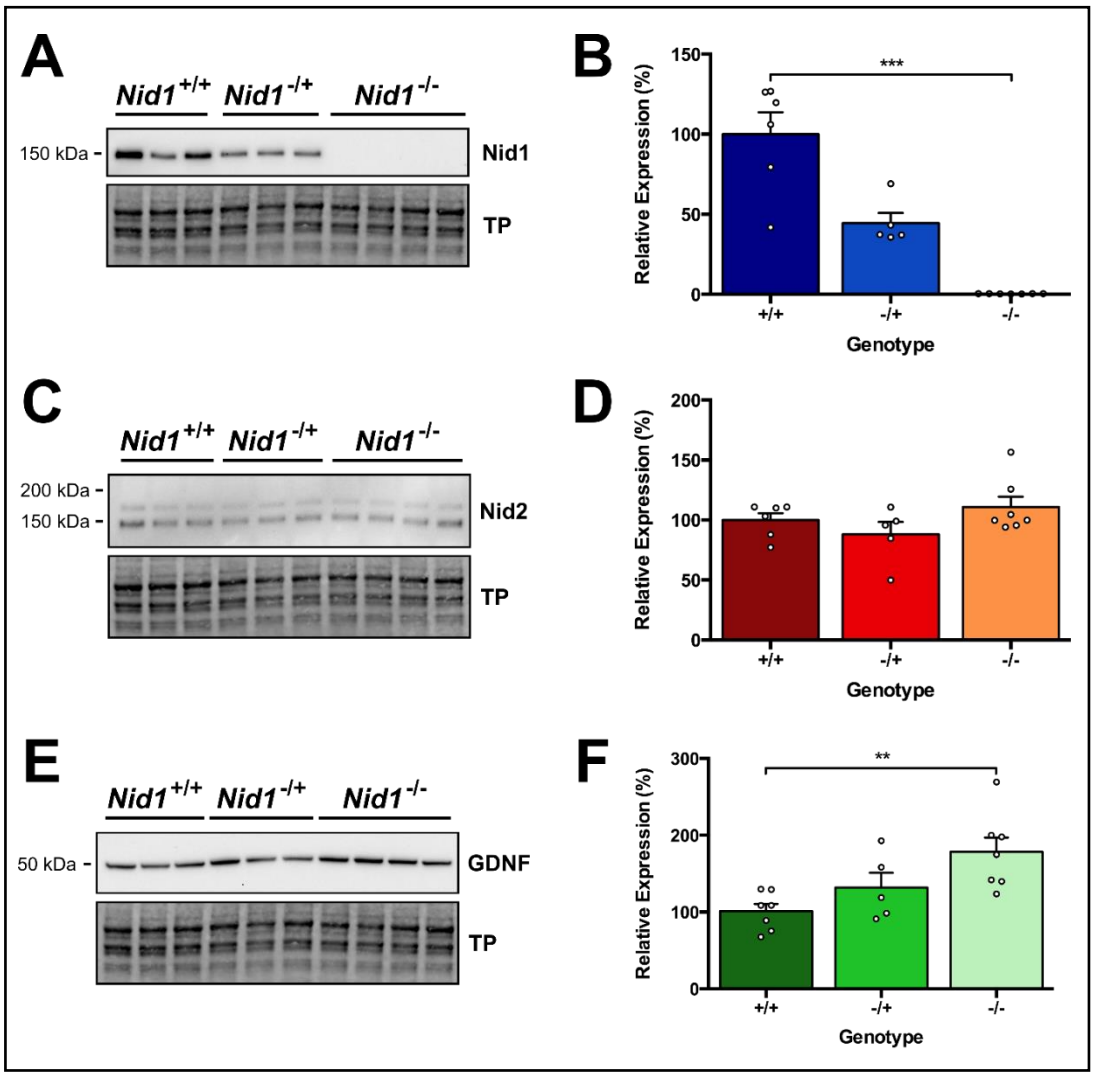

Figure 4.8 Expression of nidogens and GDNF in brain from nidogen-1 knock out mice.

(A) Brain tissue from wild type (*Nid1*$^{+/+}$), heterozygous null (*Nid1*$^{-/+}$) and homozygous null (*Nid1*$^{-/-}$) mice were probed for nidogen-1 protein expression via western blot. A blot of representative tissue samples is shown. **(B)** Nidogen-1 bands were quantified, normalised to total protein and expressed as a percentage of the mean of wild type levels. **(C, D)** Quadriceps were also probed for nidogen-2 expression and **(E, F)** GDNF expression. Data are expressed as mean ± SEM and were analysed using the Kruskal-Wallis test with Dunn's multiple comparisons test (** $P \leq 0.01$; *** $P \leq 0.005$). Data points on graphs indicate number of biological replicates for each group. *TP - total protein.*

As the *Nid1*$^{-/-}$ mice display seizure-like activity, the brain tissue was also examined (Figure 4.8). Expression of nidogen-1 was undetectable in *Nid1*$^{-/-}$ samples (Figure 4.8A). However, in contrast to the muscle tissue investigated, there appeared to be dose dependent nidogen-1 protein expression in *Nid1*$^{-/+}$ brain, although this did not reach statistical significance (Figure 4.8B). Nidogen-1 expression in this group was also not significantly different to the knock out, indicating a possible haploinsufficiency in the brain which was unable to reach statistical significance due to the presence of some low-expressing wild type samples.

Interestingly, nidogen-2 expression appears unaltered in *Nid1*$^{-/-}$ brain in contrast to knock out muscle tissue (Figure 4.8C, D). This indicates that nidogen-2 is unable to compensate for nidogen-1 loss in the brain, perhaps revealing a different role for nidogen-1 in brain and muscle, as well as different co-regulatory mechanisms. The lack of a compensatory mechanism in the brain of these knock out mice could explain the dramatic seizure activity observed in these animals.

In addition to the different nidogen-2 pattern observed in brain compared to muscle, GDNF also shows a different pattern in brain. In *Nid1*$^{-/-}$ brain GDNF is significantly upregulated *($P \leq 0.005$*, Figure 4.8F). As GDNF expression has been previously shown to increase as a result of seizure activity (Mikuni et al., 1999), it is possible that this is a downstream effect of the seizures seen in nidogen-1 knock out mice. However, a correlation analysis revealed that expression of nidogen-1 is inversely correlated with GDNF expression in individual animals (r= -0.6863, *$P \leq 0.05$*, Figure 4.9). As all *Nid1*$^{-/-}$ mice were found to present with seizure episodes with no obvious difference in their severity, if GDNF expression were simply a downstream effect of seizure

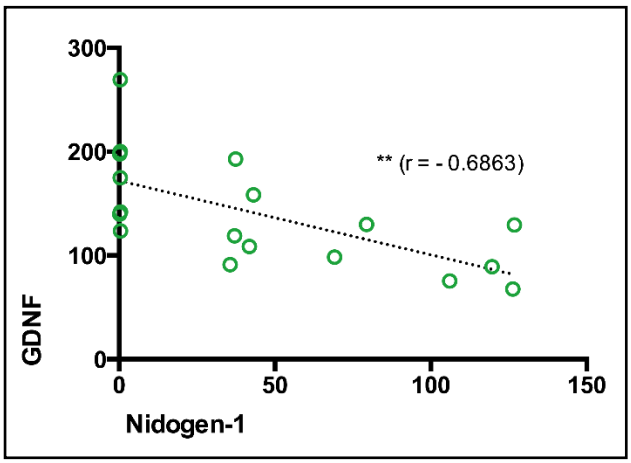

Figure 4.9 Correlation of nidogen-1 and GDNF expression in Nid1-/- brain.

The correlation of GDNF and nidogen expression in brain tissue from *Nid1*$^{-/-}$, *Nid1*$^{-/+}$ and *Nid1*$^{+/+}$ mice was analysed using Spearman correlation. ** *$P \leq 0.01$;* N = 16 biological replicates

activity in the brain, increased GDNF would not be expected to correlate with the downregulation of nidogen-1. This is not a correlation found in muscle, so may show a specific relation between nidogen-1 function in the brain.

4.5 Conclusions

Prior to this work, a quantification of nidogen protein expression over different postnatal ages had not been reported. Neither had an analysis of expression during disease progression in a model of neuromuscular degeneration, where basement membrane remodelling may be expected to occur. My experiments indicate that expression levels show substantial variation, and no obvious pattern can be discerned. No significant differences were found between wild type mice and the $SOD1^{G93A}$ mouse model of ALS. Collection of larger sample sizes than those used in this pilot experiment may result in more significant difference between these genotypes.

An interesting finding from these experiments was the observation of different nidogen-2 species migrating at different molecular weights in SDS-PAGE between the early (PND 17) age group and adult ages. This correlates with the timescale that Fox et al. found a change in nidogen-2 distribution in the muscle, from ubiquitous expression in all muscle basement membranes, to a restriction to the NMJ (Fox et al., 2008). The altered distribution may therefore represent a change in function associated with different proteolytic fragments or post-translational modifications. Further investigation into this phenomenon could examine the specific identity of these modifications via affinity purification and proteomic analysis.

A new nidogen-1 knock out mouse model has been generated by collaborators at the MRC Harwell Institute. This model harbours a conditional nidogen-1 allele flanked by loxP sites. This will allow the production of conditional nidogen-1 mutants with the gene knocked out in specific cell or tissue types. In this study, a ubiquitous nidogen-1 knock out line was used, derived from crossing the nidogen-1 floxed model with a Cre-actin mouse line. My work has confirmed the absence of detectable nidogen-1 protein in brain and muscle tissue. In addition, nidogen-2 was upregulated in nidogen-1 knock out muscle tissue, in agreement with previous suggestions in the literature of a possible compensatory role. Muscle tissue therefore appears to possess a transcription regulation mechanism

whereby reduced levels of nidogen-1 feeds back to increase nidogen-2 expression. However, I have shown that this compensation does not occur in the brain, which suggests that there may be alternative functions for nidogens in different tissues. In the brain, nidogen-1 may have a function for which nidogen-2 cannot compensate, and so there is no feedback from this pathway to upregulate nidogen-2 expression in the absence of nidogen-1.

GDNF was also found to have differential regulation in nidogen-1 knock out brain and muscle. Expression of GDNF was unaffected by the absence of nidogen-1 in muscle tissue. However, nidogen-1 knock out brain tissue showed a significant increase in GDNF expression. The level of GDNF expression was negatively correlated with the level of nidogen-1 expression which is perhaps indicative of a shared pathway. Basement membrane components have been shown to potentiate the signalling of various trophic signalling molecules. Indeed, engineered growth factors with artificially increased affinity for the extracellular matrix show higher levels of trophic activity than the endogenous wild type versions (Martino et al., 2014). Therefore, there is precedent for nidogen playing a facilitatory role with GDNF signalling in the CNS. Nidogen interaction with neurotrophic pathways therefore warrants further investigation.

Chapter 5. Nidogens and neurotrophins

5.1 Specific Aims

In Chapter 4, I showed that nidogen-1 expression levels negatively correlated with GDNF expression in the brains of wild type mice and those homozygous or heterozygous for a nidogen-1 knock out allele. While correlation does not necessarily indicate causation, it is possible that nidogens are involved in signalling pathways of trophic molecules such as GDNF.

It is well established that other basement membrane components can participate in growth factor signalling, through a range of mechanisms. Binding of growth factors to the basement membrane can act to sequester and decrease the diffusion of soluble factors, thereby creating a 3-dimensional gradient. For example, fibroblast growth factors (FGFs) bind to the heparan sulfate proteoglycan perlecan which creates a reservoir of FGF. This reservoir is released from the extracellular matrix for soluble ligand signalling via cleavage by heparanase (Patel et al., 2007). In an alternative mechanism, interactions with basement membrane components can potentiate growth factor signalling as they act as captors to enhance local concentrations or even as cofactors. Vascular endothelial growth factor (VEGF) for example, binds to the basement membrane component fibronectin and this interaction promotes the downstream effects of VEGF signalling (Wijelath et al., 2006).

Binding of growth factors to the basement membrane therefore localises a pool of these molecules at physiologically relevant sites to regulate their behaviour. Considering this, I wanted to investigate whether nidogens play a role in neurotrophic signalling in motor neurons. To address this question my aims were as follows:

a) Assess whether nidogens colocalise with neurotrophin receptors in motor neurons;
b) Investigate the effect of nidogens on downstream neurotrophin signalling.

5.2 Expression of nidogens in mixed ventral horn cultures

To investigate the involvement of nidogens in neurotrophin signalling, the model system I chose was primary mixed ventral horn cultures. Preparation of this culture provides a large population of primary motor neurons derived from the ventral horn of the spinal cord which is dissected from mouse embryos at gestational age 12.5-13.5 days. However, since this culture also contains a mixture of other cell types, it is not a pure neuronal culture system. As I was predominantly interested in the neuronal component of nidogen signalling, I decided to first characterise the expression and distribution of nidogens in different cell types throughout this mixed culture. Astrocytes comprise a significant proportion of the spinal cord cell population, with a plethora of important roles, from modulation of neurotransmission to mediation of inflammatory responses and maintenance of the blood brain barrier (Chung et al., 2015; Sofroniew, 2014; Whetstone et al., 2003). Astrocytes can express components of the basement membrane such as laminin and type IV collagen (Liesi and Kauppila, 2002; van der Laan et al., 1997) and have been shown to secrete nidogen-1 in culture (Grimpe et al., 1999). Astrocytes were examined in mixed ventral horn cultures for expression of nidogen-1 and nidogen-2 by immunofluorescence using glial fibrillary acidic protein (GFAP) as a marker of astrocytes (Figure 5.1). Cultures were maintained on glass coverslips coated with a laminin preparation which contains nidogens. Immunoreactivity against nidogen-1 indicated no significant expression associated with GFAP-positive astrocytes above that observed on the coverslip coating (Figure 5.1A). Nidogen-2 did associate with GFAP-positive astrocytes, but this was not at levels different to that of surrounding GFAP-negative cells (Figure 5.1B).

OLIG2 is a basic helix-loop-helix (bHLH) transcription factor that specifies the transition of multipotent neural stem cells in the spinal cord to oligodendrocyte precursor cells (OPCs; Ono et al., 2008). These OPCs subsequently differentiate into oligodendrocytes as well as motor neurons and type II astrocytes in temporally regulated pathways (Masahira et al., 2006; Suzuki et al., 2017). Immunostaining for OLIG2 as a marker for cells of OPC lineage revealed expression of both nidogens in these cells in ventral horn cultures (Figure 5.2). Nidogen-1 was found in a very intense perinuclear staining pattern in OLIG2-

positive cells, in contrast to the more diffuse, punctate staining seen in OLIG2-negative cells (Figure 5.2A). Nidogen-2 was not observed in the high intensity globular pattern of nidogen-1 and instead showed a punctate pattern distributed throughout OLIG2-positive cells with a more branched morphology (Figure 5.2B). A perinuclear accumulation was also seen for nidogen-2 in these cells.

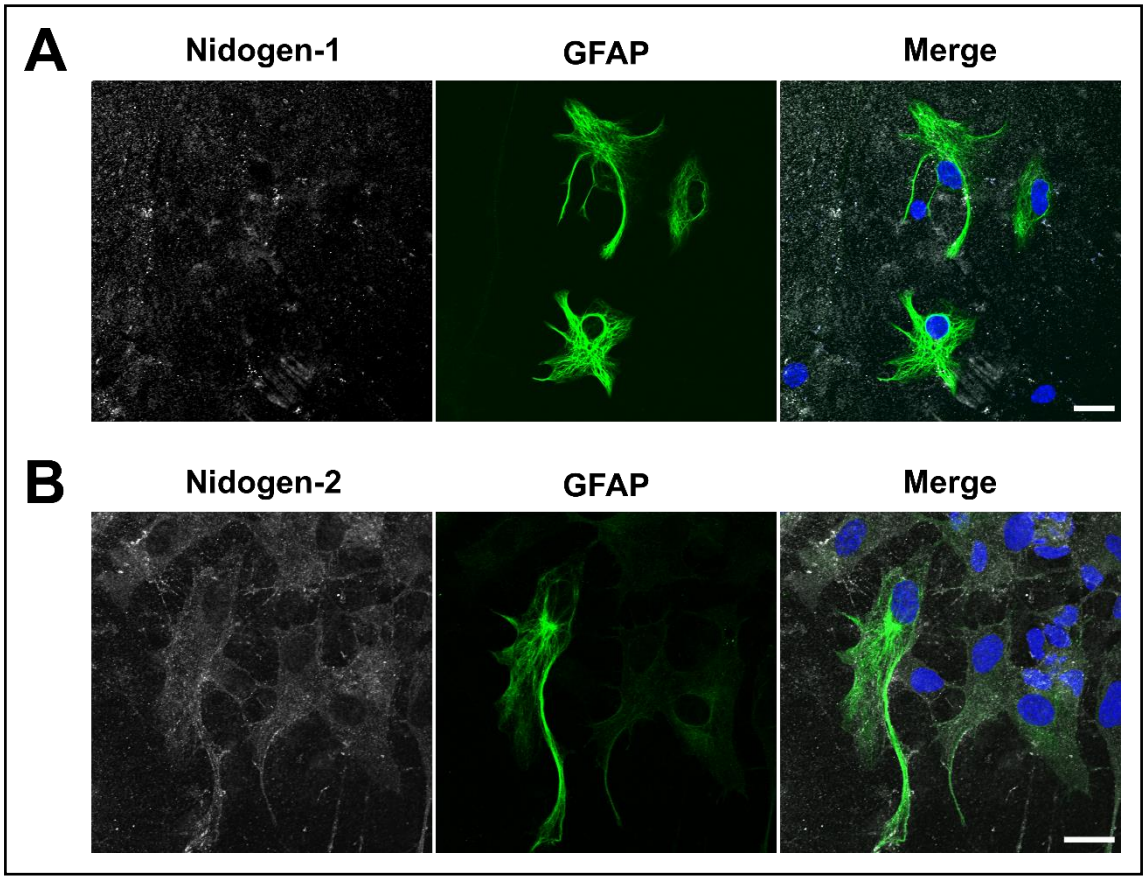

Figure 5.1 Nidogens in astrocytes

Astrocytes in mixed spinal cord ventral horn cultures were identified using glial fibrillary acidic protein (GFAP) as a marker at DIV6. **(A)** Nidogen-1 was not overtly associated with GFAP-positive astrocytes. **(B)** Nidogen-2 showed associated with GFAP-positive astrocytes, but not above that seen in other nearby cell types. DAPI-positive nuclei are blue. Scale bar = 20 µm

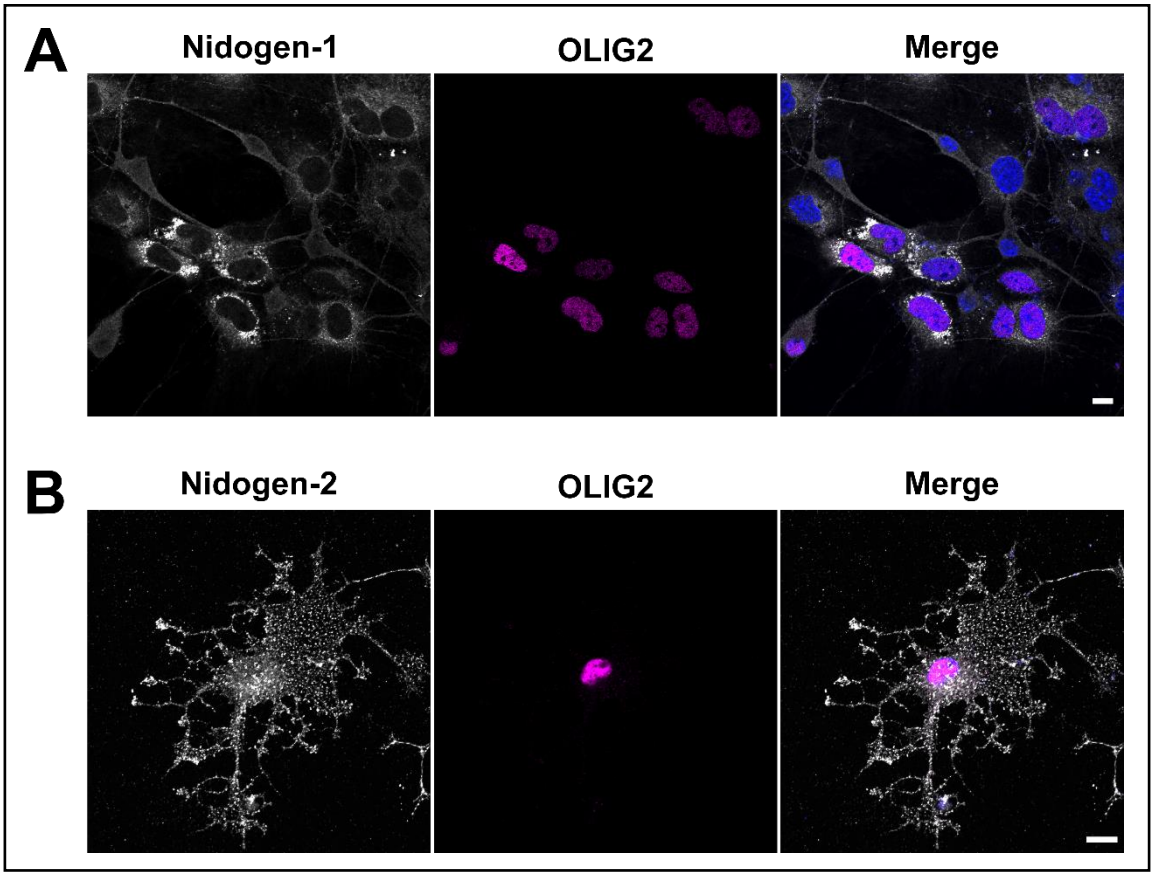

Figure 5.2 Nidogens in cells of oligodendrocyte precursor cell lineage

Oligodendrocyte precursor cells (OPCs) and cells of that lineage were identified in mixed spinal cord ventral horn cultures at DIV6 using the transcription factor OLIG2 as a marker. **(A)** Nidogen-1 appears strongly in OLIG2-positive cells compared to surrounding cell types. Nidogen-1 was observed surrounding the nucleus of these cells. **(B)** Nidogen-2 was also present in OLIG2-positive cells. However, these cells had a morphology suggestive of differentiated oligodendrocytes rather than OPCs. DAPI-positive nuclei are blue. Scale bar = 10 µm

As OLIG2 is a marker for a range of cell types downstream of the OPC stage, to understand whether the expression patterns of nidogens observed in these cells is related to their stage of differentiation I stained cultures for SOX10, a marker of maturing oligodendrocytes. SOX10 is a high-mobility-group (HMG) transcription factor responsible for regulation of myelin gene expression in differentiating oligodendrocytes (Küspert et al., 2011; Stolt et al., 2002). Both nidogens showed similar patterns of expression in SOX10-positive cells, with high expression in the cell bodies and diffuse puncta in the cellular processes (Figure 5.3).

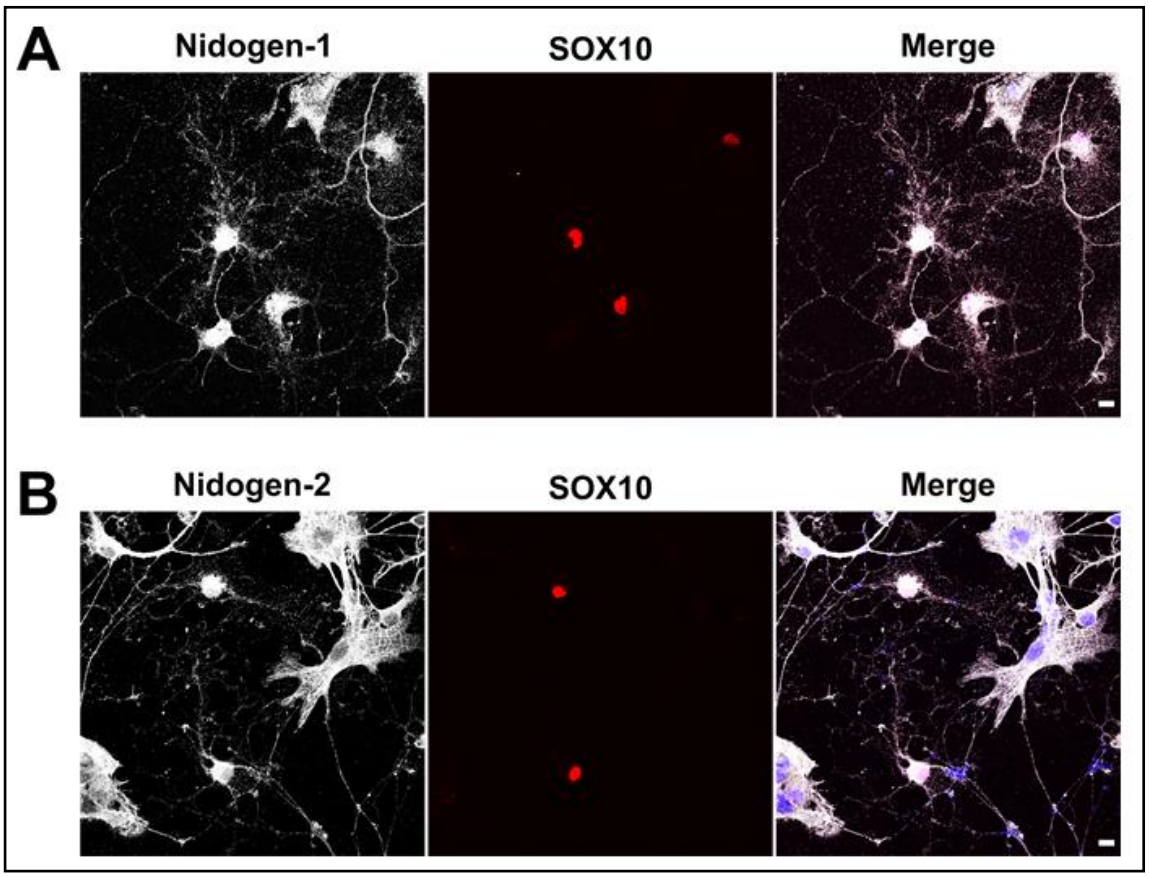

Figure 5.3 Nidogens in maturing oligodendrocytes

Maturing oligodendrocytes were identified in mixed spinal cord ventral horn cultures at DIV6 using the transcription factor SOX10 as a marker. Nidogen-1 **(A)** and nidogen-2 **(B)** were both present in SOX10-positive cells with highest intensity in the cell bodies. DAPI-positive nuclei are blue. Scale bar = 10 µm

Mesenchymal cells such as fibroblasts comprise a substantial proportion of mixed ventral horn cultures as these cells are mitotic and therefore continue to proliferate while terminally differentiated neurons and glia do not. Mesenchymal cells have previously been shown to secrete nidogen-1 in primary epithelial organoids (Pujuguet et al., 2000). However, this has not been shown for nidogen-2 or in neuronal tissue. I therefore investigated nidogen expression in fibroblasts within my ventral horn cultures using vimentin as a marker. Both nidogen-1 and nidogen-2 were found to be associated with vimentin-positive cells (Figure 5.4). Nidogen-1 was present in intense perinuclear granules which were not clearly present in nidogen-2 expressing cells (Figure 5.4A). Nidogen-2 appeared to be particularly enriched at the edges of cells indicating a role in adhesion and migration of these cells (Figure 5.4B).

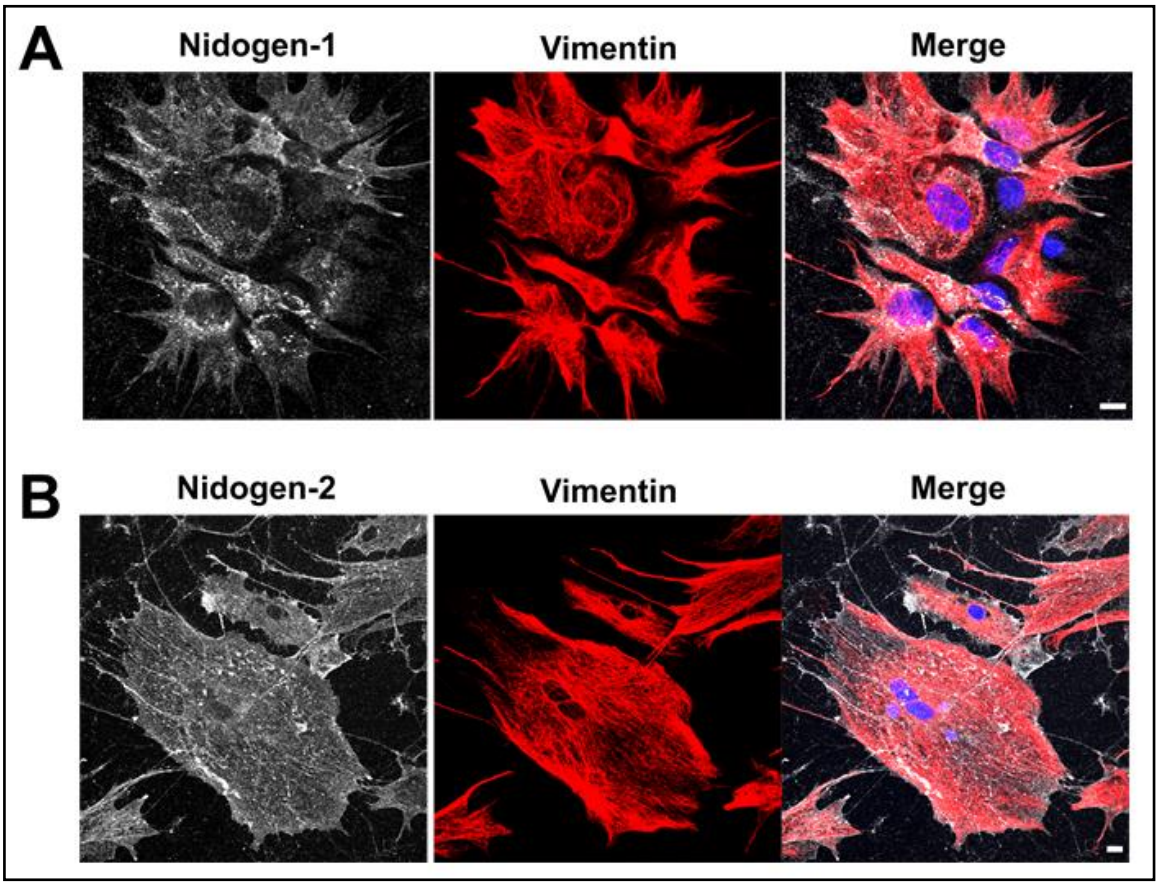

Figure 5.4 Nidogens in fibroblasts

Fibroblasts were identified in mixed spinal cord ventral horn cultures at DIV6 using the intermediate filament protein vimentin as a marker. **(A)** Nidogen-1 was observed associated with vimentin-positive cells with regions of enriched nidogen-1 surrounding the nuclei. **(B)** Nidogen-2 was also associated with vimentin-positive cells but showed a more homogeneous distribution than nidogen-1. DAPI-positive nuclei are blue. Scale bar = 10 µm

In summary, nidogens appear to be present in large puncta within OLIG2-positive OPCs, SOX10-positive oligodendrocytes and vimentin-positive fibroblasts with perinuclear enrichment, suggesting the presence of nidogens in the secretory pathway of these cell types. A more diffuse staining which encompassed the cell areas was also observed, which suggests the incorporation of nidogens into the extracellular matrix involved into the adhesion of these cells to the substrate. This diffuse staining was also observed in GFAP-positive astrocytes for nidogen-2 but not nidogen-1. This could indicate a greater role of nidogen-2 in astrocyte adhesion, but it is possible that the greater abundance of nidogen-1 than nidogen-2 in the laminin coating preparation means that astrocytes do not noticeably sequester nidogen-1 above coating levels. Nidogens are therefore ubiquitously expressed throughout the cells of mixed ventral horn cultures.

5.3 Interactions between nidogens and Trk receptors

Nidogens have previously been shown to interact with the binding fragment of tetanus neurotoxin (HcT; Bercsenyi et al., 2014). Independently, HcT has been shown to localise to signalling endosomes positive for the neurotrophin receptors TrkB and $p75^{NTR}$ (Deinhardt et al., 2006; Lalli and Schiavo, 2002). TrkB and $p75^{NTR}$ are receptors for the neurotrophin BDNF. Thus, it may be that HcT gains access to motor neurons by hijacking an endogenous neurotrophin signalling pathway that is modulalted by nidogens. This proposed signalling model is outlined in Figure 5.5. Neuromuscular activity has been shown to induce expression and release of neurotrophic factors such as BDNF, GDNF and NT-4 by skeletal muscle (Funakoshi et al., 1995; Gómez-Pinilla et al., 2001; Wehrwein et al., 2002). These neurotrophins bind to their cognate receptors on the motor neuron presynaptic terminal and initiate downstream signalling pathways. HcT has been shown to bind to nidogens, which is known to form stable links with laminin within the basement membrane (Bercsenyi et al., 2014). We propose that this complex may interact with neurotrophin receptors and be internalised together into signalling endosome. This interaction may occur by binding of nidogens to the trophic factors and/or their receptors, or via some other components of the receptor complex such as the leukocyte antigen-related (LAR) protein phosphatase. The laminin-nidogen complex has been reported to bind to LAR, and LAR in turn has been associated with BDNF-TrkB signalling (O'Grady et al., 1998; Yang et al., 2006).

To investigate this potential mechanism of nidogen involvement in neurotrophin signalling, I looked at the colocalisation of nidogens with Trk receptors in motor neurons. Both nidogen-1 and nidogen-2 colocalised with a pan-Trk marker in neurons in ventral horn cultures (Figure 5.6). However, discontinuation of the commercial pan-Trk antibody prohibited the collection of enough samples to quantify the degree of colocalisation. Using confocal microscopy, determination of colocalisation of immunofluorescent signals is also limited by the resolution. As I wanted to assess colocalisation resulting from a protein-protein interaction in signalling endosomes of between 50-100 nm (Lalli et al., 2003), and the approximate resolution of confocal microscopy is 300-600 nm in the *xy* plane, an alternative method would provide more information.

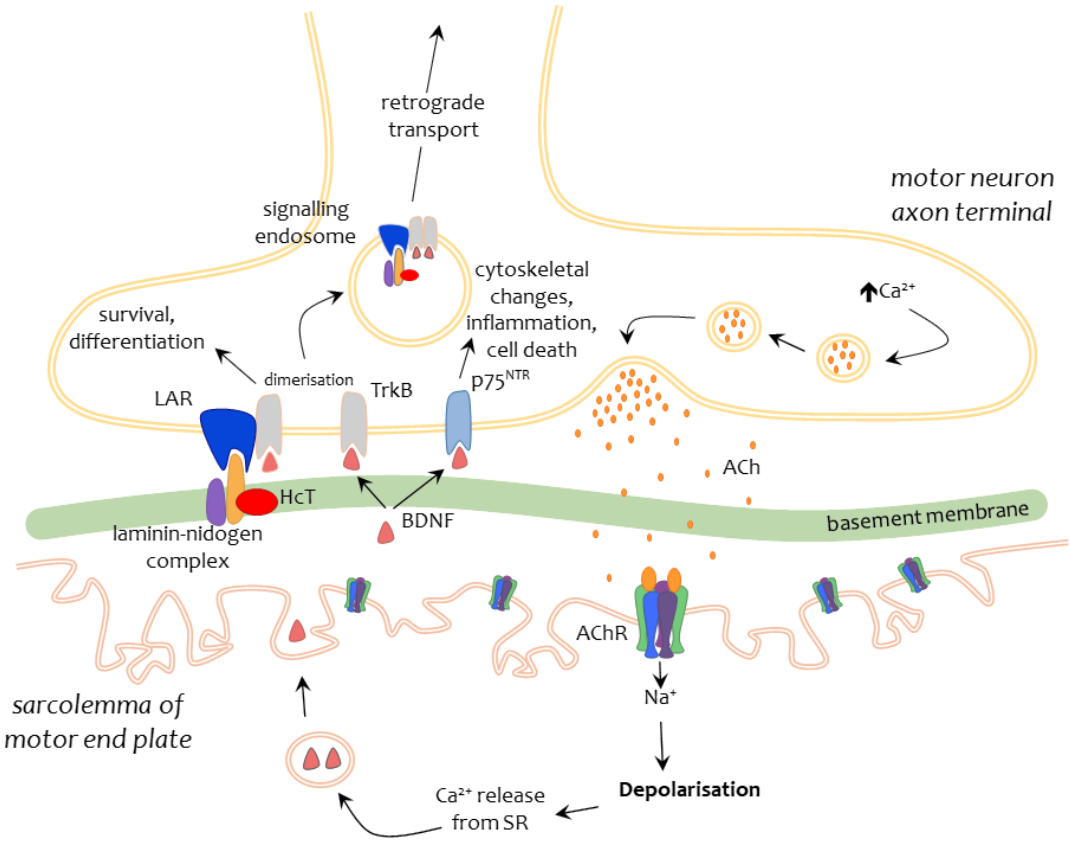

Figure 5.5 Proposed nidogen signalling model

Nidogens are found in the basement membrane in a complex with laminin and other components of this specialised extracellular matrix. The binding fragment of the tetanus neurotoxin (HcT) binds to nidogens, whilst the laminin-nidogen complex binds to the leukocyte antigen related protein phosphatase (LAR). LAR activity has been shown to correlate with BDNF and Trk receptor signalling. The Trk and $p75^{NTR}$ neurotrophin receptors have been found to colocalise with HcT in signalling endosomes. Thus, we propose that nidogen, LAR and HcT are all internalised together in a complex with neurotrophin receptors and retrogradely transported for signalling pathways.

ACh – acetylcholine; AChR – acetylcholine receptor; SR – sarcoplasmic reticulum; BDNF – bone derived neurotrophic factor

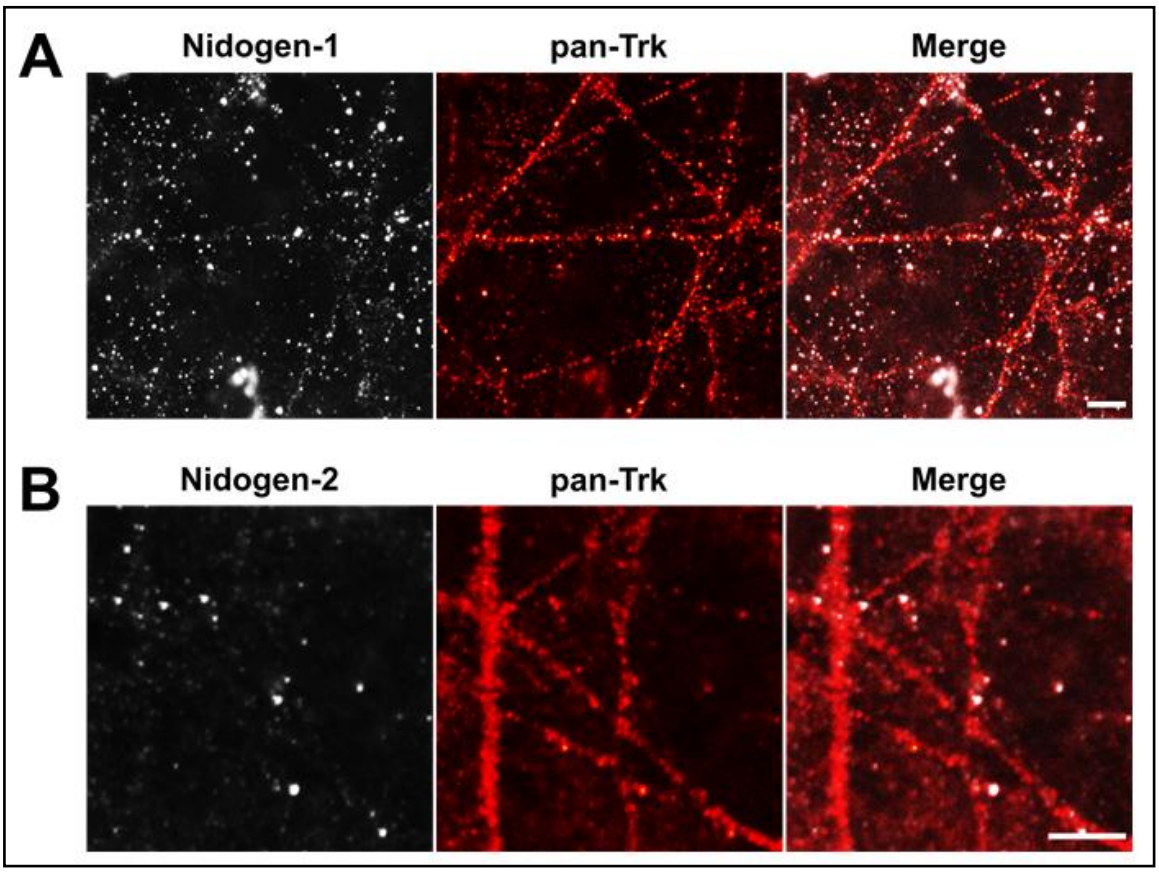

Figure 5.6 Nidogens colocalise with Trk neurotrophin receptors

Motor neurons from mixed spinal cord ventral horn cultures were stained for nidogens and Trk receptors at DIV6. A pan-Trk antibody which recognises all the Trk receptors (TrkA, TrkB, and TrkC) was used. Nidogen-1 **(A)** and nidogen-2 **(B)** puncta in neurites of cultured motor neurons were found to colocalise with pan-Trk puncta. Scale bar = 5 µm

Proximity ligation assays (PLAs) use a similar system to normal immunofluorescence but include a DNA ligation and amplification to report protein-protein interactions (Figure 5.7). Primary antibodies, generated in different species, specific to the two proteins of interest are incubated with the sample (Figure 5.7A). After washing unbound primary antibody from the sample, PLA probes specific to the primary species are added (Figure 5.7B). These probes are conjugated to short oligonucleotide sequences, which, upon addition of a connector oligonucleotide and ligase enzyme, hybridise to form a circular template (Figure 5.7C). This ligation step can only occur if the epitopes of the two proteins of interest are within 40 nm of each other. Subsequent addition of dNTPs and polymerase allow rolling circle amplification to occur. Fluorescently-labelled complementary oligonucleotide probes are added to the amplification mixture and anneal to repeated sequences in the amplified material (Figure 5.7D). This process therefore generates a discrete amplified fluorescent signal that denotes

proximity between the two proteins of interest within 40 nm. PLA was used to assess interaction between nidogen-2 and Trk. For optimal ligation using PLA, the epitopes for the two antibodies should be located in topologically equivalent regions of the proteins to exclude interference of plasma membrane or increase of the distance between the probes above detection limits. Unfortunately, again due to antibody availability, the pan-Trk antibody used in these experiments was a monoclonal antibody raised against the intracellular region of Trk, while nidogen-2 is an extracellular protein (Figure 5.7A). Thus, the plasma membrane was permeabilised with detergents to attempt to overcome this limitation.

In PLAs, the experimental condition included both nidogen-2 and pan-Trk antibodies (denoted Nid2 and Trk respectively) and single primary antibody conditions were used as controls. PLA resulted in many positive signal dots in the experimental condition (Nid2-Trk; Figure 5.8A). However, there were also several PLA dots observed in the single antibody control conditions (Nid2 control and Trk control; Figure 5.8A). The number of PLA dots per field of view was counted and divided by the number of DAPI-positive nuclei in the field to obtain a measurement of PLA dots per cell (Figure 5.8B). The number of PLA dots per cell in the Nid2-Trk condition was significantly different to the Trk control ($P \leq 0.005$) but not to the Nid2 control. The experimental signal therefore cannot be determined to indicate genuine proximity of nidogen-2 and Trk receptors.

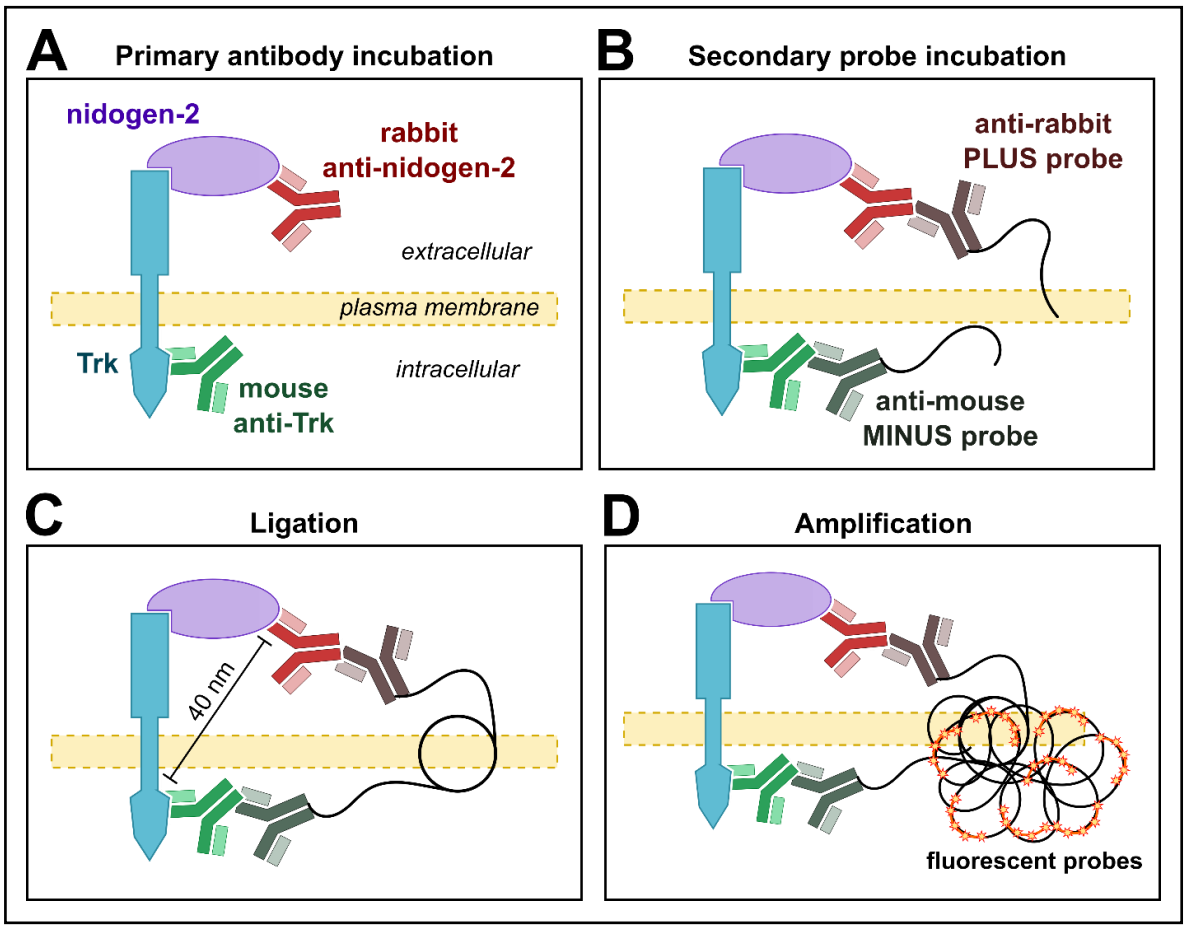

Figure 5.7 Proximity ligation assay mechanism

Proximity ligation assays (PLA) allow the detection of protein-protein interactions using a method similar to normal immunofluorescence techniques. **(A)** After cell fixation and blocking, primary antibodies specific to two proteins of interest (in this case nidogen-2 and Trk) and from different species are added to the sample. **(B)** After the primary antibodies have bound to their targets and the excess antibody has been removed, PLA probes are incubated with the sample. These probes consist of secondary antibodies, directed against the species of the primary antibodies, conjugated to short oligonucleotide probes. **(C)** If the epitopes of the proteins of interest are less than 40 nm apart, the PLUS and MINUS probes may hybridise and circularise upon addition of connector oligonucleotides and ligase. **(D)** Addition of polymerase allows rolling circle amplification to occur. Fluorescently-labelled complementary oligonucleotide probes anneal to repeated stretches of the amplified sequence generating a distinct signal representing an incidence of colocalisation between the proteins of interest. However, due to antibody limitations the Trk antibody used in these experiments was a monoclonal antibody raised to the intracellular domain of Trk.

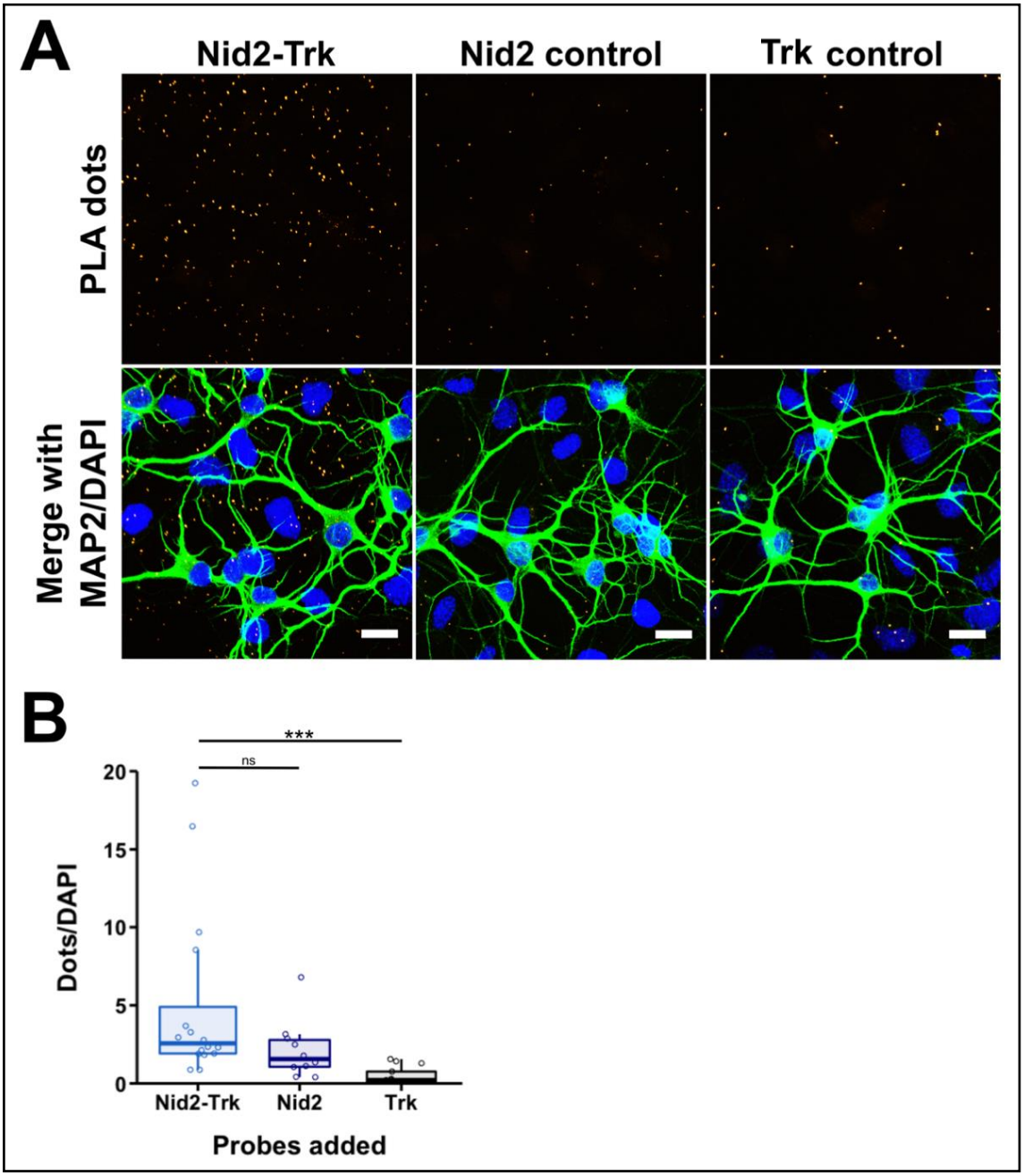

Figure 5.8 Proximity ligation assay between nidogen-2 and Trk receptors

Proximity ligation assays (PLA) were performed on DIV6 mixed spinal cord ventral horn cultures to determine colocalisation of nidogen-2 (Nid2) and Trk receptors within a 40 nm range. A Trk antibody which recognises all the Trk receptors (TrkA, TrkB, and TrkC) was used. **(A)** PLA dots represent instances of Nid2 and Trk colocalisation. Nid2-Trk is the experimental condition. Nid2 and Trk single antibody control conditions were analysed to assess background signal levels. Scale bar = 20 µm. **(B)** The number of PLA dots per field of view were quantified for each condition and divided by the number of DAPI-positive nuclei in the field as a measure of PLA signal per cell. Statistical significance was analysed by one-way ANOVA with Tukey's multiple comparisons test. *** $P \leq 0.005$; ns – not significant. N=3.

However, it is possible that nidogen-2 and Trk receptors do not interact at significant levels under basal conditions in the culture conditions used here. Addition of a ligand or pathway stimulator could induce a concerted interaction at levels high enough to be above the threshold for PLA detection. As our signalling model proposes that HcT, nidogen and Trk receptors are part of a shared pathway, addition of HcT to the culture conditions could stimulate nidogen-Trk interaction. In fact, addition of HcT to the ventral horn cultures induces a dramatic increase in nidogen-1 (Figure 5.9) and nidogen-2 (Figure 5.10) puncta in neurites. Additionally, HcT has been shown to activate TrkB receptor phosphorylation and downstream signalling cascades possibly through induction of a ternary receptor complex (Gil et al., 2003). I therefore repeated the PLA assay with nidogen-2 and Trk after stimulation with HcT (Figure 5.11). In this setting, the PLA signal generated was significantly higher than both the Nid2 and Trk controls ($P \leq 0.05$ and $P \leq 0.001$ respectively; Figure 5.11B). This indicates that HcT promotes the formation of a complex where nidogen-2 and Trk are within 40 nm of each other.

As a positive control for the Nid2-Trk PLA experiment, I also performed a PLA to confirm the previously reported interaction between nidogens and HcT (Bercsenyi et al., 2014). The exogenously applied HcT carries an HA tag allowing detection with an anti-HA antibody. Nidogen-2 and HcT-HA (Nid2-HA) showed a robust PLA signal that was greatly enriched in the neuronal component of the mixed ventral horn culture (Figure 5.12A). This signal was significantly different from both the Nid2 and the HA controls, confirming the interaction of nidogen-2 with HcT ($P \leq 0.005$; Figure 5.12B). Interestingly, the number of PLA dots in the Nid2-HA condition is far greater than the number in Nid2-Trk. Unfortunately, this assay cannot reveal if this is due to the greater prevalence or stability of the Nid2-HcT interaction. The geometry of the interaction between the HcT and nidogen-2 antibodies may simply be more amenable to this assay than Trk and nidogen-2, or this result could also reflect a higher affinity of the HA antibody.

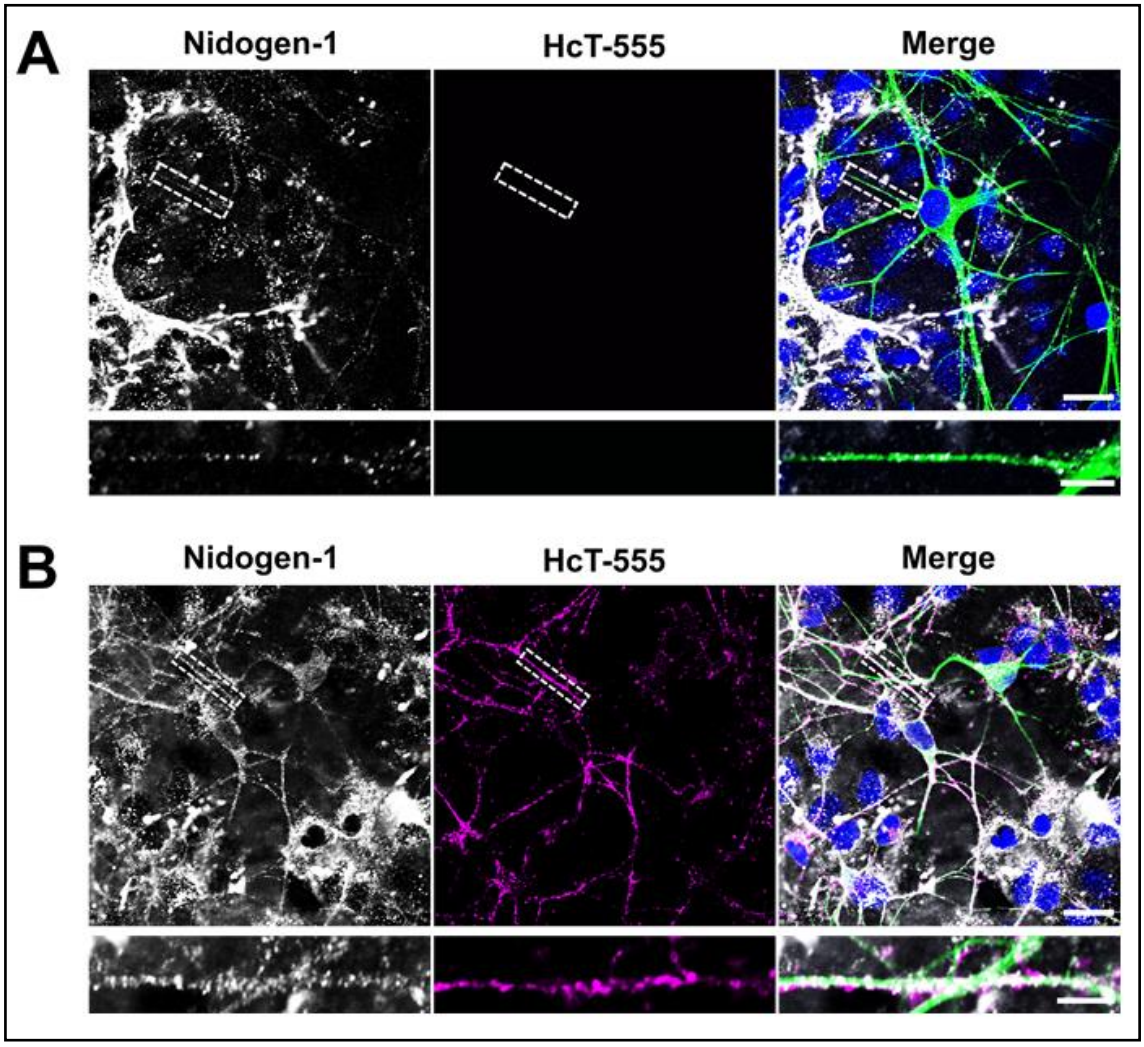

Figure 5.9 Increase in neuronal nidogen-1 upon HcT stimulation

(A) Nidogen-1 is present in distinct puncta in neurites of motor neurons in mixed spinal cord ventral horn cultures under basal conditions as can be seen in the magnified region indicated by the white dashed box. **(B)** Upon addition of HcT (conjugated to an Alexa-555 fluorophore for visualisation), levels of nidogen-1 are dramatically increased within neurons in the culture. Merged panels include staining with an anti-βIII-tubulin antibody as a neuronal marker and DAPI to indicate nuclei. Scale bar in main panels = 20 µm. Scale of magnified panels = 5 µm. Representative images from at least three independent observations.

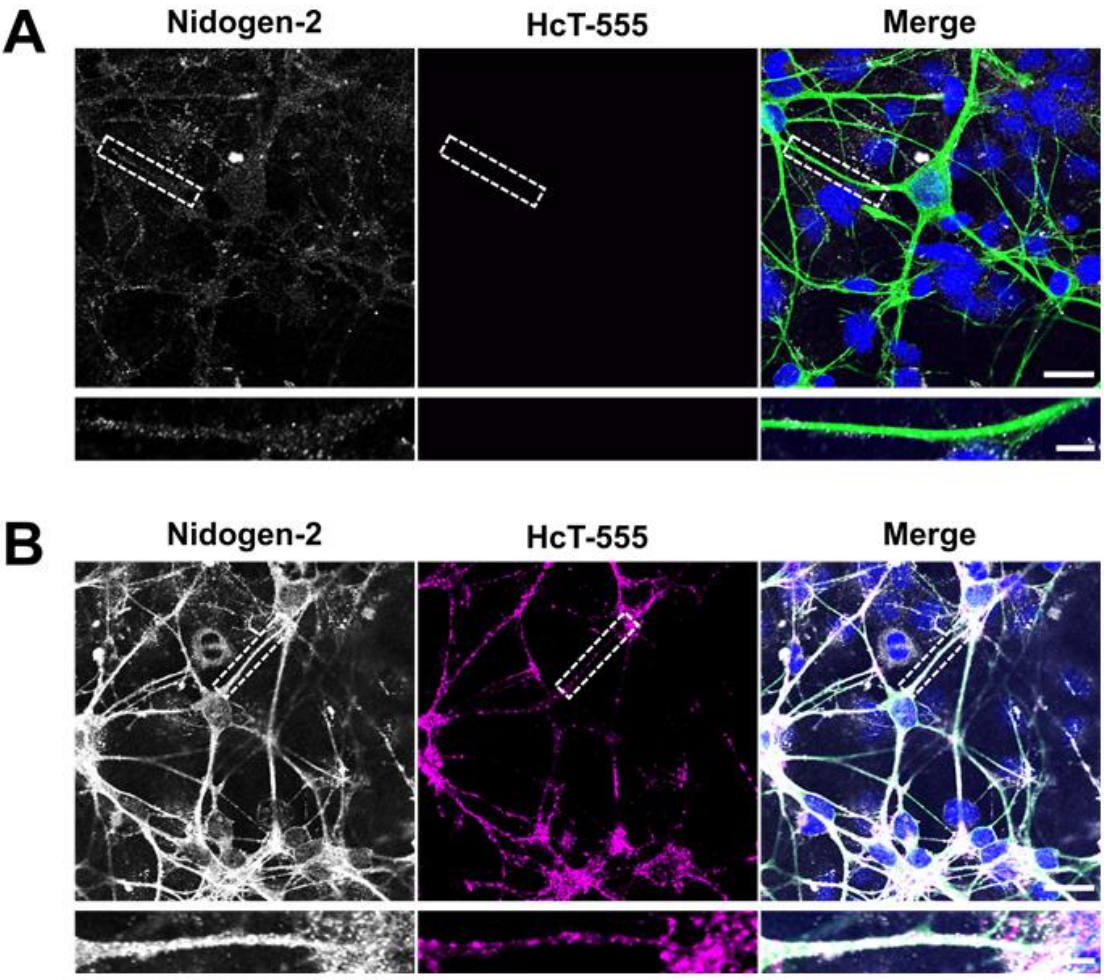

Figure 5.10 Increase in neuronal nidogen-2 upon HcT stimulation

(A) Nidogen-2 is present in distinct puncta in neurites of motor neurons in mixed spinal cord ventral horn cultures under basal conditions as can be seen in the magnified region indicated by the white dashed box. **(B)** Upon addition of HcT (conjugated to an Alexa-555 fluorophore for visualisation), levels of nidogen-2 are dramatically increased within neurons in the culture. Merged panels include staining with an anti-βIII-tubulin antibody as a neuronal marker and DAPI to indicate nuclei. Scale bar in main panels = 20 µm. Scale of magnified panels = 5 µm. Representative images from at least three independent observations.

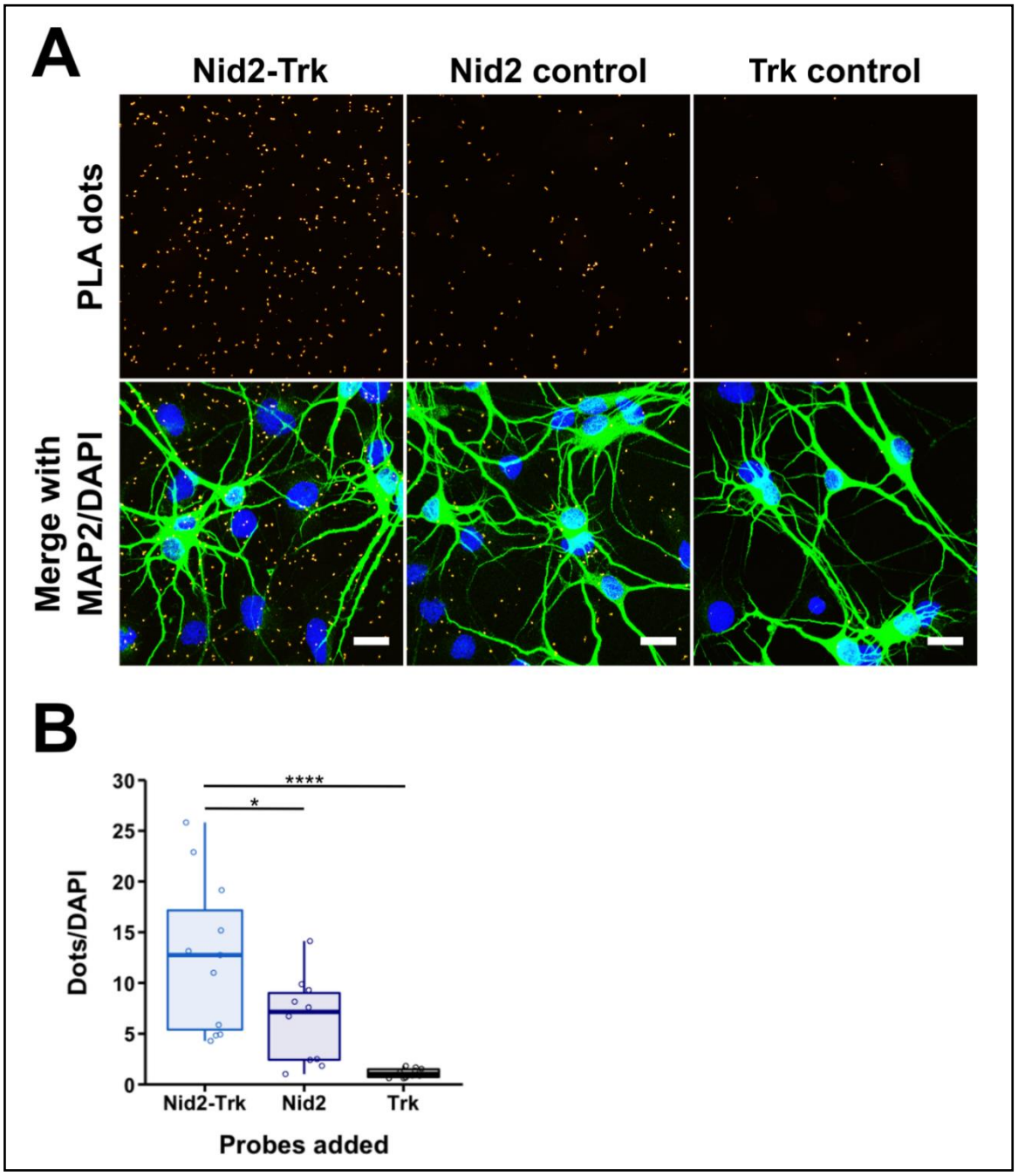

Figure 5.11 Proximity ligation assay between nidogen-2 and Trk receptors with HcT stimulation

Proximity ligation assays (PLA) were performed on DIV6 mixed spinal cord ventral horn cultures to determine whether nidogen-2 (Nid2) and Trk receptors were induced to colocalise upon addition of HcT. A panTrk antibodies recognising TrkA, TrkB, and TrkC was used. **(A)** PLA dots represent instances of Nid2 and Trk colocalisation. Nid2-Trk is the experimental condition. Nid2 and Trk single antibody control conditions were analysed to assess background signal levels. Scale bar = 20 µm. **(B)** The number of PLA dots per field of view were quantified for each condition and divided by the number of DAPI-positive nuclei in the field as a measure of PLA signal per cell. Statistical significance was analysed by one-way ANOVA with Tukey's multiple comparisons test. * $P \leq 0.05$; *** $P \leq 0.005$. N=3.

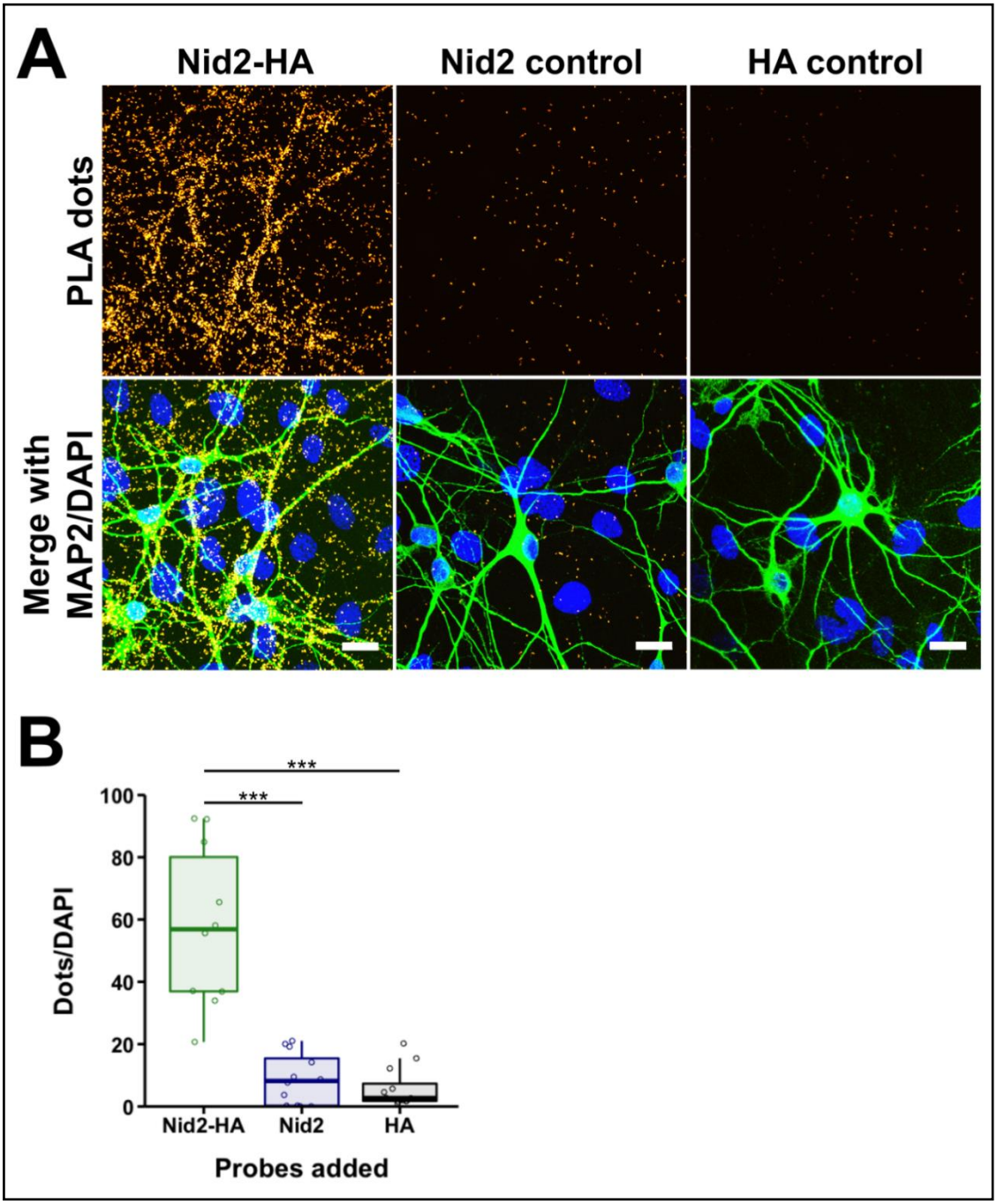

Figure 5.12 Proximity ligation assay between nidogen-2 and HcT

Proximity ligation assays (PLA) were performed on DIV6 mixed spinal cord ventral horn cultures to reveal the assay sensitivity for the known interaction between nidogen-2 (Nid2) and HcT. **(A)** PLA dots represent instances of Nid2 colocalisation with HcT using an antibody against the HA tag of HcT. Nid2-HA is the experimental condition. Nid2 and HA single antibody control conditions were analysed to assess background signal levels. Scale bar = 20 µm. **(B)** The number of PLA dots per field of view were quantified for each condition and divided by the number of DAPI-positive nuclei in the field as a measure of PLA signal per cell. Statistical significance was analysed by one-way ANOVA with Tukey's multiple comparisons test. *** $P \leq 0.005$. N=3.

5.4 Nidogens and BDNF/TrkB signalling

Basement membrane components can potentiate or negatively regulate growth factor signalling or even act as independent non-canonical ligands for trophic receptors (Kim et al., 2011). To understand the significance of nidogen-2 interaction with Trk receptors I therefore investigated the impact of purified recombinant nidogen proteins and the laminin-nidogen complex on BDNF/TrkB signalling. Primary mixed ventral horn cultures were treated at DIV5 with the recombinant proteins alone or in combination with BDNF. Subsequent protein lysates were probed for activation of the TrkB signalling pathway by phosphorylation of the TrkB receptors and the downstream effectors ERK1/2 and AKT (Figure 5.13A). Activation of these molecules was quantified as the amount of phosphorylated protein relative to the expression of the total protein (Figure 5.13B-D). Treatment of cells only with the recombinant proteins did not result in phosphorylation of TrkB receptors, whereas BDNF treatment did (Figure 5.13A-B). Co-treatment of laminin or nidogens with BDNF did not appear to alter the level of TrkB phosphorylation. Addition of the single proteins also did not induce activation of ERK1/2 or AKT (Figure 5.13C and D). Interestingly, application of nidogen-2 with BDNF appeared to induce a greater degree of phosphorylated ERK1/2 than BDNF alone or with laminin or nidogen-1 (Figure 5.13C). However, the difference between these conditions was not significant. There was no discernible difference in the level of activated AKT between BDNF application alone or in combination with laminin or nidogens (Figure 5.13D). These data indicate that nidogens do not potentiate or negatively regulate the initial BDNF/TrkB downstream signalling pathways.

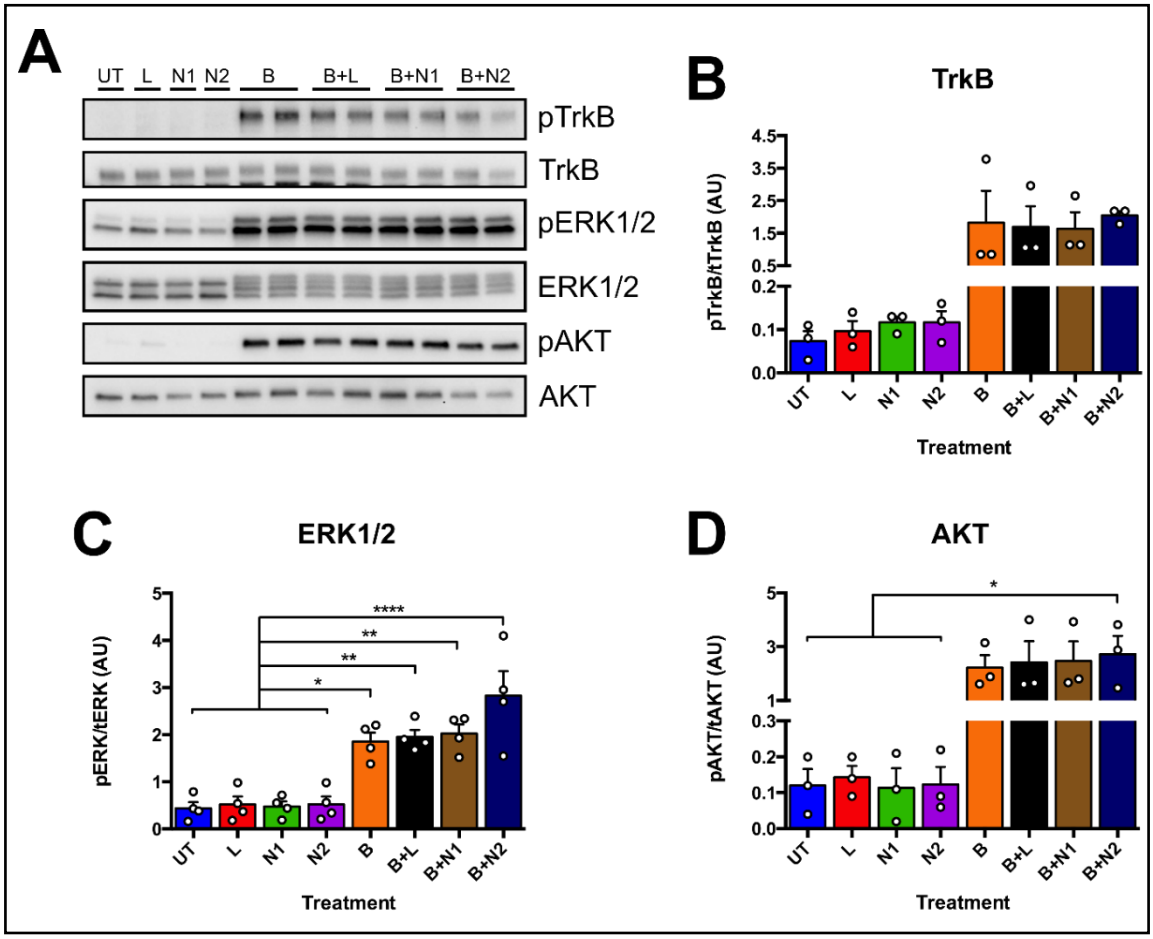

Figure 5.13 Effect of nidogens and laminin on the downstream signalling of BDNF and TrkB receptors.

The impact of laminin and nidogens on BDNF/TrkB signalling was assessed by application of these proteins to DIV5 mixed spinal cord ventral horn cultures and quantification of the subsequent activation of TrkB receptors and two downstream effectors, ERK1/2 and AKT, via phosphorylation. Nidogens and laminin were added to cultures for 5 minutes with and without co-application of BDNF. Cells were lysed and proteins separated by SDS-PAGE. **(A)** Western blots were probed for phosphorylated TrkB, ERK1/2 and AKT (pTrkB Tyr515, pERK1/2 Thr202/Tyr204, and pAKT Ser473 respectively). **(B-D)** Western blots were quantified and levels of the phosphorylated proteins were normalised to levels of the corresponding total protein to indicate activation. Statistical significance was analysed by one-way ANOVA with Tukey's multiple comparisons test. * $P \leq 0.05$; ** $P \leq 0.01$; *** $P \leq 0.005$; **** $P \leq 0.001$. TrkB N=3; ERK1/2 N=4; AKT N=3.

UT – untreated; L – laminin; N1 – nidogen-1; N2 – nidogen-2; B – BDNF

5.5 Nidogens and the GDNF receptor

Examination of the nidogen-1 knock out mouse model generated by collaborators at the MRC Harwell Institute revealed a possible link between nidogens and GDNF (Chapter 4). As the signal levels between PLA of Nid2-Trk and Nid2-HcT-HA are very different, it is possible that nidogen may also interact with other trophic molecules. Taking these observations together, I decided to perform a PLA on nidogen-2 and the GDNF co-receptor GFRα1 (Figure 5.14). In this assay I included experimental conditions with and without application of the GFRα1 ligand to see if interaction between nidogen-2 and the receptor was GDNF-dependent. The PLA signal for nidogen-2 and GFRα1 was significantly greater than the signal of the Nid2 or GFRα1 controls, suggesting their colocalisation ($P \leq 0.005$ and $P \leq 0.001$; Figure 5.14B). However, upon addition of GDNF, this signal was significantly reduced ($P \leq 0.05$; Figure 5.14B). The PLA signal for Nid2-GFRα1 without GDNF was not significantly different to the Nid2 control signal, indicating a lack of genuine interaction (Figure 5.14B). This was unexpected considering the potentiation of the Nid2-Trk interaction by HcT addition (Figure 5.10 and Figure 5.11) and suggests a competition between nidogen-2 and GDNF for GFRα1 binding. Nidogen may therefore have specific roles for different receptors.

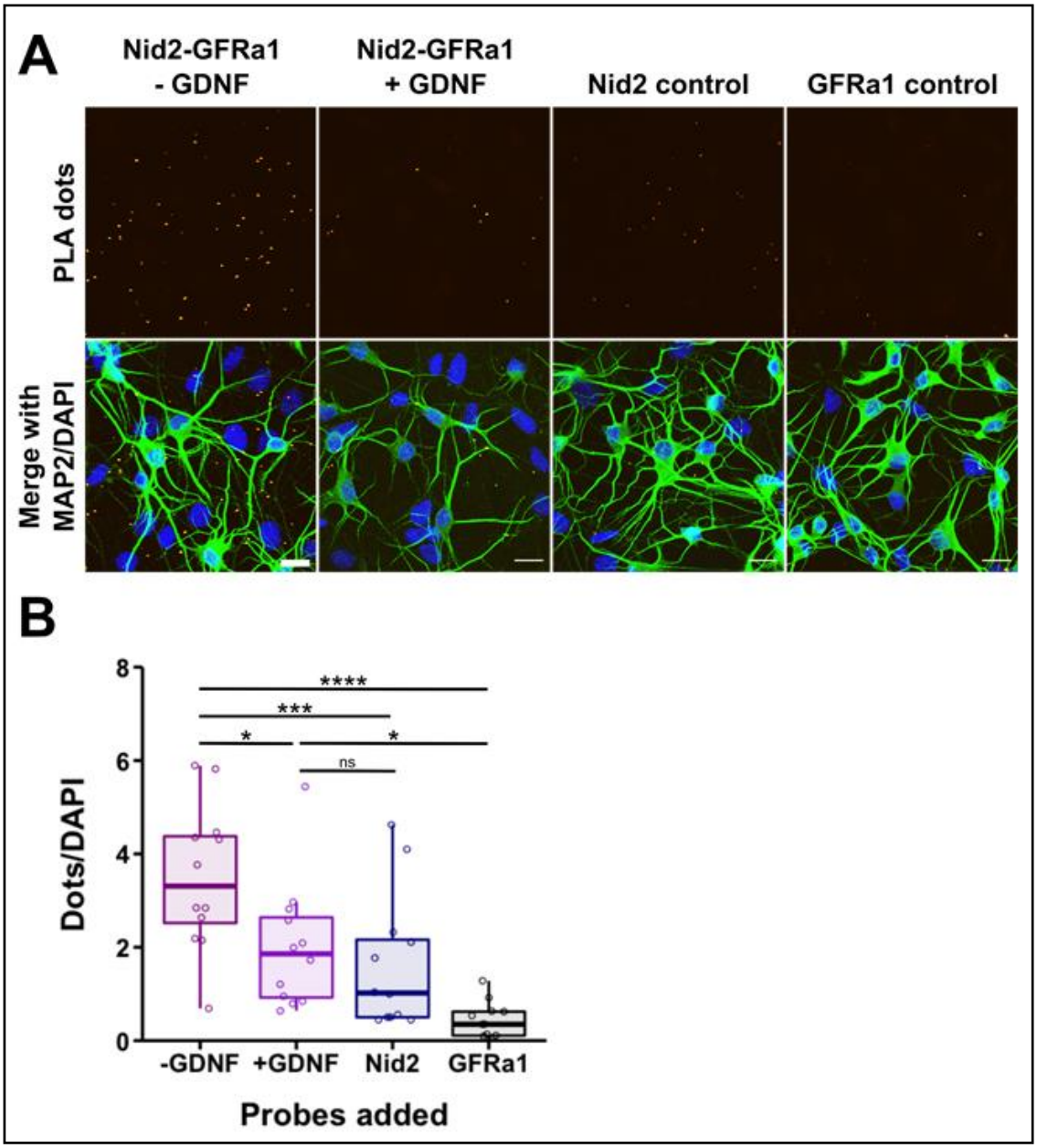

Figure 5.14 Proximity ligation assay between nidogen-2 and GFRα1

Proximity ligation assays (PLA) were performed on DIV6 mixed spinal cord ventral horn cultures to reveal colocalisation between nidogen-2 (Nid2) and the GDNF co-receptor GFRα1 with and without stimulation by GDNF. **(A)** PLA dots represent instances of Nid2 colocalisation with GFRα1. Nid2-GFRα1 ± GDNF are the experimental conditions. Nid2 and GFRα1 single antibody control conditions were analysed to assess background signal levels. Scale bar = 20 µm. **(B)** The number of PLA dots per field of view were quantified for each condition and divided by the number of DAPI-positive nuclei in the field as a measure of PLA signal per cell. Statistical significance was analysed by one-way ANOVA with Tukey's multiple comparisons test. * $P \leq 0.05$; *** $P \leq 0.005$; **** $P \leq 0.001$; ns – not significant. N=3.

5.6 Conclusions

Nidogens were found widely expressed by various cells types derived from the ventral spinal cord. Interaction of nidogen-2 with Trk receptors was not observed by PLA under basal conditions. However, this interaction was induced upon addition of HcT. HcT therefore appears to stimulate a nidogen-2-Trk pathway in ligand replacement mechanism, or by initiating the formation of a ternary complex via interactions with both molecules. The interaction of nidogen-2 with HcT was more robustly detected by PLA in comparison to the nidogen-2-Trk association. It is important to bear in mind the epitope localisation of the pan-Trk antibody relative to nidogen-2. Nidogen-2 is an extracellular molecule and the Trk antibody targets an intracellular region of the receptor. This may therefore have masked the true levels of colocalisation between Trk and nidogen-2 as the epitopes may have been further than 40 nm apart, or the plasma membrane may have interfered with probe ligation.

Nidogens did not significantly increase BDNF-dependent phosphorylation of TrkB or its downstream effector molecules ERK1/2 and AKT arguing against a role for nidogen in modulation of receptor responses. However, the concentrations used in these culture conditions may be saturating therefore masking any potentiating activity of nidogens. Titration of BDNF dosing may reveal a synergistic effect for nidogens when the neurotrophin concentration is limited. These experiments were also performed at a single time point (5 minutes). This was based on previous work, which identified maximal downstream signalling between 2 and 10 minutes after BDNF application. However, it is possible that the addition of nidogens may alter the kinetics of this signalling pathway, which could be detected in a time course experiment. Alternatively, nidogens may not play a role in modulating neurotrophin signalling but may be involved in capture or sequestration of neurotrophins *in situ*.

Intriguingly, colocalisation of nidogen-2 with the GDNF co-receptor GFRα1 was reduced upon application of the receptor ligand. This is suggestive of a competition between nidogen-2 and GDNF for GFRα1 interaction, perhaps involving nidogen-2 and an alternative GFRα1 ligand in GDNF-limited conditions. For example, in the absence of GDNF, GFRα1 has been shown to interact with neural cell adhesion molecule (NCAM) and inhibit the homodimerisation or multimerisation of NCAM molecules, thereby negatively modulating homophilic

NCAM signalling (Paratcha et al., 2003). In the presence of GDNF, GFRα1 potentiates GDNF-NCAM interactions, mediating GDNF-dependent cell adhesion (ibid.). This interaction in independent of the other GDNF receptor RET. It is possible that upon addition of GDNF to these cultures, there is a shift in the signalling involving GFRα1 from NCAM towards the RET receptor pathway, and that the nidogen-2-GFRα1 interaction is associated with the NCAM pathway. NCAM and the GDNF receptors have been localised to the neuromuscular junction where nidogens have also been found (Chapter 3; Sariola and Saarma, 2003).

In summary, I have shown that nidogen-2 exists in complexes with Trk receptors and the GDNF co-receptor GFRα1 *in vitro*. It remains to be seen what the precise effects of these interactions may be.

Chapter 6. Discussion

The aim of this project was to improve our understanding of the role of nidogens, a relatively understudied family of basement membrane components, at the NMJ. This followed from the recent work in our laboratory that identified nidogens as critical mediators of tetanus neurotoxin (TeNT) entry into motor neuron terminals, and the subsequent induction of characteristic spastic paralysis (Bercsenyi et al., 2014). I aimed to examine the expression of nidogens throughout the neuromuscular system and to uncover novel interactors and signalling mechanisms using a combination of biochemical and immunocytochemical approaches. My results suggest that nidogens may be involved in neurotrophic signalling.

6.1 Nidogens in the brain

The expression patterns of nidogen-1 and nidogen-2 were investigated in the brain, spinal cord, sciatic nerve and hind limb muscles to understand whether nidogens were particularly enriched in specific regions of these neuromuscular samples. While these tissues do not represent a comprehensive analysis of the entire neuromuscular system, they were chosen to represent the central and peripheral nervous systems (brain and spinal cord, and sciatic nerve respectively) and skeletal muscles, to provide an indication of potentially tissue-specific requirements for nidogens.

Immunohistochemical analysis of mouse brain sections showed that both nidogen-1 and nidogen-2 are tightly associated with the vasculature and meninges (Chapter 3). Nidogen-1 has previously been shown to localise to meninges and CNS blood vessels (Halfter et al., 2002), however this is the first time, to my knowledge, that the distribution of nidogen-2 expression within the brain has also been shown.

The blood brain barrier (BBB) is a physical barrier which separates the body's circulation from the neural tissue of the central nervous system (CNS), and regulates ion transport, immune cell infiltration and blood flow. This barrier comprises several different cell types, such as the endothelial cells of the vasculature, contractile pericytes which adhere to the surface of the blood vessels, and astrocytes which act as the interface between neuronal activity and

the CNS blood supply (Daneman and Prat, 2015; Attwell et al., 2016). The basement membrane is a critical acellular component of the BBB and mutations in collagen IV and laminin isoforms result in loss of BBB integrity and intracerebral haemorrhage (Gould et al., 2005; Yao et al., 2014). The role of nidogens in maintenance of the BBB has not been properly investigated. However, one study has shown that the basement membrane of capillaries in the cortex is morphologically altered in mice lacking nidogen-1, manifesting in thin and discontinuous ensheathment of the brain microvasculature (Dong et al., 2002). Interestingly, both the nidogen-1 homozygous null mice discussed by Dong and colleagues and the novel nidogen-1 knock-out mice introduced in this thesis displayed seizure-like phenotypes (Chapter 5). BBB deficits have been associated with seizure activity and epileptogenesis, although the precise role they may play in pathology remains unclear (van Vliet et al., 2015; Marchi et al., 2011). It is possible that the loss of BBB basement membrane integrity caused by lack of nidogen-1 could allow pathological immune cell infiltration, an event that has been linked to (Vezzani and Granata, 2005; Zattoni et al., 2011). Impairment of the BBB as a consequence of epileptic activity has been reported in the literature, however the basement membrane defects reported by Dong and colleagues were evident at 18 days of age while neurological phenotypes were reported at 4-12 weeks of age (Dong et al., 2002). While the authors do not confirm the actual age of onset for seizure events, the early presence of basement membrane defects in the brain argues against them being a downstream effect of epileptic damage.

While the discontinuous basement membrane found in nidogen-1 null mice discussed above was only demonstrated at the BBB, the state of the pial basement membrane, which plays an important role in brain development, was not mentioned. As I have seen in my experiments, nidogen-1 is highly expressed in the pial basement membrane and it would be interesting to see if similar defects were present here. A study investigating a mouse model with a mutation in the nidogen binding site of the laminin γ1 chain reported a loss of nidogen-1 localisation to the pial basement membrane, and a subsequent disruption of neuronal migration in the cortex (Halfter et al., 2002). Specifically, these mice displayed disordered localisation of Cajal-Retzius cells, a neuronal subtype which expresses reelin and is essential for the development of cortical lamination

(D'Arcangelo et al., 1995; Marín-Padilla, 1998). As dysregulation of reelin has been linked to the development of epilepsy (Duveau et al., 2011; Haas et al., 2002), it is possible that these mice might have displayed the seizure-like phenotype observed in nidogen-1 knock-out mice. However, as these mice die at birth due to lung and kidney failure, the possible onset of seizure events was not investigated (Willem et al., 2002). Overall, these reports demonstrate a possible role for nidogen-1 in dysregulation of neuronal activity, perhaps because of defects in the BBB and meningeal basement membranes.

6.2 Nidogens in peripheral nerves

My investigations into nidogen expression in the sciatic nerve and hindlimb muscles showed that nidogens were also strongly expressed in the basement membrane associated with the vasculature in these tissues. This was consistent with a previous report that looked at the diaphragm muscle and its innervating nerves (Fox et al., 2008). Interestingly, these authors and I both noted that while nidogen-1 is homogenously expressed across the perineurium, endoneurium, and vascular basement membranes within peripheral nerve, nidogen-2 appears predominantly associated with the vasculature (Chapter 3; Fox et al., 2008). This suggests a differential requirement for nidogen-2 by blood vessels and myelinated axons. It is interesting that nidogen-1 was so robustly expressed by the Schwann cell-associated basement membrane compared to nidogen-2, as this matrix is required for correct myelination of axons (Bunge et al., 1986). It has been shown that nidogen-1 induces migration and supports survival of Schwann cells *in vitro,* apparently via a β1 integrin-dependent mechanism (Lee et al., 2007). The effect of nidogen-2 on Schwann cells was not reported. Further investigation is needed to examine whether nidogen-1 and nidogen-2 have different effects on Schwann cell function, but this could represent a clear functional distinction between the isoforms, which has so far been lacking.

Thus far, only sections of peripheral nerve have been described when examining nidogen expression, which cause significant loss of tissue integrity, especially when examining extremely small structures such as axons. In this thesis I presented longitudinal images of nidogen expression in single teased sciatic nerve axons (Chapter 3). This preparation revealed that nidogen-2 was particularly enriched at the nodes of Ranvier. While the presence of nidogens at

the node of Ranvier has not previously been investigated, other extracellular matrix proteins have been found to localise to this important region of action potential propagation. Basement membrane components and their interactors have specific and crucial roles for nodal formation and maintenance (Court et al., 2006). Dystroglycan and the laminin γ1 chain are both enriched at nodes of Ranvier, and lack of these molecules results in reduced Na^+ channel clustering during node assembly (Occhi et al., 2005; Saito et al., 2003). Gliomedin is an extracellular molecule secreted by Schwann cells and incorporated into the basement membrane at nodes of Ranvier via interactions with HSPGs (Eshed et al., 2007). Secreted gliomedin is a ligand for neural cell adhesion molecule (NCAM) expressed on the axolemma at nodal gaps which also regulates clustering of Na^+ channels at nodes (Eshed et al., 2007; Lustig et al., 2001). As nidogen-2 is enriched at this site, and binds to laminin γ1, it may also play a role in regulating the organisation of nodes of Ranvier.

Within muscles, nidogen expression surrounded innervating axons, external to the myelin sheath, in agreement with the expression pattern observed in cross sections of the sciatic nerve. In addition, there was distinct nidogen expression at the NMJ, in a similar pattern to that seen for BTX, a marker of the postsynaptic membrane. This indicates a robust expression of nidogens at the synaptic basement membrane, which is also consistent with previous reports (Chapter 3; Fox et al., 2008). Nidogen-1 and nidogen-2 single knock-out mice display mild motor phenotypes and altered NMJ morphology (Dong et al., 2002; Fox et al., 2008), but the mechanisms behind this have not been identified. The enrichment of nidogens at the synaptic basement membrane suggests a specific requirement for these extracellular glycoproteins at this site, perhaps in maintenance of pre- and post-synaptic adhesion or maintenance of efficient neurotransmission. To try to understand their role here, I investigated expression levels of both nidogens over different ages in rodent muscles.

6.3 Nidogens in muscle

Semi-quantification of nidogen expression in muscles of different ages indicated a slight trend for higher expression in younger muscles, as well as the presence of different isoforms of nidogen-2 (Chapter 4). It has been previously reported that over post-natal development of muscles, the expression pattern of nidogen-

2 changes from a widespread distribution comparable to that of nidogen-1, to restricted expression mainly at synaptic sites (Fox et al., 2008). This observation was reported to occur during the first two postnatal weeks, such that extrasynaptic nidogen-2 was undetectable at postnatal day (PND) 21. While this time point does not appear to coincide with a strong downregulation of nidogen-2 expression in my investigation, the presence of alternative isoforms at younger ages suggest that these isoforms may have differential expression and perhaps a specific function. It would be interesting to identify the nature of these isoforms – whether they are alternative splice variants or products of post-translational modification, such as proteolytic cleavage events. Generation of isoform-specific antibodies could reveal if these species display different localisation. Indeed, one study reported the identification of a monoclonal antibody, termed 9H6, that specifically bound to rat NMJs (Chiu and Ko, 1994). Sequence analysis and treatment with N-glycanase indicated that the target of this antibody could be a glycosylated isoform of nidogen-1, which displayed NMJ-specific localisation.

Agrin is an interesting example of an extracellular molecule with a number of isoforms, which display differing activities and expression patterns. An NMJ-specific form, Z^+ agrin, has a specific synaptic function, which is distinct from other forms that are more ubiquitously expressed and have a role in cell adhesion rather than post-synaptic neurotransmitter receptor clustering (Burgess et al., 2000). Therefore, it is not inconceivable that nidogens may also exists as different isoforms with specific activities.

To understand whether nidogens play a role in remodelling or pathological states in muscles, I investigated the expression profiles of nidogen-1 and nidogen-2 in different muscle types over disease progression in the $SOD1^{G93A}$ mouse model of ALS (Chapter 4). This mouse displays presymptomatic motor neuron pathology, NMJ denervation and severe motor deficits (Bilsland et al., 2010; Kalmar et al., 2008). Motor neurons innervating different muscles display varying levels of susceptibility to degeneration, resulting in slow-twitch muscles being the most resistant to pathology (Frey et al., 2000; Tremblay et al., 2017). The mechanisms that protect slow-twitch muscles and their innervating motor neurons remain unclear, but identification of factors which show different expression between muscles types may help identify these protective properties. I therefore looked at a variety of muscles to see if different profiles emerged

depending on muscle fibre composition. The tibialis anterior (TA) and extensor digitorum longus (EDL) were examined as fast-twitch muscles, the soleus (SOL) represented slow-twitch muscles and the gastrocnemius is comprised of a mixture of both fast- and slow-twitch fibres. No clear pattern was found either in particular muscle types or over disease progression, although there was high variability in the expression of nidogens within groups, which perhaps masked a trend. I believe that this variability was more attributable to biological variation than technical, as samples processed at the same time displayed different extents and directional differences in protein expression. This suggests that lower expression in some samples was unlikely to be due to protein degradation during tissue processing.

While western blotting is a useful technique for demonstrating relative changes in protein expression, it does have several limitations. It is a semi-quantitative technique and therefore protein expression levels must be reported as relative to another protein or proteins. In addition, more subtle changes in protein expression are difficult to detect, while technical variability due to sample processing and antibody detection can be significant. Ideally, alternative techniques would have been used alongside the western blotting reported here, but time limitations prevented this. To consolidate the changes in protein levels in the wild type and $SOD1^{G93A}$ mouse muscles, expression could have been measured in muscles using immunohistochemistry (IHC) to quantify the relative intensity of staining in tissue sections. However, while this technique provides more information regarding the localisation of proteins, it is also highly dependent on antibody affinity and sample processing. IHC can also be affected by the bioavailability of the antigen. For example, certain conditions or treatments may induce remodelling that reveals an antigen, thereby allowing greater antibody binding, an increase in signal intensity, and an erroneous increase in protein expression. Therefore, these antibody-reliant approaches should be confirmed with alternative methodologies.

One such alternative is quantitative reverse transcription PCR (RT-qPCR), which can indicate changes in gene expression levels. While levels of mRNA do not always directly correlate with protein levels, a high availability of mRNA is suggestive of higher protein expression, unless downstream protein processing pathways are implicated (Liu et al., 2016).

Another method, which would provide localisation data and both absolute and relative protein levels, is laser capture microdissection-mass spectrometry (LCM-MS) (MacDonald et al., 2019; Sethi et al., 2012). This technique uses a directed laser to dissect regions of interest, for example NMJs, and capture them for proteomic analysis (Nazarian et al., 2005). Future work could use a combination of LCM-MS with validation using the other techniques mentioned to gain a comprehensive understanding of nidogen expression at the NMJs of different muscles during postnatal development, as well as changes in expression of other proteins in the nidogen knock out models.

6.4 A novel nidogen-1 knock-out mouse model

In addition to looking at nidogen expression in a model of degenerative disease, I also investigated a novel nidogen-1 KO model (Chapter 4). This was generated by collaborators at MRC Harwell and involved targeting essential exons of the nidogen-1 gene for Cre-mediated recombination to generate a null allele. Although several nidogen-1 knock-out mouse models have been described in the literature, this model was generated to provide greater control over *Nid1* gene expression. Flanking the critical exon with loxP sites creates a conditional null allele which can be used to produce tissue-specific or developmentally-restricted nidogen-1 knock-out mice. As nidogen-1 is so ubiquitously expressed throughout the body, it will be particularly useful to be able to tease out the cell-specific requirements for this protein.

In this thesis I investigated the strain with constitutive and ubiquitous knock-out of nidogen-1, as generated by genetic crosses of the floxed *Nid1* mice with actin-Cre mice. As previously touched upon, this novel nidogen-1 knock-out model displays seizure-like activity and temporary hind-limb paralysis, which appears to be stress-induced. This is comparable to the phenotype observed in a previously described model (Dong et al., 2002). I examined the expression of both nidogen-1 and nidogen-2 in wild-type, heterozygous and homozygous littermates of this model. Two different muscles were examined, the quadriceps and the triceps surae, as well as the brain. In this model, as found in other models of nidogen-1 KO, nidogen-2 appeared upregulated in homozygous null muscles. Interestingly however, this compensatory upregulation was not apparent in the brain. This suggests the presence of feedback mechanisms specific to the muscle which

lead to a lack of nidogen-1 inducing an increase in nidogen-2. This could indicate either an essential role for nidogen-1 in muscles that requires compensation with nidogen-2, or a specific role for nidogen-1 in the brain which nidogen-2 cannot perform. Indeed, gene regulatory modelling studies have indicated that the context of regulatory pathways is just as important as the identity of the pathway components (Sonawane et al., 2017). This is evidenced by the 'specific' expression of certain transcription factors by several different tissues, but the downstream effects of their expression resulting in much more specific physiological functions in single tissues (ibid.). Taken together with the incidence of seizure activity nidogen-1 knock-out mice and the lack neurological deficits found in nidogen-2 mice, it seems likely that nidogen-1 has a specific function in the brain.

6.5 Nidogens in motor neurons

To gain a greater understanding of the potential role of nidogens in neuronal signalling, I investigated nidogens in primary mixed ventral horn cultures (Chapter 5). Previous work in our laboratory showed that nidogens were essential for the efficient entry of TeNT into motor neurons at the NMJ (Bercsenyi et al., 2014). Interestingly, I found that addition of the heavy chain binding fragment of TeNT (HcT) to primary neuronal cultures induced an upregulation in nidogen-1 and nidogen-2 puncta in motor neurons (Chapter 5). While this was not quantified, it was qualitatively quite striking. The mechanisms behind this were not investigated but may indicate that nidogen internalisation into motor neurons is induced by a ligand not present under basal conditions in mixed ventral horn cultures. In this scenario, HcT may possess a similar binding capacity to the unknown endogenous ligand and can therefore initiate nidogen mobilisation from the basement membrane. As the ligand appears not to be produced by any of the cell types in the mixed neuronal culture derived from spinal cords, it is possible that it may be a target-derived factor synthesised by muscles.

6.6 Interaction of nidogens and neurotrophins

Neurotrophins are essential factors for the development, survival and maintenance of neurons and their signalling. They are important in the development of myofibres and the NMJ and in neuronal cell migration and axonal targeting in the brain (Huang and Reichardt, 2001; Sakuma and Yamaguchi,

2011). They are also involved in maintenance of neuronal function and plasticity of neural networks (Gómez-Palacio-Schjetnan and Escobar, 2013). As these processes appear affected by an absence of nidogens, I decided to investigate the possible interactions between nidogens and neurotrophin candidates (Chapter 5). I used proximity ligation assays (PLA) in mixed ventral horn cultures to examine the interactions of nidogens with the Trk family of neurotrophin receptors in motor neurons. These experiments revealed that while, under basal culture conditions, there is minimal interaction between nidogen-2 and Trk receptors, association is amplified by the addition of HcT. This indicates that the association of nidogen-2 with Trk receptors may not be direct but requires a co-receptor or ligand which forms a ternary complex. Nidogen-2 showed a robust signal in PLA experiments with HcT, providing further evidence for an interaction between these proteins. Although the signals were vastly different between the Nid2-Trk and Nid2-HcT assays, this does not necessarily mean that these molecules are not part of a single pathway. The kinetics of the Nid2-Trk association may be faster, representing a transient interaction of nidogen-2 with the neurotrophin receptor, while nidogen-2 and HcT may remain together after internalisation into motor neurons.

To understand whether interaction of nidogen-2 is physiologically relevant to the intracellular signalling of Trk receptors, I investigated the expression of downstream effector molecules with and without addition of nidogen-2. The BDNF receptors TrkB and $p75^{NTR}$ have been shown to colocalise with HcT, which in turn colocalises with nidogen-2 in motor neurons. As a result of this, I decided to examine the impact of nidogen-2 on TrkB signalling. The presence of nidogen-2 alone did not appear to affect the activation of signalling molecules downstream of TrkB, and nidogen-2 also did not appear to potentiate or inhibit BDNF-elicited TrkB signalling. As the PLA experiments were performed with a pan-Trk antibody, it is possible that nidogen-2 may be interacting with other members of the Trk receptor family. Alternatively, nidogen-2 may affect the kinetics of receptor signalling, such that the effect was outside of the time window observed in these experiments. A 5-minute time point was used in these experiments as the presence of activated early TrkB effector molecules has been shown to decline after 10 minutes (Terenzio et al., 2014). However, association of nidogen-2 with

TrkB or BDNF have altered the rate of effector dephosphorylation or degradation, which would not have been picked up in this assay.

As another important neurotrophin in the brain and at the NMJ is GDNF, I also performed PLA to examine interactions between nidogen-2 and the GDNF-specific receptor GFRα1. GDNF forms a complex with the GPI-anchored GFRα1 and initiates intracellular signalling cascades via the RET receptor tyrosine kinase. Intriguingly, there did appear to be an association of nidogen-2 with GFRα1 which was reduced upon the addition of GDNF to the culture medium. These experiments were performed in permeabilising conditions, so it is not clear if this interaction is extracellular or intracellular. If the interaction occurs extracellularly, it may be that nidogen-2 helps to maintain cell surface expression of GFRα1, and upon GDNF binding, it releases GFRα1 to allow internalisation and downstream signalling. Perhaps nidogen-2 and GDNF compete for binding to GFRα1. Alternatively, nidogen-2 may be involved in GFRα1 signalling in the absence of GDNF. GFRα1 expression has been found in cells lacking RET. In these cells, GFRα1 can form a complex with neural cell adhesion molecule (NCAM) which activates Fyn and FAK downstream signalling pathways (Paratcha et al., 2003). GFRα1 interaction with NCAM inhibits homophilic binding between NCAM molecules and subsequently decreases NCAM-mediated cell adhesion, independent of GDNF. The possibility that nidogen-2 may be involved in GFRα1-NCAM signalling warrants further investigation.

6.7 Future Perspectives

My work has opened many new avenues for investigation into the role of nidogens in neuromuscular function. Our nidogen-1 knock-out model was only recently generated, and so the experiments presented here are only the beginning of the characterisation of this novel strain. It is reassuring that our model recapitulates the neurological phenotypes observed in other nidogen-1 knock-out mice produced by different methods. The aetiology of the seizures and hindlimb paralysis need to be investigated. EEG recordings of mutant brains as well as assessment of network morphology and quantification of inflammatory markers may reveal the aetiology of the seizures. Investigating the presence of NMJ abnormalities in these mice may also clarify the cause of hindlimb paralysis in these mice.

While nidogen-2 did not appear affect the downstream signalling of TrkB in the experiments presented here, it would be worth performing the experiment over a time course to determine whether the kinetics of this pathway are affected. The interactions observed by PLA between nidogen-2 and TrkB with HcT addition, and nidogen-2 with GFRα1 in the absence of GDNF could also be confirmed via co-immunoprecipitation. It would also be interesting to understand whether GDNF and nidogen-2 are competitive ligands for GFRα1, and whether they initiate different intracellular signalling cascades.

While the impact of other components of the basement membrane have been shown to impact trophic signalling via interactions with growth factors and their receptors, this has not so far been demonstrated for nidogens. My experiments suggest that nidogens are well placed to take part in neurotrophic signalling and do indeed interact with trophic receptors. Validation of these interactions by other methods and determination of the effects on their signalling will shed new light on the role of basement membrane in the neuromuscular system.

6.8 Conclusion

The work presented in this thesis represents my efforts to understand the role of nidogens in neuronal signalling and neuromuscular function. Despite the exact mechanisms by which nidogens may regulate neural plasticity and neuromuscular junction maintenance have remained elusive, I present novel evidence for the interaction of nidogens and components of neurotrophic signalling pathways. A greater understanding of how these components of the basement membrane and intracellular signalling cascades interact will provide a new platform for therapeutic intervention in neurological diseases where drug delivery is a significant hurdle. It also demonstrates the complexity of basement membrane biology and the existence of yet more functions we have yet to understand.

References

Ackley, B.D., Kang, S.H., Crew, J.R., Suh, C., Jin, Y., Kramer, J.M., 2003. The basement membrane components nidogen and type XVIII collagen regulate organization of neuromuscular junctions in Caenorhabditis elegans. J. Neurosci. 23, 3577–87.

Alazami, A.M., Patel, N., Shamseldin, H.E., Anazi, S., Al-Dosari, M.S., Alzahrani, F., Hijazi, H., Alshammari, M., Aldahmesh, M.A., Salih, M.A., Faqeih, E., Alhashem, A., Bashiri, F.A., Al-Owain, M., Kentab, A.Y., Sogaty, S., Al Tala, S., Temsah, M.-H., Tulbah, M., Aljelaify, R.F., Alshahwan, S.A., Seidahmed, M.Z., Alhadid, A.A., Aldhalaan, H., AlQallaf, F., Kurdi, W., Alfadhel, M., Babay, Z., Alsogheer, M., Kaya, N., Al-Hassnan, Z.N., Abdel-Salam, G.M.H., Al-Sannaa, N., Al Mutairi, F., El Khashab, H.Y., Bohlega, S., Jia, X., Nguyen, H.C., Hammami, R., Adly, N., Mohamed, J.Y., Abdulwahab, F., Ibrahim, N., Naim, E.A., Al-Younes, B., Meyer, B.F., Hashem, M., Shaheen, R., Xiong, Y., Abouelhoda, M., Aldeeri, A.A., Monies, D.M., Alkuraya, F.S., 2015. Accelerating novel candidate gene discovery in neurogenetic disorders via whole-exome sequencing of prescreened multiplex consanguineous families. Cell Rep. 10, 148–61.

Arikawa-Hirasawa, E., Le, A.H., Nishino, I., Nonaka, I., Ho, N.C., Francomano, C.A., Govindraj, P., Hassell, J.R., Devaney, J.M., Spranger, J., Stevenson, R.E., Iannaccone, S., Dalakas, M.C., Yamada, Y., 2002. Structural and functional mutations of the perlecan gene cause Schwartz-Jampel syndrome, with myotonic myopathy and chondrodysplasia. Am. J. Hum. Genet. 70, 1368–75.

Attwell, D., Mishra, A., Hall, C.N., O'Farrell, F.M., Dalkara, T., 2016. What is a pericyte? J. Cereb. Blood Flow Metab. 36, 451–455.

Aumailley, M., 2013. The laminin family. Cell Adh. Migr. 7, 48–55.

Aumailley, M., Battaglia, C., Mayer, U., Reinhardt, D., Nischt, R., Timpl, R., Fox, J.W., 1993. Nidogen mediates the formation of ternary complexes of basement membrane components. Kidney Int. 43, 7–12.

Aumailley, M., Bruckner-Tuderman, L., Carter, W.G., Deutzmann, R., Edgar, D., Ekblom, P., Engel, J., Engvall, E., Hohenester, E., Jones, J.C.R., Kleinman,

H.K., Marinkovich, M.P., Martin, G.R., Mayer, U., Meneguzzi, G., Miner, J.H., Miyazaki, K., Patarroyo, M., Paulsson, M., Quaranta, V., Sanes, J.R., Sasaki, T., Sekiguchi, K., Sorokin, L.M., Talts, J.F., Tryggvason, K., Uitto, J., Virtanen, I., Von Der Mark, K., Wewer, U.M., Yamada, Y., Yurchenco, P.D., 2005. A simplified laminin nomenclature. Matrix Biol.

Aumailley, M., Pesch, M., Tunggal, L., Gaill, F., Fässler, R., 2000. Altered synthesis of laminin 1 and absence of basement membrane component deposition in (beta)1 integrin-deficient embryoid bodies. J. Cell Sci. 113 Pt 2, 259–68.

Aumailley, M., Wiedemann, H., Mann, K., Timpl, R., 1989. Binding of nidogen and the laminin-nidogen complex to basement membrane collagen type IV. Eur. J. Biochem. 184, 241–8.

Ayers, J.I., McMahon, B., Gill, S., Lelie, H.L., Fromholt, S., Brown, H., Valentine, J.S., Whitelegge, J.P., Borchelt, D.R., 2017. Relationship between mutant Cu/Zn superoxide dismutase 1 maturation and inclusion formation in cell models. J. Neurochem.

Bader, B.L., Smyth, N., Nedbal, S., Miosge, N., Baranowsky, A., Mokkapati, S., Murshed, M., Nischt, R., 2005. Compound genetic ablation of nidogen 1 and 2 causes basement membrane defects and perinatal lethality in mice. Mol. Cell. Biol. 25, 6846–56.

Bai, X., Dilworth, D.J., Weng, Y.-C., Gould, D.B., 2009. Developmental distribution of collagen IV isoforms and relevance to ocular diseases. Matrix Biol. 28, 194–201.

Balbona, K., Tran, H., Godyna, S., Ingham, K.C., Strickland, D.K., Argraves, W.S., 1992. Fibulin binds to itself and to the carboxyl-terminal heparin-binding region of fibronectin. J. Biol. Chem. 267, 20120–5.

Bangratz, M., Sarrazin, N., Devaux, J., Zambroni, D., Echaniz-Laguna, A., René, F., Borio, D., Davoine, C.S., Fontaine, B., Feltri, M.L., Benoit, E., Nicole, S., 2012. A mouse model of schwartz-jampel syndrome reveals myelinating schwann cell dysfunction with persistent axonal depolarization in vitro and distal peripheral nerve hyperexcitability when perlecan is lacking. Am. J. Pathol. 180, 2040–2055.

Bauché, S., Boerio, D., Davoine, C.S., Bernard, V., Stum, M., Bureau, C., Fardeau, M., Romero, N.B., Fontaine, B., Koenig, J., Hantaï, D., Gueguen, A., Fournier, E., Eymard, B., Nicole, S., 2013. Peripheral nerve hyperexcitability with preterminal nerve and neuromuscular junction remodeling is a hallmark of Schwartz-Jampel syndrome. Neuromuscul. Disord. 23, 998–1009.

Beenken, A., Mohammadi, M., 2009. The FGF family: biology, pathophysiology and therapy. Nat. Rev. Drug Discov. 8, 235–53.

Behrens, D.T., Villone, D., Koch, M., Brunner, G., Sorokin, L., Robenek, H., Bruckner-Tuderman, L., Bruckner, P., Hansen, U., 2012. The epidermal basement membrane is a composite of separate laminin- or collagen IV-containing networks connected by aggregated perlecan, but not by nidogens. J. Biol. Chem. 287, 18700–9.

Bellot, F., Crumley, G., Kaplow, J.M., Schlessinger, J., Jaye, M., Dionne, C.A., 1991. Ligand-induced transphosphorylation between different FGF receptors. EMBO J. 10, 2849–54.

Bercsenyi, K., Schmieg, N., Bryson, J.B., Wallace, M., Caccin, P., Golding, M., Zanotti, G., Greensmith, L., Nischt, R., Schiavo, G., 2014. Tetanus toxin entry. Nidogens are therapeutic targets for the prevention of tetanus. Science 346, 1118–23.

Betz, W., Sakmann, B., 1973. Effects of proteolytic enzymes on function and structure of frog neuromuscular junctions. J. Physiol. 230, 673–688.

Bhat, J.M., Hutter, H., 2016. Pioneer Axon Navigation Is Controlled by AEX-3, a Guanine Nucleotide Exchange Factor for RAB-3 in Caenorhabditis elegans. Genetics 203, 1235–1247.

Bilsland, L.G., Sahai, E., Kelly, G., Golding, M., Greensmith, L., Schiavo, G., 2010. Deficits in axonal transport precede ALS symptoms in vivo. Proc. Natl. Acad. Sci. U. S. A. 107, 20523–20528.

Bönnemann, C.G., 2011. The collagen VI-related myopathies: muscle meets its matrix. Nat. Rev. Neurol. 7, 379–90.

Bowman, W., 1840. On the Minute Structure and Movements of Voluntary Muscle. Philos. Trans. R. Soc. London 130, 457–501.

Brown, J.C., Wiedemann, H., Timpl, R., 1994. Protein binding and cell adhesion properties of two laminin isoforms (AmB1eB2e, AmB1sB2e) from human placenta. J. Cell Sci. 107 (Pt 1, 329–38.

Bunge, R.P., Bunge, M.B., Eldridge, C.F., 1986. Linkage Between Axonal Ensheathment and Basal Lamina Production by Schwann Cells. Annu. Rev. Neurosci. 9, 305–328.

Burgess, R.W., Nguyen, Q.T., Son, Y.-J., Lichtman, J.W., Sanes, J.R., 1999. Alternatively Spliced Isoforms of Nerve-and Muscle-Derived Agrin: Their Roles at the Neuromuscular Junction. Neuron 23, 33–44.

Burgess, R.W., Skarnes, W.C., Sanes, J.R., 2000. Agrin Isoforms with Distinct Amino Termini: Differential Expression, Localization, and Function. J. Cell Biol. 151, 41–52.

Carlin, B., Jaffe, R., Bender, B., Chung, A.E., 1981. Entactin, a novel basal lamina-associated sulfated glycoprotein. J. Biol. Chem. 256, 5208–5214.

Casino, P., Gozalbo-Rovira, R., Rodríguez-Díaz, J., Banerjee, S., Boutaud, A., Rubio, V., Hudson, B.G., Saus, J., Cervera, J., Marina, A., 2018. Structures of collagen IV globular domains: insight into associated pathologies, folding and network assembly. IUCrJ 5, 765–779.

Chen, J., Billings, S.E., Nishimune, H., 2011. Calcium channels link the muscle-derived synapse organizer laminin β2 to Bassoon and CAST/Erc2 to organize presynaptic active zones. J. Neurosci. 31, 512–25.

Chen, T.T., Luque, A., Lee, S., Anderson, S.M., Segura, T., Iruela-Arispe, M.L., 2010. Anchorage of VEGF to the extracellular matrix conveys differential signaling responses to endothelial cells. J. Cell Biol. 188, 595–609.

Cheng, Y.S., Champliaud, M.F., Burgeson, R.E., Marinkovich, M.P., Yurchenco, P.D., 1997. Self-assembly of laminin isoforms. J. Biol. Chem. 272, 31525–32.

Chiu, A.Y., Ko, J., 1994. a Novel Epitope of Entactin Is Present At the Mammalian Neuromuscular-Junction. J. Neurosci. 14, 2809–2817.

Chung, W.-S., Allen, N.J., Eroglu, C., 2015. Astrocytes Control Synapse Formation, Function, and Elimination. Cold Spring Harb. Perspect. Biol. 7, a020370.

Colognato, H., Winkelmann, D.A., Yurchenco, P.D., 1999. Laminin polymerization induces a receptor-cytoskeleton network. J. Cell Biol. 145, 619–31.

Colombelli, C., Palmisano, M., Eshed-Eisenbach, Y., Zambroni, D., Pavoni, E., Ferri, C., Saccucci, S., Nicole, S., Soininen, R., McKee, K.K., Yurchenco, P.D., Peles, E., Wrabetz, L., Feltri, M.L., 2015. Perlecan is recruited by dystroglycan to nodes of ranvier and binds the clustering molecule gliomedin. J. Cell Biol. 208, 313–329.

Costell, M., Gustafsson, E., Aszódi, A., Mörgelin, M., Bloch, W., Hunziker, E., Addicks, K., Timpl, R., Fässler, R., 1999. Perlecan maintains the integrity of cartilage and some basement membranes. J. Cell Biol. 147, 1109–22.

Court, F.A., Wrabetz, L., Feltri, M.L., 2006. Basal lamina: Schwann cells wrap to the rhythm of space-time. Curr. Opin. Neurobiol. 16, 501–507.

D'Arcangelo, G., G. Miao, G., Chen, S.-C., Scares, H.D., Morgan, J.I., Curran, T., 1995. A protein related to extracellular matrix proteins deleted in the mouse mutant reeler. Nature 374, 719–723.

Daneman, R., Prat, A., 2015. The blood-brain barrier. Cold Spring Harb. Perspect. Biol. 7, a020412.

Daniels, M.P., 2012. The role of agrin in synaptic development, plasticity and signaling in the central nervous system. Neurochem. Int. 61, 848–53.

Darbro, B.W., Mahajan, V.B., Gakhar, L., Skeie, J.M., Campbell, E., Wu, S., Bing, X., Millen, K.J., Dobyns, W.B., Kessler, J.A., Jalali, A., Cremer, J., Segre, A., Manak, J.R., Aldinger, K.A., Suzuki, S., Natsume, N., Ono, M., Hai, H.D., Viet, L.T., Loddo, S., Valente, E.M., Bernardini, L., Ghonge, N., Ferguson, P.J., Bassuk, A.G., 2013. Mutations in Extracellular Matrix Genes NID1 and LAMC1 Cause Autosomal Dominant Dandy-Walker Malformation and Occipital Cephaloceles. Hum. Mutat. 34, 1075–1079.

de Bentzmann, S., Tristan, A., Etienne, J., Brousse, N., Vandenesch, F., Lina, G., 2004. Staphylococcus aureus isolates associated with necrotizing pneumonia bind to basement membrane type I and IV collagens and laminin. J. Infect. Dis. 190, 1506–15.

De Vos, K.J., Chapman, A.L., Tennant, M.E., Manser, C., Tudor, E.L., Lau, K.-F.,

Brownlees, J., Ackerley, S., Shaw, P.J., McLoughlin, D.M., Shaw, C.E., Leigh, P.N., Miller, C.C.J., Grierson, A.J., 2007. Familial amyotrophic lateral sclerosis-linked SOD1 mutants perturb fast axonal transport to reduce axonal mitochondria content. Hum. Mol. Genet. 16, 2720–2728.

Deinhardt, K., Salinas, S., Verastegui, C., Watson, R., Worth, D., Hanrahan, S., Bucci, C., Schiavo, G., 2006. Rab5 and Rab7 control endocytic sorting along the axonal retrograde transport pathway. Neuron 52, 293–305.

Denies, M.S., Johnson, J., Maliphol, A.B., Bruno, M., Kim, A., Rizvi, A., Rustici, K., Medler, S., 2014. Diet-induced obesity alters skeletal muscle fiber types of male but not female mice. Physiol. Rep. 2, e00204.

Dickinson, M.E., Flenniken, A.M., Ji, X., Teboul, L., Wong, M.D., White, J.K., Meehan, T.F., Weninger, W.J., Westerberg, H., Adissu, H., Baker, C.N., Bower, L., Brown, J.M., Caddle, L.B., Chiani, F., Clary, D., Cleak, J., Daly, M.J., Denegre, J.M., Doe, B., Dolan, M.E., Edie, S.M., Fuchs, H., Gailus-Durner, V., Galli, A., Gambadoro, A., Gallegos, J., Guo, S., Horner, N.R., Hsu, C.-W., Johnson, S.J., Kalaga, S., Keith, L.C., Lanoue, L., Lawson, T.N., Lek, M., Mark, M., Marschall, S., Mason, J., McElwee, M.L., Newbigging, S., Nutter, L.M.J., Peterson, K.A., Ramirez-Solis, R., Rowland, D.J., Ryder, E., Samocha, K.E., Seavitt, J.R., Selloum, M., Szoke-Kovacs, Z., Tamura, M., Trainor, A.G., Tudose, I., Wakana, S., Warren, J., Wendling, O., West, D.B., Wong, L., Yoshiki, A., International Mouse Phenotyping Consortium, Jackson Laboratory, Infrastructure Nationale PHENOMIN, I.C. de la S. (ICS), Charles River Laboratories, MRC Harwell, Toronto Centre for Phenogenomics, Wellcome Trust Sanger Institute, RIKEN BioResource Center, MacArthur, D.G., Tocchini-Valentini, G.P., Gao, X., Flicek, P., Bradley, A., Skarnes, W.C., Justice, M.J., Parkinson, H.E., Moore, M., Wells, S., Braun, R.E., Svenson, K.L., de Angelis, M.H., Herault, Y., Mohun, T., Mallon, A.-M., Henkelman, R.M., Brown, S.D.M., Adams, D.J., Lloyd, K.C.K., McKerlie, C., Beaudet, A.L., Bućan, M., Murray, S.A., 2016. High-throughput discovery of novel developmental phenotypes. Nature 537, 508–514.

Domogatskaya, A., Rodin, S., Tryggvason, K., 2012. Functional Diversity of Laminins. Annu. Rev. Cell Dev. Biol. 28, 523–553.

Dong, L., Chen, Y., Lewis, M., Hsieh, J.-C., Reing, J., Chaillet, J.R., Howell, C.Y.,

Melhem, M., Inoue, S., Kuszak, J.R., DeGeest, K., Chung, A.E., 2002. Neurologic defects and selective disruption of basement membranes in mice lacking entactin-1/nidogen-1. Lab. Invest. 82, 1617–1630.

Donoghue, M.J., Sanes, J.R., 1994. All muscles are not created equal. Trends Genet. 10, 396–401.

Durkin, M.E., Chakravarti, S., Bartos, B.B., Liu, S.-H., Friedman, R.L., Chung, A.E., 1988. Amino acid sequence and domain structure of entactin. Homology with epidermal growth factor precursor and low density lipoprotein receptor. J. Cell Biol. 107, 2749–2756.

Duveau, V., Madhusudan, A., Caleo, M., Knuesel, I., Fritschy, J.-M., 2011. Impaired reelin processing and secretion by Cajal-Retzius cells contributes to granule cell dispersion in a mouse model of temporal lobe epilepsy. Hippocampus 21, 935–44.

Dziadek, M., Clements, R., Mitrangas, K., Reiter, H., Fowler, K., 1988. Analysis of degradation of the basement membrane protein nidogen, using a specific monoclonal antibody. Eur. J. Biochem. 172, 219–25.

Dziadek, M., Edgar, D., Paulsson, M., Timpl, R., Fleischmajer, R., 1986. Basement membrane proteins produced by Schwann cells and in neurofibromatosis. Ann. N. Y. Acad. Sci. 486, 248–259.

Dziadek, M., Paulsson, M., Timpl, R., 1985. Identification and interaction repertoire of large forms of the basement membrane protein nidogen. EMBO J. 4, 2513–8.

Engel, J., Odermatt, E., Engel, A., Madri, J.A., Furthmayr, H., Rohde, H., Timpl, R., 1981. Shapes, domain organizations and flexibility of laminin and fibronectin, two multifunctional proteins of the extracellular matrix. J. Mol. Biol. 150, 97–120.

Ernst, C., Christie, B.R., 2006. Isolectin-IB 4 as a vascular stain for the study of adult neurogenesis. J. Neurosci. Methods 150, 138–42.

Eshed, Y., Feinberg, K., Carey, D.J., Peles, E., 2007. Secreted gliomedin is a perinodal matrix component of peripheral nerves. J. Cell Biol. 177, 551–562.

Exposito, J.-Y., Valcourt, U., Cluzel, C., Lethias, C., 2010. The fibrillar collagen family. Int. J. Mol. Sci. 11, 407–26.

Farach-Carson, M.C., Carson, D.D., 2007. Perlecan--a multifunctional extracellular proteoglycan scaffold. Glycobiology 17, 897–905.

Farrawell, N.E., Lambert-Smith, I.A., Warraich, S.T., Blair, I.P., Saunders, D.N., Hatters, D.M., Yerbury, J.J., 2015. Distinct partitioning of ALS associated TDP-43, FUS and SOD1 mutants into cellular inclusions. Sci. Rep. 5, 13416.

Ferns, M.J., Campanelli, J.T., Hoch, W., Scheller, R.H., Hall, Z., 1993. The Ability of Agrin to Cluster AChRs Depends on Alternative Splicing and on Cell Surface Proteoglycans. Neuron 11, 491–502.

ffrench-Constant, C., 1995. Alternative splicing of fibronectin--many different proteins but few different functions. Exp. Cell Res. 221, 261–71.

Fidler, A.L., Darris, C.E., Chetyrkin, S. V., Pedchenko, V.K., Boudko, S.P., Brown, K.L., Gray Jerome, W., Hudson, J.K., Rokas, A., Hudson, B.G., 2017. Collagen IV and basement membrane at the evolutionary dawn of metazoan tissues. Elife 6, e24176.

Fischer, L.R., Culver, D.G., Tennant, P., Davis, A.A., Wang, M., Castellano-Sanchez, A., Khan, J., Polak, M.A., Glass, J.D., 2004. Amyotrophic lateral sclerosis is a distal axonopathy: Evidence in mice and man. Exp. Neurol.

Folkman, J., Klagsbrun, M., Sasse, J., Wadzinski, M., Ingber, D., Vlodavsky, I., 1988. A heparin-binding angiogenic protein--basic fibroblast growth factor--is stored within basement membrane. Am. J. Pathol. 130, 393–400.

Fox, J.W., Mayer, U., Nischt, R., Aumailley, M., Reinhardt, D., Wiedemann, H., Mann, K., Timpl, R., Krieg, T., Engel, J., 1991. Recombinant nidogen consists of three globular domains and mediates binding of laminin to collagen type IV. EMBO J. 10, 3137–46.

Fox, M.A., Ho, M.S.P., Smyth, N., Sanes, J.R., 2008. A synaptic nidogen: developmental regulation and role of nidogen-2 at the neuromuscular junction. Neural Dev. 3, 24.

Frey, D., Schneider, C., Xu, L., Borg, J., Spooren, W., Caroni, P., 2000. Early and selective loss of neuromuscular synapse subtypes with low sprouting competence in motoneuron diseases. J. Neurosci. 20, 2534–42.

Funakoshi, H., Belluardo, N., Arenas, E., Yamamoto, Y., Casabona, A., Persson, H., Ibáñez, C.F., 1995. Muscle-derived neurotrophin-4 as an activity-

dependent trophic signal for adult motor neurons. Science 268, 1495–9.

Galpin, A.J., Raue, U., Jemiolo, B., Trappe, T.A., Harber, M.P., Minchev, K., Trappe, S., 2012. Human skeletal muscle fiber type specific protein content. Anal. Biochem. 425, 175–182.

Gee, S.H., Blacher, R.W., Douville, P.J., Provost, P.R., Yurchenco, P.D., Carbonetto, S., 1993. Laminin-binding protein 120 from brain is closely related to the dystrophin-associated glycoprotein, dystroglycan, and binds with high affinity to the major heparin binding domain of laminin. J. Biol. Chem. 268, 14972–80.

Gesemann, M., 1995. Acetylcholine receptor-aggregating activity of agrin isoforms and mapping of the active site. J. Cell Biol. 128, 625–636.

Gil, C., Chaib-Oukadour, I., Aguilera, J., 2003. C-terminal fragment of tetanus toxin heavy chain activates Akt and MEK/ERK signalling pathways in a Trk receptor-dependent manner in cultured cortical neurons. Biochem. J. 373, 613–20.

Gillet, Y., Issartel, B., Vanhems, P., Fournet, J.-C., Lina, G., Bes, M., Vandenesch, F., Piémont, Y., Brousse, N., Floret, D., Etienne, J., 2002. Association between Staphylococcus aureus strains carrying gene for Panton-Valentine leukocidin and highly lethal necrotising pneumonia in young immunocompetent patients. Lancet (London, England) 359, 753–9.

Gómez-Palacio-Schjetnan, A., Escobar, M.L., 2013. Neurotrophins and synaptic plasticity. Curr. Top. Behav. Neurosci. 15, 117–36.

Gómez-Pinilla, F., Ying, Z., Opazo, P., Roy, R.R., Edgerton, V.R., 2001. Differential regulation by exercise of BDNF and NT-3 in rat spinal cord and skeletal muscle. Eur. J. Neurosci. 13, 1078–1084.

Gould, D.B., Phalan, F.C., Breedveld, G.J., van Mil, S.E., Smith, R.S., Schimenti, J.C., Aguglia, U., van der Knaap, M.S., Heutink, P., John, S.W.M., 2005. Mutations in Col4a1 cause perinatal cerebral hemorrhage and porencephaly. Science 308, 1167–71.

Grimpe, B., Probst, J.C., Hager, G., 1999. Suppression of nidogen-1 translation by antisense targeting affects the adhesive properties of cultured astrocytes. Glia 28, 138–149.

Gubbiotti, M.A., Neill, T., Iozzo, R. V., 2017. A current view of perlecan in physiology and pathology: A mosaic of functions. Matrix Biol. 57–58, 285–298.

Haas, C.A., Dudeck, O., Kirsch, M., Huszka, C., Kann, G., Pollak, S., Zentner, J., Frotscher, M., 2002. Role for reelin in the development of granule cell dispersion in temporal lobe epilepsy. J. Neurosci. 22, 5797–802.

Halfter, W., Dong, S., Yip, Y.-P., Willem, M., Mayer, U., 2002. A critical function of the pial basement membrane in cortical histogenesis. J. Neurosci. 22, 6029–40.

Halfter, W., Yip, J., 2014. An organizing function of basement membranes in the developing nervous system. Mech. Dev. 133, 1–10.

Helbling-Leclerc, A., Zhang, X., Topaloglu, H., Cruaud, C., Tesson, F., Weissenbach, J., Tomé, F.M.S., Schwartz, K., Fardeau, M., Tryggvason, K., 1995. Mutations in the laminin alpha 2-chain gene (LAMA2) cause merosin-deficient congenital muscular dystrophy. Nat. Genet. 11, 216–8.

Henderson, C.E., Phillips, H.S., Pollock, R.A., Davies, A.M., Lemeulle, C., Armanini, M., Simmons, L., Moffet, B., Vandlen, R.A., Simpson LC corrected to Simmons, L., Koliatsos, V.E., Rosenthal, A., 1994. GDNF: a potent survival factor for motoneurons present in peripheral nerve and muscle. Science 266, 1062–4.

Hohenester, E., Yurchenco, P.D., 2013. Laminins in basement membrane assembly. Cell Adh. Migr. 7, 56–63.

Hopf, M., Göhring, W., Kohfeldt, E., Yamada, Y., Timpl, R., 1999. Recombinant domain IV of perlecan binds to nidogens, laminin-nidogen complex, fibronectin, fibulin-2 and heparin. Eur. J. Biochem. 259, 917–25.

Hopf, M., Göhring, W., Mann, K., Timpl, R., 2001. Mapping of binding sites for nidogens, fibulin-2, fibronectin and heparin to different IG modules of perlecan 1 1Edited by M. F. Moody. J. Mol. Biol. 311, 529–541.

Hoppeler, H., 2016. Molecular networks in skeletal muscle plasticity. J. Exp. Biol. 219, 205–13.

Huang, E.J., Reichardt, L.F., 2001. Neurotrophins: Roles in Neuronal Development and Function. Annu. Rev. Neurosci. 24, 677–736.

Hudson, B.G., Kalluri, R., Gunwar, S., Weber, M., Ballester, F., Hudson, J.K., Noelken, M.E., Sarras, M., Richardson, W.R., Saus, J., 1992. The pathogenesis of Alport syndrome involves type IV collagen molecules containing the alpha 3(IV) chain: evidence from anti-GBM nephritis after renal transplantation. Kidney Int. 42, 179–87.

Hughes, S.M., Chi, M.M.Y., Lowry, O.H., Gundersen, K., 1999. Myogenin induces a shift of enzyme activity from glycolytic to oxidative metabolism in muscles of transgenic mice. J. Cell Biol. 145, 633–42.

Hynes, R.O., 2002. Integrins. Cell 110, 673–687.

Hynes, R.O., 2012. The evolution of metazoan extracellular matrix. J. Cell Biol. 196, 671–9.

Ibraghimov-Beskrovnaya, O., Ervasti, J.M., Leveille, C.J., Slaughter, C.A., Sernett, S.W., Campbell, K.P., 1992. Primary structure of dystrophin-associated glycoproteins linking dystrophin to the extracellular matrix. Nature 355, 696–702.

Kalluri, R., 2003. Basement membranes: Structure, assembly and role in tumour angiogenesis. Nat. Rev. Cancer 3, 422–433.

Kalmar, B., Novoselov, S., Gray, A., Cheetham, M.E., Margulis, B., Greensmith, L., 2008. Late stage treatment with arimoclomol delays disease progression and prevents protein aggregation in the SOD1 mouse model of ALS. J. Neurochem. 107, 339–50.

Kami, K., Morikawa, Y., Kawai, Y., Senba, E., 1999. Leukemia inhibitory factor, glial cell line-derived neurotrophic factor, and their receptor expressions following muscle crush injury. Muscle Nerve 22, 1576–1586.

Kashtan, C., 2017. Alport syndrome: facts and opinions. F1000Research 6, 50.

Khoshnoodi, J., Pedchenko, V., Hudson, B.G., 2008. Mammalian collagen IV. Microsc. Res. Tech. 71, 357–70.

Kieran, D., Hafezparast, M., Bohnert, S., Dick, J.R.T., Martin, J., Schiavo, G., Fisher, E.M.C., Greensmith, L., 2005. A mutation in dynein rescues axonal transport defects and extends the life span of ALS mice. J. Cell Biol. 169, 561–7.

Kim, M., Ogawa, M., Fujita, Y., Yoshikawa, Y., Nagai, T., Koyama, T., Nagai, S.,

Lange, A., Fässler, R., Sasakawa, C., 2009. Bacteria hijack integrin-linked kinase to stabilize focal adhesions and block cell detachment. Nature 459, 578–82.

Kim, N., Stiegler, A.L., Cameron, T.O., Hallock, P.T., Gomez, A.M., Huang, J.H., Hubbard, S.R., Dustin, M.L., Burden, S.J., 2008. Lrp4 is a receptor for Agrin and forms a complex with MuSK. Cell 135, 334–42.

Kim, S.-H., Turnbull, J., Guimond, S., 2011. Extracellular matrix and cell signalling: the dynamic cooperation of integrin, proteoglycan and growth factor receptor. J. Endocrinol. 209, 139–51.

Kim, S., Wadsworth, W.G., 2000. Positioning of longitudinal nerves in C. elegans by nidogen. Science 288, 150–154.

Kohfeldt, E., Sasaki, T., Göhring, W., Timpl, R., 1998. Nidogen-2: a new basement membrane protein with diverse binding properties. J. Mol. Biol. 282, 99–109.

Köhling, R., Nischt, R., Vasudevan, A., Ho, M., Weiergräber, M., Schneider, T., Smyth, N., 2006. Nidogen and nidogen-associated basement membrane proteins and neuronal plasticity. Neurodegener. Dis. 3, 56–61.

Kuang, W., Xu, H., Vachon, P.H., Engvall, E., 1998. Disruption of the lama2 gene in embryonic stem cells: laminin alpha 2 is necessary for sustenance of mature muscle cells. Exp. Cell Res. 241, 117–25.

Küspert, M., Hammer, A., Bösl, M.R., Wegner, M., 2011. Olig2 regulates Sox10 expression in oligodendrocyte precursors through an evolutionary conserved distal enhancer. Nucleic Acids Res. 39, 1280–93.

Lalli, G., Bohnert, S., Deinhardt, K., Verastegui, C., Schiavo, G., 2003. The journey of tetanus and botulinum neurotoxins in neurons. Trends Microbiol. 11, 431–437.

Lalli, G., Schiavo, G., 2002. Analysis of retrograde transport in motor neurons reveals common endocytic carriers for tetanus toxin and neurotrophin receptor p75NTR. J. Cell Biol. 156, 233–9.

Land, B.R., Harris, W. V, Salpeter, E.E., Salpeter, M.M., 1984. Diffusion and binding constants for acetylcholine derived from the falling phase of miniature endplate currents. Proc. Natl. Acad. Sci. U. S. A.

Laurila, P., Leivo, I., 1993. Basement membrane and interstitial matrix components form separate matrices in heterokaryons of PYS-2 cells and fibroblasts. J. Cell Sci. 104 (Pt 1, 59–68.

Lee, H.K., Seo, I.A., Park, H.K., Park, Y.M., Ahn, K.J., Yoo, Y.H., Park, H.T., 2007. Nidogen is a prosurvival and promigratory factor for adult Schwann cells. J. Neurochem. 102, 686–698.

Lee, S., Jilani, S.M., Nikolova, G. V., Carpizo, D., Iruela-Arispe, M.L., 2005. Processing of VEGF-A by matrix metalloproteinases regulates bioavailability and vascular patterning in tumors. J. Cell Biol. 169, 681–91.

Lerner, R.A., Glassock, R.J., Dixon, F.J., 1967. The role of anti-glomerular basement membrane antibody in the pathogenesis of human glomerulonephritis. J. Exp. Med. 126, 989–1004.

Li, A.C.Y., Thompson, R.P.H., 2003. Basement membrane components. J. Clin. Pathol. 56, 885–7.

Li, S., Harrison, D., Carbonetto, S., Fassler, R., Smyth, N., Edgar, D., Yurchenco, P.D., 2002. Matrix assembly, regulation, and survival functions of laminin and its receptors in embryonic stem cell differentiation. J. Cell Biol. 157, 1279–90.

Liesi, P., Kauppila, T., 2002. Induction of type IV collagen and other basement-membrane-associated proteins after spinal cord injury of the adult rat may participate in formation of the glial scar. Exp. Neurol. 173, 31–45.

Lisi, M.T., Cohn, R.D., 2007. Congenital muscular dystrophies: New aspects of an expanding group of disorders. Biochim. Biophys. Acta - Mol. Basis Dis. 1772, 159–172.

Liu, Y., Beyer, A., Aebersold, R., 2016. On the Dependency of Cellular Protein Levels on mRNA Abundance. Cell 165, 535–50.

Lustig, M., Zanazzi, G., Sakurai, T., Blanco, C., Levinson, S.R., Lambert, S., Grumet, M., Salzer, J.L., 2001. Nr-CAM and neurofascin interactions regulate ankyrin G and sodium channel clustering at the node of Ranvier Voltage-dependent sodium (Na) channels are myelinated axons and play a key role in promoting rapid and efficient conduction of action potentials b. Curr. Biol. 11, 1864–1869.

MacDonald, M.L., Favo, D., Garver, M., Sun, Z., Arion, D., Ding, Y., Yates, N., Sweet, R.A., Lewis, D.A., 2019. Laser capture microdissection-targeted mass spectrometry: a method for multiplexed protein quantification within individual layers of the cerebral cortex. Neuropsychopharmacology 44, 743–748.

Macdonald, P.R., Lustig, A., Steinmetz, M.O., Kammerer, R.A., 2010. Laminin chain assembly is regulated by specific coiled-coil interactions. J. Struct. Biol. 170, 398–405.

Makarenkova, H.P., Hoffman, M.P., Beenken, A., Eliseenkova, A. V., Meech, R., Tsau, C., Patel, V.N., Lang, R.A., Mohammadi, M., 2009. Differential interactions of FGFs with heparan sulfate control gradient formation and branching morphogenesis. Sci. Signal. 2, ra55.

Mallineni, S.K., Yiu, C.K.Y., King, N.M., 2012. Schwartz-Jampel syndrome: a review of the literature and case report. Spec. Care Dent. 32, 105–111.

Marín-Padilla, M., 1998. Cajal-Retzius cells and the development of the neocortex. Trends Neurosci. 21, 64–71.

Martino, M.M., Briquez, P.S., Güç, E., Tortelli, F., Kilarski, W.W., Metzger, S., Rice, J.J., Kuhn, G.A., Müller, R., Swartz, M.A., Hubbell, J.A., 2014. Growth factors engineered for super-affinity to the extracellular matrix enhance tissue healing. Science 343, 885–8.

Masahira, N., Takebayashi, H., Ono, K., Watanabe, K., Ding, L., Furusho, M., Ogawa, Y., Nabeshima, Y., Alvarez-Buylla, A., Shimizu, K., Ikenaka, K., 2006. Olig2-positive progenitors in the embryonic spinal cord give rise not only to motoneurons and oligodendrocytes, but also to a subset of astrocytes and ependymal cells. Dev. Biol. 293, 358–69.

Maselli, R.A., Ng, J.J., Anderson, J.A., Cagney, O., Arredondo, J., Williams, C., Wessel, H.B., Abdel-Hamid, H., Wollmann, R.L., 2009. Mutations in LAMB2 causing a severe form of synaptic congenital myasthenic syndrome. J. Med. Genet. 46, 203–8.

Mazzon, C., Anselmo, A., Soldani, C., Cibella, J., Ploia, C., Moalli, F., Burden, S.J., Dustin, M.L., Sarukhan, A., Viola, A., 2012. Agrin is required for survival and function of monocytic cells. Blood 119, 5502–11.

McKee, K.K., Harrison, D., Capizzi, S., Yurchenco, P.D., 2007. Role of laminin terminal globular domains in basement membrane assembly. J. Biol. Chem. 282, 21437–47.

McMahan, U.J., Sanes, J.R., Marshall, L.M., 1978. Cholinesterase is associated with the basal lamina at the neuromuscular junction. Nature.

Mehuron, T., Kumar, A., Duarte, L., Yamauchi, J., Accorsi, A., Girgenrath, M., 2014. Dysregulation of matricellular proteins is an early signature of pathology in laminin-deficient muscular dystrophy. Skelet. Muscle 4, 14.

Meier, H., Southard, J.L., 1970. Muscular dystrophy in the mouse caused by an allele at the dy-locus. Life Sci. 9, 137–44.

Michelson, A.M., Russell, E.S., Harman, P.J., 1955. Dystrophia Muscularis: A HEREDITARY PRIMARY MYOPATHY IN THE HOUSE MOUSE. Proc. Natl. Acad. Sci. U. S. A. 41, 1079–84.

Mikuni, N., Babb, T.L., Chakravarty, D.N., Christi, W., 1999. Time course of transient expression of GDNF protein in rat granule cells of the bilateral dentate gyri after unilateral intrahippocampal kainic acid injection. Neurosci. Lett. 262, 215–8.

Miner, J.H., Yurchenco, P.D., 2004. Laminin functions in tissue morphogenesis. Annu. Rev. Cell Dev. Biol. 20, 255–84.

Miosge, N., Sasaki, T., Timpl, R., 2002. Evidence of nidogen-2 compensation for nidogen-1 deficiency in transgenic mice. Matrix Biol. 21, 611–621.

Miura, M., Terajima, J., Izumiya, H., Mitobe, J., Komano, T., Watanabe, H., 2006. OspE2 of Shigella sonnei is required for the maintenance of cell architecture of bacterium-infected cells. Infect. Immun. 74, 2587–95.

Montanaro, F., Lindenbaum, M., Carbonetto, S., 1999. alpha-Dystroglycan is a laminin receptor involved in extracellular matrix assembly on myotubes and muscle cell viability. J. Cell Biol. 145, 1325–40.

Morrissey, M.A., Sherwood, D.R., 2015. An active role for basement membrane assembly and modification in tissue sculpting. J. Cell Sci. 128, 1661–8.

Murshed, M., Smyth, N., Miosge, N., Karolat, J.R., Krieg, T., Paulsson, M., Nischt, R., 2000. The Absence of Nidogen 1 Does Not Affect Murine Basement Membrane Formation 20, 7007–7012.

Nakamura, T., 2018. Roles of short fibulins, a family of matricellular proteins, in lung matrix assembly and disease. Matrix Biol. 73, 21–33.

Nazarian, J., Bouri, K., Hoffman, E.P., 2005. Intracellular expression profiling by laser capture microdissection: three novel components of the neuromuscular junction. Physiol. Genomics 21, 70–80.

Nguyen, Q.T., Parsadanian, A.S., Snider, W.D., Lichtman, J.W., 1998. Hyperinnervation of neuromuscular junctions caused by GDNF overexpression in muscle. Science (80-.).

Nguyen, Q.T., Sanes, J.R., Lichtman, J.W., 2002. Pre-existing pathways promote precise projection patterns. Nat. Neurosci. 5, 861–7.

Nicole, S., Davoine, C.S., Topaloglu, H., Cattolico, L., Barral, D., Beighton, P., Hamida, C. Ben, Hammouda, H., Cruaud, C., White, P.S., Samson, D., Urtizberea, J.A., Lehmann-Horn, F., Weissenbach, J., Hentati, F., Fontaine, B., 2000. Perlecan, the major proteoglycan of basement membranes, is altered in patients with Schwartz-Jampel syndrome (chondrodystrophic myotonia). Nat. Genet. 26, 480–483.

Noakes, P.G., Gautam, M., Mudd, J., Sanes, J.R., Merlie, J.P., 1995. Aberrant differentiation of neuromuscular junctions in mice lacking s-laminin/laminin beta 2. Nature 374, 258–62.

O'Grady, P., Thai, T.C., Saito, H., 1998. The laminin-nidogen complex is a ligand for a specific splice isoform of the transmembrane protein tyrosine phosphatase LAR. J. Cell Biol. 141, 1675–84.

O'Toole, J.J., Deyst, K. a, Bowe, M. a, Nastuk, M. a, McKechnie, B. a, Fallon, J.R., 1996. Alternative splicing of agrin regulates its binding to heparin alpha-dystroglycan, and the cell surface. Proc. Natl. Acad. Sci. U. S. A. 93, 7369–74.

Occhi, S., Zambroni, D., Del Carro, U., Amadio, S., Sirkowski, E.E., Scherer, S.S., Campbell, K.P., Moore, S.A., Chen, Z.-L., Strickland, S., Di Muzio, A., Uncini, A., Wrabetz, L., Feltri, M.L., 2005. Both laminin and Schwann cell dystroglycan are necessary for proper clustering of sodium channels at nodes of Ranvier. J. Neurosci. 25, 9418–27.

Ono, K., Takebayashi, H., Ikeda, K., Furusho, M., Nishizawa, T., Watanabe, K.,

Ikenaka, K., 2008. Regional- and temporal-dependent changes in the differentiation of Olig2 progenitors in the forebrain, and the impact on astrocyte development in the dorsal pallium. Dev. Biol. 320, 456–68.

Ornitz, D.M., Itoh, N., 2016. The Fibroblast Growth Factor signaling pathway. Wiley Interdiscip. Rev. Dev. Biol. 4, 215–66.

Ozbek, S., Balasubramanian, P.G., Chiquet-Ehrismann, R., Tucker, R.P., Adams, J.C., 2010. The evolution of extracellular matrix. Mol. Biol. Cell 21, 4300–5.

Pan, T.C., Sasaki, T., Zhang, R.Z., Fässler, R., Timpl, R., Chu, M.L., 1993. Structure and expression of fibulin-2, a novel extracellular matrix protein with multiple EGF-like repeats and consensus motifs for calcium binding. J. Cell Biol. 123, 1269–77.

Paratcha, G., Ledda, F., Ibáñez, C.F., 2003. The neural cell adhesion molecule NCAM is an alternative signaling receptor for GDNF family ligands. Cell 113, 867–879.

Patel, V.N., Knox, S.M., Likar, K.M., Lathrop, C.A., Hossain, R., Eftekhari, S., Whitelock, J.M., Elkin, M., Vlodavsky, I., Hoffman, M.P., 2007. Heparanase cleavage of perlecan heparan sulfate modulates FGF10 activity during ex vivo submandibular gland branching morphogenesis. Development 134, 4177–86.

Patton, B.L., 2000. Laminins of the neuromuscular system. Microsc. Res. Tech. 51, 247–61.

Paulsson, M., Deutzmann, R., Timpl, R., Dalzoppo, D., Odermatt, E., Engel, J., 1985. Evidence for coiled-coil alpha-helical regions in the long arm of laminin. EMBO J. 4, 309–16.

Pedchenko, V., Vanacore, R., Hudson, B., 2011. Goodpasture's disease: molecular architecture of the autoantigen provides clues to etiology and pathogenesis. Curr. Opin. Nephrol. Hypertens. 20, 290–6.

Pelaseyed, T., Bergström, J.H., Gustafsson, J.K., Ermund, A., Birchenough, G.M.H., Schütte, A., van der Post, S., Svensson, F., Rodríguez-Piñeiro, A.M., Nyström, E.E.L., Wising, C., Johansson, M.E. V, Hansson, G.C., 2014. The mucus and mucins of the goblet cells and enterocytes provide the first

defense line of the gastrointestinal tract and interact with the immune system. Immunol. Rev. 260, 8–20.

Peter, A.K., Cheng, H., Ross, R.S., Knowlton, K.U., Chen, J., 2011. The costamere bridges sarcomeres to the sarcolemma in striated muscle. Prog. Pediatr. Cardiol. 31, 83–88.

Pitts, E.V., Potluri, S., Hess, D.M., Balice-Gordon, R.J., 2006. Neurotrophin and Trk-mediated signaling in the neuromuscular system. Int. Anesthesiol. Clin. 44, 21–76.

Podos, S.D., Ferguson, E.L., 1999. Morphogen gradients: new insights from DPP. Trends Genet. 15, 396–402.

Potthoff, M.J., Wu, H., Arnold, M.A., Shelton, J.M., Backs, J., McAnally, J., Richardson, J.A., Bassel-Duby, R., Olson, E.N., 2007. Histone deacetylase degradation and MEF2 activation promote the formation of slow-twitch myofibers. J. Clin. Invest. 117, 2459–67.

Pujuguet, P., Simian, M., Liaw, J., Timpl, R., Werb, Z., Bissell, M.J., 2000. Nidogen-1 regulates laminin-1-dependent mammary-specific gene expression. J. Cell Sci. 113 (Pt 5, 849–58.

Pun, S., Sigrist, M., Santos, A.F., Ruegg, M.A., Sanes, J.R., Jessell, T.M., Arber, S., Caroni, P., 2002. An intrinsic distinction in neuromuscular junction assembly and maintenance in different skeletal muscles. Neuron 34, 357–370.

Reeben, M., Laurikainen, A., Hiltunen, J.O., Castrén, E., Saarma, M., 1998. The messenger RNAs for both glial cell line-derived neurotrophic factor receptors, c-ret and GDNFRalpha, are induced in the rat brain in response to kainate-induced excitation. Neuroscience 83, 151–9.

Ricard-Blum, S., 2011. The collagen family. Cold Spring Harb. Perspect. Biol. 3, a004978.

Ries, A., Göhring, W., Fox, J.W., Timpl, R., Sasaki, T., 2001. Recombinant domains of mouse nidogen-1 and their binding to basement membrane proteins and monoclonal antibodies. Eur. J. Biochem. 268, 5119–5128.

Ruoslahti, E., Yamaguchi, Y., 1991. Proteoglycans as modulators of growth factor activities. Cell 64, 867–9.

Saarma, M., 2009. GFL Neurotrophic Factors: Physiology and Pharmacology. In: Encyclopedia of Neuroscience. Elsevier, pp. 711–720.

Saito, F., Moore, S.A., Barresi, R., Henry, M.D., Messing, A., Ross-Barta, S.E., Cohn, R.D., Williamson, R.A., Sluka, K.A., Sherman, D.L., Brophy, P.J., Schmelzer, J.D., Low, P.A., Wrabetz, L., Feltri, M.L., Campbell, K.P., 2003. Unique role of dystroglycan in peripheral nerve myelination, nodal structure, and sodium channel stabilization. Neuron 38, 747–758.

Saksela, O., Rifkin, D.B., 1990. Release of basic fibroblast growth factor-heparan sulfate complexes from endothelial cells by plasminogen activator-mediated proteolytic activity. J. Cell Biol. 110, 767–75.

Sakuma, K., Yamaguchi, A., 2011. The Recent Understanding of the Neurotrophin's Role in Skeletal Muscle Adaptation. J. Biomed. Biotechnol. 2011, 1–12.

Salmivirta, K., Talts, J.F., Olsson, M., Sasaki, T., Timpl, R., Ekblom, P., 2002. Binding of mouse nidogen-2 to basement membrane components and cells and its expression in embryonic and adult tissues suggest complementary functions of the two nidogens. Exp. Cell Res. 279, 188–201.

Sanes, J.R., 2003. The basement membrane/basal lamina of skeletal muscle. J. Biol. Chem. 278, 12601–4.

Sanes, J.R., Engvall, E., Butkowski, R., Hunter, D.D., 1990. Molecular heterogeneity of basal laminae: isoforms of laminin and collagen IV at the neuromuscular junction and elsewhere. J. Cell Biol. 111, 1685–99.

Sariola, H., Saarma, M., 2003. Novel functions and signalling pathways for GDNF. J. Cell Sci. 116, 3855–62.

Sarker, S.A., Gyr, K., 1992. Non-immunological defence mechanisms of the gut. Gut 33, 987–993.

Sasaki, T., Göhring, W., Pan, T.C., Chu, M.L., Timpl, R., 1995. Binding of mouse and human fibulin-2 to extracellular matrix ligands. J. Mol. Biol. 254, 892–9.

Savige, J., 2014. Alport syndrome: its effects on the glomerular filtration barrier and implications for future treatment. J. Physiol. 592, 4013–23.

Schindelin, J., Arganda-Carreras, I., Frise, E., Kaynig, V., Longair, M., Pietzsch, T., Preibisch, S., Rueden, C., Saalfeld, S., Schmid, B., Tinevez, J.-Y., White,

D.J., Hartenstein, V., Eliceiri, K., Tomancak, P., Cardona, A., 2012. Fiji: an open-source platform for biological-image analysis. Nat. Methods 9, 676–82.

Schlessinger, J., Plotnikov, A.N., Ibrahimi, O.A., Eliseenkova, A. V., Yeh, B.K., Yayon, A., Linhardt, R.J., Mohammadi, M., 2000. Crystal structure of a ternary FGF-FGFR-heparin complex reveals a dual role for heparin in FGFR binding and dimerization. Mol. Cell 6, 743–50.

Schmieg, N., Menendez, G., Schiavo, G., Terenzio, M., 2014. Signalling endosomes in axonal transport: Travel updates on the molecular highway. Semin. Cell Dev. Biol. 27, 32–43.

Schymeinsky, J., Nedbal, S., Miosge, N., Pöschl, E., Rao, C., Beier, D.R., Skarnes, W.C., Timpl, R., Bader, B.L., 2002. Gene Structure and Functional Analysis of the Mouse Nidogen-2 Gene: Nidogen-2 Is Not Essential for Basement Membrane Formation in Mice. Mol. Cell. Biol. 22, 6820–6830.

Sethi, S., Vrana, J.A., Theis, J.D., Leung, N., Sethi, A., Nasr, S.H., Fervenza, F.C., Cornell, L.D., Fidler, M.E., Dogan, A., 2012. Laser microdissection and mass spectrometry-based proteomics aids the diagnosis and typing of renal amyloidosis. Kidney Int. 82, 226–34.

Sherwood, D.R., 2015. A developmental biologist's "outside-the-cell" thinking. J. Cell Biol. 210, 369–72.

Sleigh, J.N., Burgess, R.W., Gillingwater, T.H., Cader, M.Z., 2014. Morphological analysis of neuromuscular junction development and degeneration in rodent lumbrical muscles. J. Neurosci. Methods 227, 159–65.

Sofroniew, M. V., 2014. Multiple roles for astrocytes as effectors of cytokines and inflammatory mediators. Neuroscientist 20, 160–72.

Sonawane, A.R., Platig, J., Fagny, M., Chen, C.-Y., Paulson, J.N., Lopes-Ramos, C.M., DeMeo, D.L., Quackenbush, J., Glass, K., Kuijjer, M.L., 2017. Understanding Tissue-Specific Gene Regulation. Cell Rep. 21, 1077–1088.

Stolt, C.C., Rehberg, S., Ader, M., Lommes, P., Riethmacher, D., Schachner, M., Bartsch, U., Wegner, M., 2002. Terminal differentiation of myelin-forming oligodendrocytes depends on the transcription factor Sox10. Genes Dev. 16, 165–70.

Stum, M., Davoine, C.-S., Vicart, S., Guillot-Noël, L., Topaloglu, H., Carod-Artal,

F.J., Kayserili, H., Hentati, F., Merlini, L., Urtizberea, J.A., Hammouda, E.-H., Quan, P.C., Fontaine, B., Nicole, S., 2006. Spectrum of HSPG2 (Perlecan) mutations in patients with Schwartz-Jampel syndrome. Hum. Mutat. 27, 1082–1091.

Susuki, K., Rasband, M.N., 2008. Molecular mechanisms of node of Ranvier formation. Curr. Opin. Cell Biol. 20, 616–23.

Suzuki, H., Hase, A., Miyata, Y., Arahata, K., Akazawa, C., 1998. Prominent expression of glial cell line-derived neurotrophic factor in human skeletal muscle. J. Comp. Neurol. 402, 303–312.

Suzuki, N., Sekimoto, K., Hayashi, C., Mabuchi, Y., Nakamura, T., Akazawa, C., 2017. Differentiation of Oligodendrocyte Precursor Cells from Sox10-Venus Mice to Oligodendrocytes and Astrocytes. Sci. Rep. 7, 14133.

Takahashi, H., Shibuya, M., 2005. The vascular endothelial growth factor (VEGF)/VEGF receptor system and its role under physiological and pathological conditions. Clin. Sci. (Lond). 109, 227–41.

Terenzio, M., Golding, M., Russell, M.R.G., Wicher, K.B., Rosewell, I., Spencer-Dene, B., Ish-Horowicz, D., Schiavo, G., 2014. Bicaudal-D1 regulates the intracellular sorting and signalling of neurotrophin receptors. EMBO J. 33, 1582–1598.

Timpl, R., 1989. Structure and biological activity of basement membrane proteins. Eur. J. Biochem. 180, 487–502.

Timpl, R., Brown, J.C., 1994. The laminins. Matrix Biol. 14, 275–81.

Timpl, R., Brown, J.C., 1996. Supramolecular assembly of basement membranes. Bioessays 18, 123–32.

Timpl, R., Wiedemann, H., van Delden, V., Furthmayr, H., Kühn, K., 1981. A network model for the organization of type IV collagen molecules in basement membranes. Eur. J. Biochem. 120, 203–11.

Tomé, F.M., Evangelista, T., Leclerc, A., Sunada, Y., Manole, E., Estournet, B., Barois, A., Campbell, K.P., Fardeau, M., 1994. Congenital muscular dystrophy with merosin deficiency. C. R. Acad. Sci. III. 317, 351–7.

Trelstad, R.L., 1988. The extracellular matrix is a soluble and solid-phase agonist and receptor. Arch. Dermatol. 124, 706–8.

Tremblay, E., Martineau, É., Robitaille, R., 2017. Opposite Synaptic Alterations at the Neuromuscular Junction in an ALS Mouse Model: When Motor Units Matter. J. Neurosci. 37, 8901–8918.

Turck, N., Gross, I., Gendry, P., Stutzmann, J., Freund, J.-N., Kedinger, M., Simon-Assmann, P., Launay, J.-F., 2005. Laminin isoforms: biological roles and effects on the intracellular distribution of nuclear proteins in intestinal epithelial cells. Exp. Cell Res. 303, 494–503.

Turner, N., Mason, P.J., Brown, R., Fox, M., Povey, S., Rees, A., Pusey, C.D., 1992. Molecular cloning of the human Goodpasture antigen demonstrates it to be the alpha 3 chain of type IV collagen. J. Clin. Invest. 89, 592–601.

Ungar, O.J., Nadol, J.B., Santos, F., 2018. Temporal Bone Histopathology of X-linked Inherited Alport Syndrome. Laryngoscope Investig. Otolaryngol. 3, 311–314.

van der Knaap, M.S., Smit, L.M.E., Barkhof, F., Pijnenburg, Y.A.L., Zweegman, S., Niessen, H.W.M., Imhof, S., Heutink, P., 2006. Neonatal porencephaly and adult stroke related to mutations in collagen IV A1. Ann. Neurol. 59, 504–11.

van der Laan, L.J., De Groot, C.J.A., Elices, M.J., Dijkstra, C.D., 1997. Extracellular matrix proteins expressed by human adult astrocytes in vivo and in vitro: an astrocyte surface protein containing the CS1 domain contributes to binding of lymphoblasts. J. Neurosci. Res. 50, 539–48.

Vanacore, R., Ham, A.-J.L., Voehler, M., Sanders, C.R., Conrads, T.P., Veenstra, T.D., Sharpless, K.B., Dawson, P.E., Hudson, B.G., 2009. A sulfilimine bond identified in collagen IV. Science 325, 1230–4.

Vasudevan, A., Ho, M.S.P., Weiergräber, M., Nischt, R., Schneider, T., Lie, A., Smyth, N., Köhling, R., 2010. Basement membrane protein nidogen-1 shapes hippocampal synaptic plasticity and excitability. Hippocampus 20, 608–20.

Vezzani, A., Granata, T., 2005. Brain inflammation in epilepsy: experimental and clinical evidence. Epilepsia 46, 1724–43.

Vigelsø, A., Dybboe, R., Hansen, C.N., Dela, F., Helge, J.W., Guadalupe Grau, A., 2015. GAPDH and β-actin protein decreases with aging, making Stain-

Free technology a superior loading control in Western blotting of human skeletal muscle. J. Appl. Physiol. 118, 386–394.

Vlodavsky, I., Folkman, J., Sullivan, R., Fridman, R., Ishai-Michaeli, R., Sasse, J., Klagsbrun, M., 1987. Endothelial cell-derived basic fibroblast growth factor: synthesis and deposition into subendothelial extracellular matrix. Proc. Natl. Acad. Sci. U. S. A. 84, 2292–6.

Wakui, S., Furusato, M., Nikaido, T., Yokota, K., Sekiguchi, J., Ohmori, K., Kano, Y., Ushigome, S., 1990. Ultrastructural localization of fibronectin and laminin in human granulation tissue in relation to capillary development. Cell Struct. Funct. 15, 201–10.

Walsh, M.K., Lichtman, J.W., 2003. In vivo time-lapse imaging of synaptic takeover associated with naturally occurring synapse elimination. Neuron 37, 67–73.

Wang, X., Harris, R.E., Bayston, L.J., Ashe, H.L., 2008. Type IV collagens regulate BMP signalling in Drosophila. Nature 455, 72–77.

Wang, Y., Reheman, A., Spring, C.M., Kalantari, J., Marshall, A.H., Wolberg, A.S., Gross, P.L., Weitz, J.I., Rand, M.L., Mosher, D.F., Freedman, J., Ni, H., 2014. Plasma fibronectin supports hemostasis and regulates thrombosis. J. Clin. Invest. 124, 4281–93.

Way, M., Pope, B., Cross, R.A., Kendrick-Jones, J., Weeds, A.G., 1992. Expression of the N-terminal domain of dystrophin in E. coli and demonstration of binding to F-actin. FEBS Lett. 301, 243–5.

Wehrwein, E.A., Roskelley, E.M., Spitsbergen, J.M., 2002. GDNF is regulated in an activity-dependent manner in rat skeletal muscle. Muscle Nerve 26, 206–11.

Whetstone, W.D., Hsu, J.-Y.C., Eisenberg, M., Werb, Z., Noble-Haeusslein, L.J., 2003. Blood-spinal cord barrier after spinal cord injury: relation to revascularization and wound healing. J. Neurosci. Res. 74, 227–39.

Wijelath, E.S., Rahman, S., Namekata, M., Murray, J., Nishimura, T., Mostafavi-Pour, Z., Patel, Y., Suda, Y., Humphries, M.J., Sobel, M., 2006. Heparin-II domain of fibronectin is a vascular endothelial growth factor-binding domain: enhancement of VEGF biological activity by a singular growth factor/matrix

protein synergism. Circ. Res. 99, 853–60.

Willem, M., Miosge, N., Halfter, W., Smyth, N., Jannetti, I., Burghart, E., Timpl, R., Mayer, U., 2002. Specific ablation of the nidogen-binding site in the laminin gamma1 chain interferes with kidney and lung development. Development 129, 2711–22.

Williams, J.M., Duckworth, C.A., Burkitt, M.D., Watson, A.J.M., Campbell, B.J., Pritchard, D.M., 2015. Epithelial cell shedding and barrier function: a matter of life and death at the small intestinal villus tip. Vet. Pathol. 52, 445–55.

Xu, J., Rodriguez, D., Petitclerc, E., Kim, J.J., Hangai, M., Moon, Y.S., Davis, G.E., Brooks, P.C., Yuen, S.M., 2001. Proteolytic exposure of a cryptic site within collagen type IV is required for angiogenesis and tumor growth in vivo. J. Cell Biol. 154, 1069–79.

Yamashita, Y., Nakada, S., Yoshihara, T., Nara, T., Furuya, N., Miida, T., Hattori, N., Arikawa-Hirasawa, E., 2018. Perlecan, a heparan sulfate proteoglycan, regulates systemic metabolism with dynamic changes in adipose tissue and skeletal muscle. Sci. Rep. 8, 7766.

Yang, T., Massa, S.M., Longo, F.M., 2006. LAR protein tyrosine phosphatase receptor associates with TrkB and modulates neurotrophic signaling pathways. J. Neurobiol. 66, 1420–36.

Yao, Y., Chen, Z.-L., Norris, E.H., Strickland, S., 2014. Astrocytic laminin regulates pericyte differentiation and maintains blood brain barrier integrity. Nat. Commun. 5, 3413.

Yayon, A., Klagsbrun, M., Esko, J.D., Leder, P., Ornitz, D.M., 1991. Cell surface, heparin-like molecules are required for binding of basic fibroblast growth factor to its high affinity receptor. Cell 64, 841–8.

Yurchenco, P.D., 2015. Integrating Activities of Laminins that Drive Basement Membrane Assembly and Function. Curr. Top. Membr. 76, 1–30.

Yurchenco, P.D., Cheng, Y.-S., Campbell, K., Li, S., 2004. Loss of basement membrane, receptor and cytoskeletal lattices in a laminin-deficient muscular dystrophy. J. Cell Sci. 117, 735–42.

Yurchenco, P.D., Cheng, Y.S., Colognato, H., 1992. Laminin forms an independent network in basement membranes. J. Cell Biol. 117, 1119–33.

Yurchenco, P.D., Ruben, G.C., 1987. Basement membrane structure in situ: evidence for lateral associations in the type IV collagen network. J. Cell Biol. 105, 2559–68.

Yurchenco, P.D., Schittny, J.C., 1990. Molecular architecture of basement membranes. FASEB J. 4, 1577–90.

Zattoni, M., Mura, M.L., Deprez, F., Schwendener, R.A., Engelhardt, B., Frei, K., Fritschy, J.-M., 2011. Brain Infiltration of Leukocytes Contributes to the Pathophysiology of Temporal Lobe Epilepsy. J. Neurosci. 31, 4037–4050.

Zeisberg, M., Khurana, M., Rao, V.H., Cosgrove, D., Rougier, J.-P., Werner, M.C., Shield, C.F., Werb, Z., Kalluri, R., 2006. Stage-specific action of matrix metalloproteinases influences progressive hereditary kidney disease. PLoS Med. 3, e100.

Zhang, B., Luo, S., Wang, Q., Suzuki, T., Xiong, W.C., Mei, L., 2008. LRP4 serves as a coreceptor of agrin. Neuron 60, 285–97.

Zong, Y., Zhang, B., Gu, S., Lee, K., Zhou, J., Yao, G., Figueiredo, D., Perry, K., Mei, L., Jin, R., 2012. Structural basis of agrin-LRP4-MuSK signaling. Genes Dev. 26, 247–58.